T H E U N I V E R S I T Y O F M I C H I G A N

COLLEGE OF ENGINEERING

Department of Meteorology and Oceanography

Final Report

THE UTILITY OF SATELLITE CLOUD PHOTOGRAPHS IN OBJECTIVE ANALYSIS OF THE 500-MB HEIGHT FIELD

Christopher M. Hayden

Aksel C. Wiin-Nielsen
Project Director

ORA Project 08203

supported by:

ENVIRONMENTAL SCIENCE SERVICES ADMINISTRATION
CONTRACT CWB-11377
WASHINGTON, D.C.

administered through:

OFFICE OF RESEARCH ADMINISTRATION - ANN ARBOR

February 1968

TABLE OF CONTENTS

TABLE OF CONTENTS (Concluded)

LIST OF TABLES

LIST OF TABLES (Concluded)

LIST OF FIGURES

LIST OF FIGURES (Continued)

LIST OF FIGURES (Concluded)

ABSTRACT

This study was conducted to investigate the feasibility of modifying the 500 mb height field by reference to cloud formations visible in satellite photographs. Three case studies are investigated to illustrate high (North America), medium (Atlantic), and low (Pacific) data density regions.

A technique is developed whereby the height-tendency field, either instantaneous or averaged over twelve hours, is adjusted by comparison with the cloud pictures. Through the modified tendency field alterations are made to the twelve-hour forecast height field, valid at analysis time, which serves as the first-guess for the objective analysis routine. The reanalyzed forecast fields are evaluated with respect to improvement in the initial-guess and effect on the final product of an objective analysis system which duplicates that employed at NMC prior to 1965 (and which consequently closely resembles the present operational system.) The data density dependence of the latter is investigated by a procedure of withholding a varying number of observations from repeated analysis of the same synoptic situation. Reanalysis is introduced to the system via the altered guess field or through pseudo station reports abstracted from that field. It is demonstrated that the tendency technique is successful in improving the forecast guess field, though modestly in areas of good data. However, the improvement is not meaningfully reflected in the product of the objective analysis, regardless of the method of input and almost irrespective of observation density. At moderate data density the observations overwhelm the reanalysis alterations while at low density the analysis system behaves erratically.

The objective analysis system is tested primarily to determine the role of the initial guess field and to investigate the observed instability at low station density. It is found that the system gives too little weight to the guess field. Simple alterations are offered to alleviate both this deficiency and the sparse data instability.

With the modified analysis system it is shown that reanalysis by bogus station input remains inconsequential. However, input by the adjusted first-guess field can be

effective in the final analysis at station densities less that approximately one report per ten gridpoints (NMC) grid). This density is encountered at low latitudes and over the Pacific.

It is suggested that although the satellite cloud photographs cannot be used effectively to supplement conventional data without alteration in the objective analysis routine presently used at NMC, they do provide a ready tool for the evaluation of the conventional analysis by comparison of the implied tendency field with the cloud formations. This is particularly useful in sparse-data areas where any type of verification is difficult.

1. INTRODUCTION

1.1 Background

Since the advent of the TIROS series, meteorologists have been trying to draw inferences on the state of the atmosphere from the cloud photographs and radiation data received from satellites. The present study is a further effort in this direction dealing specifically with the relationships between the height field at 500 mb and the photographs relayed from the ESSA I and III satellites.

By their nature, cloud photographs give qualitative information on the state of the atmosphere. Few realized, prior to receipt of the first TIROS pictures, the degree of organization in satellite-observed cloud formations, and there has been considerable success in using these photographs to describe major storm systems (Boucher and Newcomb, 1962; Widger et. al., 1965). Much attention has also been paid to the identification and description of smaller-scale features such as tropical storms (Fritz, 1962; Whitney, 1963; Frank, 1963; Erickson, 1965; Felt, 1966), the jet stream (Whitney, 1961; Bonner and Winninghoff, 1967), lee waves (Döös, 1962; Fritz, 1965), and the like. However, outside the field of descriptive meteorology the cloud photographs have been of more limited utility, with that utility naturally greater the more closely the phenomenon under investigation is related to the presence of clouds. Many authors have related the cloud photographs to separately derived synoptic parameters. Examples in this field include precipitation studies (Nagle and Serebreny, 1962), diagnostic cloud studies (Nagle et. al., 1966), air mass wind and thermal structure (Elliot and

Thompson, 1965), vertical velocity (Musayelyan, 1964; Sanders et. al., 1965; Deardorff, 1963; Rogers and Sherr, 1965) and vorticity advection (Brodrick, 1964). A further study (Fritz, 1963), relates laboratory experiments to the photographs.

The next logical step is to infer the synoptic parameters from the cloud pictures, or to seek quantative information. Probably because of the inherent difficulty, rather limited progress has been made in this field, although again success is related to the closeness of the correspondence between cloud and the desired parameter. An example is layer-mean relative humidity (McClain, 1966). Studies have also been performed on wind speeds inferred from the satellite pictures (Timchalk et. al., 1961; Fritz et. al., 1966).

The final stage is to introduce the inferred quantities into routine operational analysis and forecasting procedures. This use of the photographs was initiated at the National Environmental Satellite Center (McClain, Brodrick and Ruzecki, 1964) under project SINAP (Satellite Input to Numerical Analysis and Prediction)[1], and has been continued at the University of Michigan (Bradley and Hayden, 1966). Prior to the present study, SINAP has been concerned with direct reanalysis of the contour (or stream function) field or reanalysis of the vorticity field at 500 mb. Experiments have been carried out for the data-sparse Pacific in cases where the forecast was unusually bad. Verification was

---

[1] A recent comprehensive review of this subject is contained in "The SINAP Problem: Present Status and Future Prospects," ESSA Tech. Rept. NESC-41, 1967.

attempted by comparing the thirty-six-hour barotropic forecast from the reanalyzed field with the original forecast field. Although some success was attained with this method by the NESC group in Washington, the results obtained here at Michigan were of questionable utility. Part of the difficulty can be attributed to the lack of familiarity of the investigators here with satellite photographs, and a further part to the deficiency inherent in the isolated swaths obtainable from the TIROS satellite. However, the major problems encountered were the extreme subjectivity of the reanalysis techniques and the internal machinations of such an extended forecast. Results of the work strongly suggested that even immodest alterations in the original field were completely lost by the forecast, most probably because the implied scale of the reanalysis was below the resolution of the forecast model.

1.2 Aim of the Study

Because of the aforesaid difficulties, the present work was designed to eschew the complete subjectivity of the reanalysis procedure and also the problems associated with forecast verification. The technique remains subjective, though less so than either the reshaping of streamlines or the introduction of vorticity centers. Numerical analysis rather than forecast is used to assess the procedure, thus removing much of the uncertainty though little of the difficulty of verification. The purpose of this study remains as before, to analyze the usefullness of satellite photographs as additional data for the 500-mb analysis. A secondary aim is to clarify the heretofore moot question of how best to introduce the photograph information into the operational analysis/forecast routine.

2. REANALYSIS PROCEDURE

2.1 Height-Tendency Field

In order to infer a physical parameter from the visible cloud structure it is only reasonable to select a variable which is closely related to the generation of clouds. The most obvious choice is the vertical wind velocity, particularly as considerable work has already been done to relate this variable to satellite-observed cloud systems. The studies mentioned above agree that in the early stages of vortex development there is good correlation between observed cloud cover and synoptic-scale vertical velocities. In later stages, where advection plays a greater role, cloud tends to overrun areas of downward motion on the western side of the vortex while a tongue of relatively clear air penetrates regions of upward motion (Leese, 1962; Rogers and Sherr, 1967). The correspondence of cloud to vertical velocity is consequently somewhat diminished, but the known discrepancies can be allowed for in a SINAP procedure.

To further document the relationship of cloud to vertical velocity, computations were made in this study with data over the Atlantic (May case). A simplified version of the omega equation (Wiin-Nielsen, 1959) was used:

$$\sigma_o \nabla^2 \omega + f_o^2 \frac{\partial^2 \omega}{\partial p^2} = \frac{2Rg}{f_o p} \{ J(\nabla^2 Z, T) + \lambda(Z, T) \} \qquad 2.1.1$$

where σ_o is an average value of the static stability,

f_o is the Coriolis parameter at 45^oN latitude,

J is the Jacobian operator,

λ is a notation for the following operator:

$$\lambda(Z,T) = -\left(\frac{\partial^2 Z}{\partial x \partial y}\right)\left(\frac{\partial^2 T}{\partial x^2} - \frac{\partial^2 T}{\partial y^2}\right) + \left(\frac{\partial^2 Z}{\partial x^2} - \frac{\partial^2 Z}{\partial y^2}\right)\left(\frac{\partial^2 T}{\partial x \partial y}\right) \qquad 2.1.2$$

Equation 2.1.1 has been further simplified by assumption of a parabolic distribution of omega:

$$\omega = \frac{\omega_5 p}{p_5}\left(2 - \frac{p}{p_5}\right) \qquad 2.1.3$$

where ω_5 is the vertical velocity at 500 mb. In this manner the vertical velocity has been computed from data at a single pressure level. The resultant fields have proved to correlate well (a strictly visual comparison tempered by the aforementioned discrepancies) with the satellite-observed cloud formation.

These results suggest that the cloud photographs can be used to correct or reanalyze the field of vertical velocity. However, since the vertical velocity is not a primary variable in objective analysis, some procedure is necessary to relate the alterations in this field to changes in the contour or stream field. The most straightforward technique is to "reverse" the omega equation so that the height field can be obtained explicitly from the vertical velocity field. A general scheme to accomplish this has been proposed by Blinova (1963) and investigated by Nemchinov et.al. (1963) in a spherical coordinate system. The inversion has also been done by Krishnamurti (1964) using the method of characteristics. The proposed techniques are, however, rather complex for a SINAP procedure, and although several attempts were made during this work to find a simple method of inverting equation 2.1.1 without the deformation term, $\lambda(A,T)$, these efforts were

unsuccessful.[1]

Because of the complications involved in working directly with the vertical velocity field, all reanalyses performed in this work have been done on the height-tendency field ($\partial Z/\partial t$). The close correspondence of these variables can be justified partly in theory and partly by experiment.

Holmström (1963) has discussed a parametric representation of the vertical structure of the atmosphere in terms of empirical orthogonal functions. These functions take the form (using the height field as an example):

$$Z(x,y,p) = F_o(p) + \sum_{k=1}^{K} F_k(p)\, z(x,y) + r(x,y,p) \qquad 2.1.4$$

where $F_o(p)$ is the horizontally-averaged height field,

$r(x,y,p)$ is the residual due to truncation of the series.

Experiments with real data using these functions revealed that:

(a) The pressure functions $F_k(p)$ are relatively time independent.

(b) The 500-mb surface can be accurately represented by inclusion of only the first mode. More specifically, for the height field at 490 mb, Holmstrom states that the residual after the first mode in the expansion was found to have a root-mean-square error of only twenty-six meters.[2]

---

[1] As pointed out by Wiin-Nielsen and confirmed by experiment with our data, this term is of far less consequence than the advective term, at least for the 500-mb level.

[2] It is interesting to note that this is close to the noise level of the objective analysis routine (see Appendix B.)

Based on these results, which have been verified by other authors (Obukhov, 1960; Bradley, 1967), Holmström (1964) developed a forecasting procedure using only a single mode. This model is briefly recapitulated here.

The quasi-geostrophic vorticity and thermodynamic equations can be written in the form:

$$\frac{\partial \zeta}{\partial t} + J(Z, \zeta+f) - f_o \frac{\partial \omega}{\partial p} = 0 \qquad 2.1.5$$

$$\frac{\partial^2 \phi}{\partial t \partial p} + \frac{1}{f_o} J(\phi, \frac{\partial \phi}{\partial p}) + \omega \sigma_o = 0 \qquad 2.1.6$$

where ϕ is the geopotential and other variables have their usual meaning. Introducing expansions for the height and vertical velocity in only a single mode:

$$Z(x,y,p) = F_o + F_1(p) z_1 \qquad 2.1.7$$

$$\omega = C_1(p) \omega_1 \qquad 2.1.8$$

and approximating the vorticity by:

$$\zeta = \frac{1}{f_o} \nabla^2 \phi \qquad 2.1.9$$

equations (2.1.5) and (2.1.6) can be rewritten as:

$$F_1 \frac{\partial \zeta_1}{\partial t} + J(\phi_1, \zeta_1 + \frac{f}{F_1}) \frac{F_1^2}{f_o} - f_o \omega_1 \frac{dC_1}{dp} = 0 \qquad 2.1.10$$

$$\frac{\partial \phi_1}{\partial t} \frac{dF_1}{dp} + \omega_1 C_1 \sigma_o = 0. \qquad 2.1.11$$

These equations are combined by eliminating the vertical velocity and taking the vertical average of the individual terms such that:

$$\bar{F}_1 = \frac{1}{P_o} \int_o^{P_o} F_1(p)\,dp \qquad 2.1.12$$

where p_o is 1000 mb.
This yields:

$$\frac{\partial \nabla^2 \phi_1}{\partial t} + J(\phi_1, \zeta_1 \frac{\overline{F_1^2}}{\bar{F}_1} + f) + \frac{f_o^2}{P_o \bar{F}_1 \sigma_o(P_o)} (\frac{dF_1}{dp})_{P_o} \frac{\partial \phi_1}{\partial t} = 0 \qquad 2.1.13$$

The last equation (2.1.13) is analogous to the equivalent barotropic forecast equation. The success of the latter as a forecast model for the 500-mb surface is in complete accordance with the accuracy of the 500-mb representation obtainable from only a single mode.

With respect to a reanalysis procedure, equation 2.1.11 demonstrates that within this framework the height tendency is proportional to the vertical velocity. Consequently we may use the height-tendency field as equivalent to the vertical velocity field to relate the cloud photographs to the 500-mb analysis. This equivalence has proved valid for the data used in this study by comparison of the tendency and omega fields computed from equations (2.1.13) and (2.1.1) respectively.

It is no easier to reverse the equivalent barotropic forecast equation than to reverse the omega equation, and in the course of this work two other techniques have been followed. Originally the subsequent procedure was used to

---

[1] It should be mentioned that to make the investigation tractable (from the point of view of economy and computer storage) all computations are done over a subset of the regular NMC 1977 point grid. The subsets are determined by the satellite coverage used in the experiments.

reanalyze the tendency and consequently the height field:

i) Find the original tendencies and forecast the original height field one hour.

ii) Compare the tendency field with the cloud photographs and alter the tendencies in accordance with discrepancies.

iii) Hindcast the forecast with the new tendency field to obtain the reanalyzed original field.

iv) Smooth the reanalyzed field and recompute the tendency field.

v) Repeat steps ii-iv if necessary.

Steps (ii) and (iii) are equivalent to reanalyzing the height field, but this procedure is less subjective than the simple reshaping of the contours since the tendency field adjustment allows more sensitive control over the magnitude of the reanalysis. This technique proved to be quite stable in the sense that alterations made in step (ii) were only modestly changed in step (iv).

The second method of reanalysis uses the gross twelve-hour tendencies determined by subtracting the twelve-hour-old analysis from the twelve-hour forecast field which forms the first guess for the objective analysis. The tendencies are compared to the cloud photographs, altered, and added to the old analysis to form a new guess field. The twelve-hour tendency field is much smoother than the instantaneous field, but its main characteristics are similar (at least to the degree of resolution sought in this study). This second method is obviously much easier to use, and there is no expensive iterative procedure involved. The major disadvantage is that it presupposes

accuracy in the twelve-hour-old analysis. In extensive regions of sparse data this assumption is not well justified.

With regard to the actual SINAP modifications it should be emphasized that only the large-scale, horizontal features of the cloud systems have been of concern in this study. There has been no attempt to distinguish the finer features or the vertical structure of the cloud formations. A one-level, 500-mb experiment dealing with the height-tendency field is too crude to permit such resolution. It will be noted that the primary target is the dense cloud shield associated with all mature vortices which is always the primary region of upward motion. Balancing regions of downward vertical velocities are inferred from the shapes of the systems apparent in the cloud photographs. Clouds associated with fronts are used only to shape the major regions of upward motion and no attempt has been made to estimate the magnitudes of vertical velocities in the frontal bands. No differentiation is made between cloud/clear areas associated with advective rather than vertical motion except to bear in mind the discrepancies discussed above and to note that with cyclogenesis on a well-defined front, clouds are always advected downstream from the cloud shield into areas of sinking motion. Small-scale cumulus clouds are ignored. Local low-level convective processes are irrelevant to a study of the 500-mb surface except to offer some indication of the location and shape of ridges in the circulation.

2.2 Temporal Continuity

The fact that the individual swaths which make up the cloud montages are not contemporary with analysis time slightly complicates comparison of the tendency fields with

the cloud photographs. In order to investigate the effect of time discontinuities a program was designed to advect to analysis time the cloud formations of each swath. The advecting wind was chosen to be one-half the geostrophic wind at 500 mb. This somewhat arbitrary choice was itself checked by advecting the clouds to the succeeding picture time. The resultant comparison of the advected with the observed clouds was sufficiently good to justify a short term advection (Fig. 2.1). The tests suggest that time differences of up to three hours can be ignored as the corresponding change in the cloud formations is below the resolution of the reanalysis technique. With time disparities of greater than three hours some compensation must be made.

2.3 First-Guess Reanalysis

As the name implies, reanalysis of the twelve-hour forecast field by either of the tendency methods detailed above serves as one technique for 500-mb contour reanalysis. The modified forecast is used as the first guess for the objective analysis scheme (Appendix A). The value of such reanalysis is dependent on the weight permitted the first guess by the analysis scheme. This question itself has been of major concern during this study, since it is very difficult to strike the delicate balance between the forecast and analysis procedures. Intrinsically this method of reanalysis is attractive in that erroneous changes (which are unavoidable in any subjective method) will tend to be smoothed out of the final analysis.

2.4 Bogus Station Reanalysis

This type of reanalysis involves the introduction of

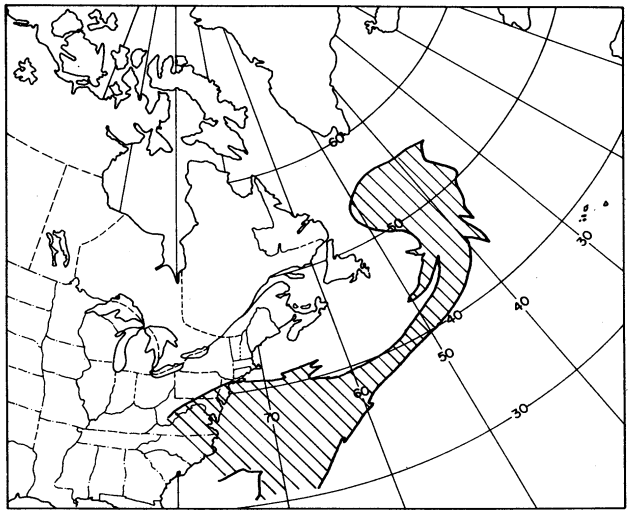

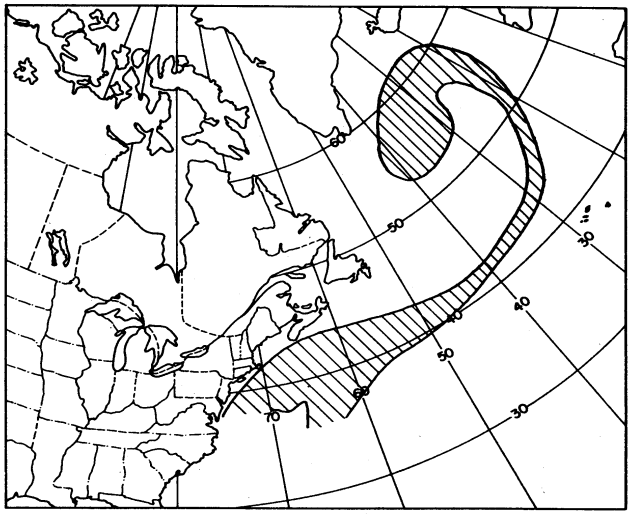

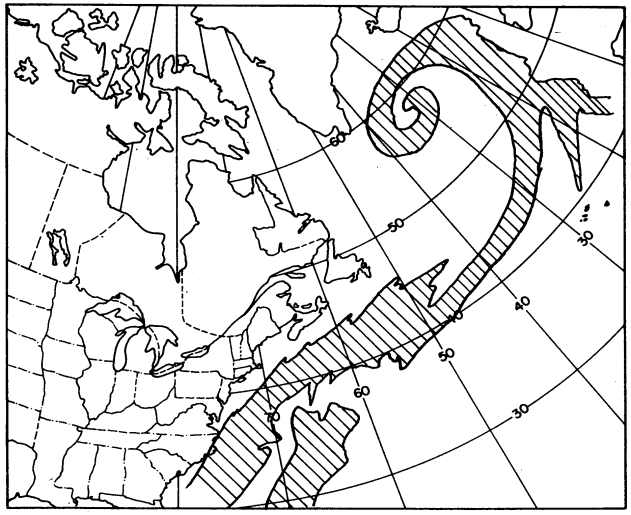

Fig. 2.1. Forecast cloud cover for 00Z, 16 May 1966. Upper left: Cloud photographs of 14 May rectified to 00Z, 15 May. Lower left: Cloud photographs of 15 May rectified to 00Z, 16 May. Above: Upper left forecast to 00Z 16 May.

pseudo station reports to be used during the objective analysis. The reports are extracted directly from the reanalyzed first-guess field and used as ordinary data. This type of input is presently used at NMC to introduce corrections to the analysis from both subjective hand-analysis and satellite photographs. The major advantage of this method is that it continues to assert an active role throughout the analysis. However, it is very difficult to produce a desired change in the analysis via a few points of information. This will become apparent in section 4.

3. VERIFICATION PROCEDURE

3.1 Statement of Problem

There are two not unrelated aspects to verification in this study. Firstly there is the question of whether the reanalysis of the first-guess field gives a closer approximation to the actual state of the atmosphere. Secondly (given the above) there is the question of whether the reanalysis is useful to the final product. Obviously if conventional data are sufficiently plentiful to exactly define the state of the atmosphere (within the limits of the analysis system), reanalysis via cloud photographs is superfluous.

Unfortunately neither of these questions is easily answered. The logical approach to the former is to choose an area of very dense data and simply compare the final product of the objective analysis with the original and reanalyzed first-guess fields. However, dense-data networks occur over land only, and cloud patterns over land are much more confused than over ocean areas (Timchalk and Hubert, 1961). Furthermore, it is certainly true that the denser the data, the better the short-term forecast. Hence the first-guess field is quite accurate and difficult to improve. In order to partially circumvent this last obstacle both the thirty-six-hour forecast (valid at analysis time) and the regular twelve-hour forecast were used as first-guess fields in the high density case study.

To investigate the second question, a procedure of withholding observations was adopted. This method has also been employed by Gandin (1963) in evaluating objective analysis. Repeated analyses have been executed for each data set while varying the amount of data used in an individual trial. Intuitively there should exist some density

at which reanalysis becomes ineffective, although this may vary from case to case in accordance with the severity of the reanalysis and the state of the atmosphere.

Several parameters have been used to elucidate both aspects of the verification problem. These are detailed in the following.

3.2 Change Correlation Coefficients, RMS Error

Five verification statistics similar to those used at NMC to validate forecast height (stream) fields at gridpoints are used in this study for comparison of any two contemporaneous fields. The twelve-hour-old NMC analysis is originally subtracted from each of the fields in order to remove the quasi-permanent variance associated with the equator-to-pole height gradient. These statistics are:

SRMS - the root-mean-square discrepancy between the twelve-hour changes in geostrophic wind speed indicated by the two fields.

SCC - the correlation coefficient of the twelve-hour changes in geostrophic wind speed indicated by the two fields.

DCC - the correlation coefficient of the twelve-hour changes in geostrophic wind direction indicated by the two fields.

TRMS - the root-mean-square discrepancy between the twelve-hour height changes indicated by the two fields.

TCC - the correlation coefficient of the twelve-hour height changes indicated by the two fields.

Combinations of the fields available at each analysis time have been chosen to elucidate particular aspects of the

SINAP problem. Five are performed for every trial:

i) Analysis from original guess vs. original guess: This comparison investigates the deficiency of the original guess, particularly as a function of data density when all artificially sparse-data analyses are used.

ii) Analysis from reanalyzed guess vs. reanalyzed guess: Similarly to (i), this combination investigates the performance of the reanalyzed guess field. A comparison of the results for this combination with those for (i) is intended as a measure of the efficiency of the reanalysis technique, again as a function of data density.

iii) Analysis from original guess vs. NMC analysis: This combination investigates the performance of the analysis system by measuring the correspondence of the final products from varying data densities with the NMC product.

iv) Analysis from reanalyzed guess vs. NMC analysis: Statistics computed with this pair are compared with those of (iii) to evaluate the effectiveness of the SINAP modifications in the final products and to determine a density "threshold of effectiveness." The latter is defined as the data density above which the difference between (iii) and (iv) becomes constant or insignificant.

v) Analysis from original guess vs. analysis from reanalyzed guess: This combination is used to complement the comparisons of (iii) and (iv) in determining the "threshold of effectiveness."

Three combinations which are independent of data density are computed once for each data set:

vi) Original guess vs. NMC analysis: This comparison measures the quality of the original guess field, at least

for those cases where the NMC analysis can be considered correct.

vii) Reanalyzed guess vs. NMC analysis: Statistics computed from these fields are compared with those of (vi) to evaluate the effectiveness of SINAP modifications in improving the first guess.

viii) Original guess vs. reanalyzed guess: These statistics measure the severity of the reanalysis.

For all of the above, statistics are computed over the entire grid (excepting edgepoint winds) and over a subregion determined by the particular reanalysis.

3.3 Areal-Root-Mean-Square Error

The grid statistics discussed above are far from a panacea for the difficulties involved in assessing an objective analysis. It is more desirable to use actual station values of the analyzed parameter as has been discussed by Thomasell (1962). From this standpoint he devised the areal-mean-error method of verification. In essence, point-error estimates are obtained from the difference between observed station heights and the height values interpolated to the stations from the surrounding gridpoints in the analysis. These errors are computed both for stations used in the analysis and for stations intentionally withheld from the analysis. Because all objective analysis schemes are designed to fit the reported data to a high degree of accuracy, the error related to the retained reports is representative of the minimum error in the field. Those regions most distant from any retained data can be though to contain (in a statistical sense) the maximum error that is represented by the withheld stations. The areal-root-

mean-square error (ARMSE) is a summation of the individual point error estimates weighted according to the number of analysis (retained) stations in the neighborhood of each error. This gives an approximation to the integral of the analysis error over the analysis area, which may be formulated mathematically by:

$$\text{ARMSE} = \left\{ \sum_{w=1}^{W} \frac{(\phi_w - S)^2}{2\sum^{W} \rho_w^{-1}} \rho_w^{-1} + \sum_{a=1}^{A} \frac{(\phi_a - S)^2}{2\sum^{W} \rho_a^{-1}} \rho_a^{-1} \right\}^{\frac{1}{2}} \qquad 3.3.1$$

where
- ϕ is the observed height,
- S is the interpolated height,
- a is a subscript for analysis (retained) stations,
- w is a subscript for withheld stations,
- ρ_w is the density of analysis stations in the neighborhood of a withheld station
- ρ_a is the density of analysis stations in the neighborhood of an analysis station.

Density is defined as the number of analysis stations within two gridlengths of the station in question. If there are no neighbors, the search is extended up to four gridlengths, but the density is weighted to give less contribution to the ARMSE. If no neighbors are available at four gridlengths the contribution is ignored. Thomasell gives a method for objective selection of withheld stations, but in this study, where the analysis stations used for the artificiallly sparse-data networks were carefully chosen to give uniform distribution, the withheld stations were chosen subjectively. In all cases they are well-removed from the analysis stations but also uniformly distributed. The ARMSE was computed for every scan of all moderately sparse analyses. This lends insight into the performance of the individual scans as well as the analysis as an entity.

3.4 Zonal Harmonic Analysis

A one-latitude, zonal harmonic analysis to compute the cosine coefficients for an evenly-extended increment of ninety degrees of longitude was built into the objective analysis program. In this manner the first six coefficients have the scale of hemispheric wave numbers 0, 2, 4, 6, 8, and 10 (although they converge to the true value of the analysis only in the analysis area). Tests with a five-point filter indicated, as expected, that attempts to resolve smaller scales resulted in pure noise. Coefficients were computed for each scan of all analyses. This feature was designed to delineate the scale of the reanalysis and to measure the effects of the individual scans on the scales of motion present in the guess fields. It was hoped that these calculations would disclose any bias effects related to the scanning radii of the objective analysis system (see Appendix A) or would determine an effective limit to the scale of the first-guess reanalysis. In actual fact the results proved too erratic to be conclusive.

3.5 Objective Analysis

The limited resolution, or large-scale treatment, stressed in the SINAP tendency technique is at least partially justified by the problem of reanalysis verification, particularly with regard to the influence of the objective analysis system. The original system used here was programmed to correspond to the four-scan, one-level analysis system operational at NMC until 1965 (Appendix A). Results with this system were difficult to evaluate for two reasons, both related to the fact that the early scans of the analysis cause considerable modification of the first-guess

field irrespective of the quality of that field or the observation density (Appendix B). In the first place this characteristic greatly hampers verification by artificially sparse-data networks. Secondly, as will become clear, the twelve-hour forecasts used in Case I and II are quite accurate, certainly more so than the fields produced after the first two scans of the objective analysis. The implications regarding the utility of reanlyzing the first-guess field via cloud photographs are obvious. Improvements by this SINAP technique are overwhelmed by the analysis procedure. It seems likely that the analysis system presently operational at NMC retains this behaviour despite the fact that the 500-mb analysis is now performed in two three-scan stages. The initial stage operates on the same first-guess field and has equivalent large-scale scanning radii. The stability check introduced prior to the second stage might help the problems associated with low data density, but it seems doubtful that it can completely recover those first-guess fields which are accurate.

Mainly because of these system-related difficulties in assessing the reanalysis, the analysis system was modified to give greater weight to the initial guess field and to limit the influence of the early scans, particularly at low data densities. A full account of the modification, and tests leading to it, is given in Appendix B. This detour from a purely objective investigation of SINAP might be challenged as compromising the existing operational structure in order to present SINAP in a more favorable light. Hopefully the motivation is not so mean. Analysis and forecast are conjugate problems, and it seems only reasonable that any analysis system should glean all possible benefit avail-

able from the forecast (or first guess). This philosophy is fairly widely accepted. Although there have been many efforts to devise analysis systems which are self-sufficient entities, they are outnumbered by those which use either a forecast as a first guess or some dynamic principle with forecasting overtones (Thompson, 1961; Richardson, 1961; Smith, 1962). All trials in this study have been executed with both the original and modified versions of the analysis system to permit evaluation not only of the height-tendency SINAP technique, but of the analysis system as well.

4. CASE STUDIES

4.1 Introduction

Three synoptic cases were selected for this study:

i) 6 - 9 January 1967, North America.
ii) 10 - 16 May 1966, Atlantic.
iii) 11 - 14 February 1967, Pacific.

These choices were made to illustrate regions of dense, moderate, and sparse data coverage. The first case follows a developing short wave over the United States. The second case features two systems which move through the classic stages of vortex development from the eastern coast of the United States through the North Atlantic. The final case is concerned primarily with two developing storms in the northern region and the life cycle of an easterly wave in the southern region of the Pacific. Because of the disparity between the cloud photographs and the first-guess fields, the dearth of observational data, and finally time commitments, no artificially sparse-data trials or reanalyses were attempted with the last case. The three cases are treated individually in the following sections.

4.2 Case I: High Data Density, North America, 6-9 January 1967

4.2.1 Introduction

Although this case was the second investigated in this work, it will be discussed first since the greater data density permits more confidence in the verification procedure. The twelve-hour, gross-tendency technique was used for all reanalyses that were performed initially with the thirty-six-hour forecast guess fields. Further reanalyses

were made using the twelve-hour forecast first-guess, excepting the eighth of January where no improvement seemed possible through the satellite photographs. No time rectification was used in this case since the times of the photographs approximate the mean time of the tendency calculations.

The decision to use the thirty-six-hour forecast was made when casual comparison of the cloud photographs with the twelve-hour forecast tendencies indicated that there was little room for improvement. It might be argued that this decision is not quite "cricket," as there is undoubtably a built-in bias caused by the use of the twelve-hour-old analyses. In many cases the persistence of this field may be a better approximation than the relatively extended forecast field. If this is true, any improvements that are made with the reanalysis are partially in consequence of the accuracy of the old analysis. This objection is quite valid and can be countered only by stressing that the gross-tendency field <u>requires</u> accuracy in the previous analysis. In this sense the thirty-six-hour forecast is to be thought of as a poor twelve-hour forecast. If the associated tendency field turns out to be completely unrealistic, the reanalysis becomes an attempt to guess the twelve-hour tendencies with no help from the forecast. During this part of the study conscious effort was made to avoid reanalyzing those portions of the gross tendency field which seemed in error, but which error was unrelated to the major cloud systems.

4.2.2 Synoptic Discussion

The basic circulation for this period is quite typical of midwinter conditions. The long wave pattern at 500 mb over the North American continent shows a deep trough centered over Hudson Bay with a trailing ridge over the Northwest. This configuration is held fairly stationary by a blocking high over the North Atlantic. During the four-day period a mature short wave moves from east of the Middle Atlantic States to a stall position east of the Maritime Provinces (Fig. 4.1 and 4.2). At this time it diffuses southeast into the low associated with the blocking high. At the start of the period a second short wave has entered the major trough and is situated over Idaho and Montana. This system moves across the Rockies with slight intensification into the Central Plains States. As it moves up the major trough it reaches maturity (12Z, 7 January) while deforming the long wave extensively in the northeast-southwest direction (Fig. 4.3). At the end of the period the storm has lost most of its identity as the center moves over the Gulf of St. Lawrence (Fig. 4.4). Surface phenomena associated with this wave reveal a large cyclone which, driven by arctic air, develops rapidly and produces blizzard conditions over the northern tier of states in the Midwest and East. The large-scale features of the cloud montages are rectified (with some license for artistry) in each figure. The cloud formations unfortunately are not as well defined as in the classical models of vortex development. This is partly due to disruptive orographic influences which deform the clouds, but also due to the technical difficulty of differentiating cloud from snow cover (stippled in drawings). It is of interest to note that the sharp cloud edge on the downstream side of the minor trough identifies the jet stream.

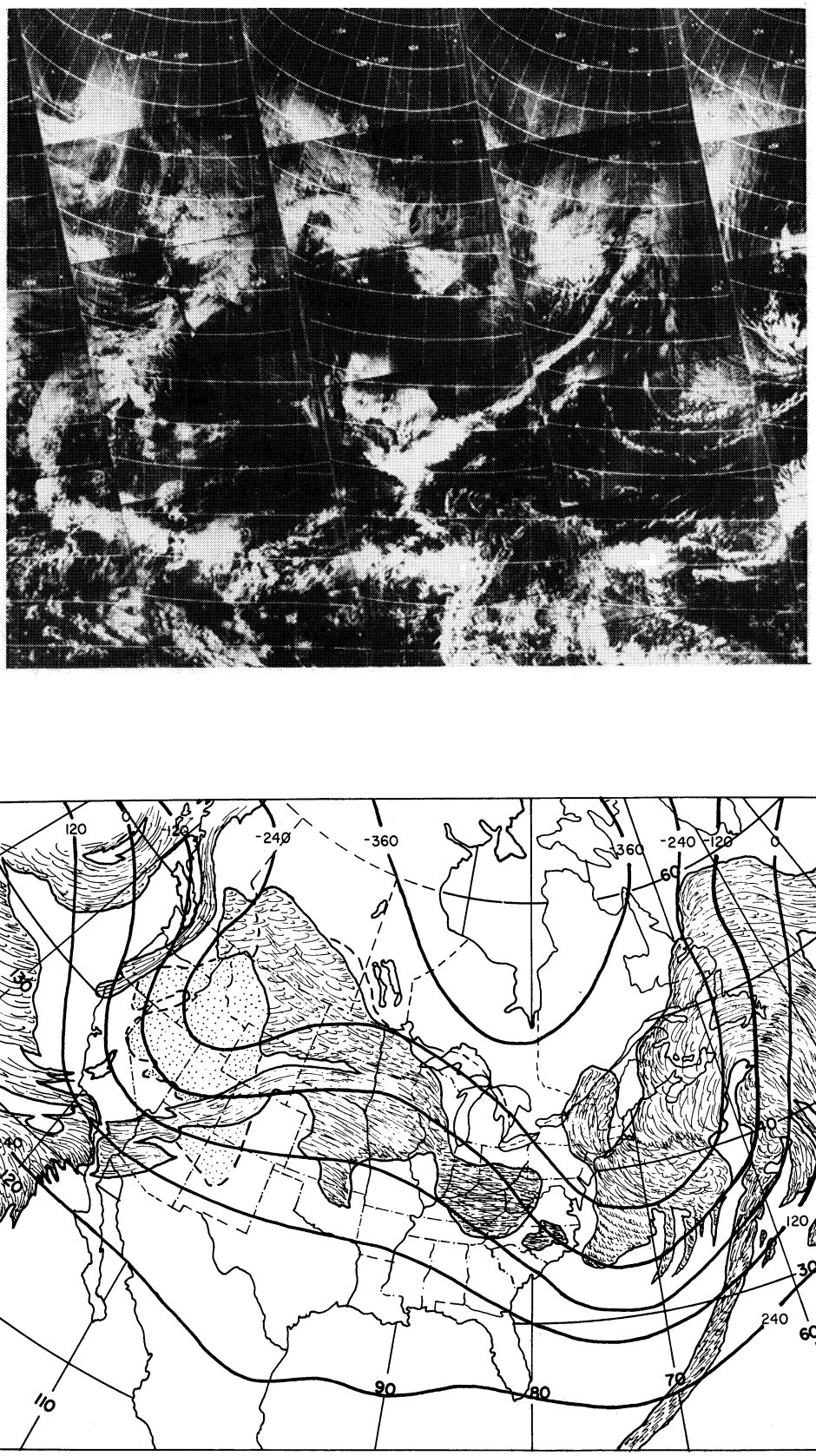

Fig. 4.1. Cloud montage and NMC 500 mb analysis for 00Z, 6 January 1967. (D values in meters.)

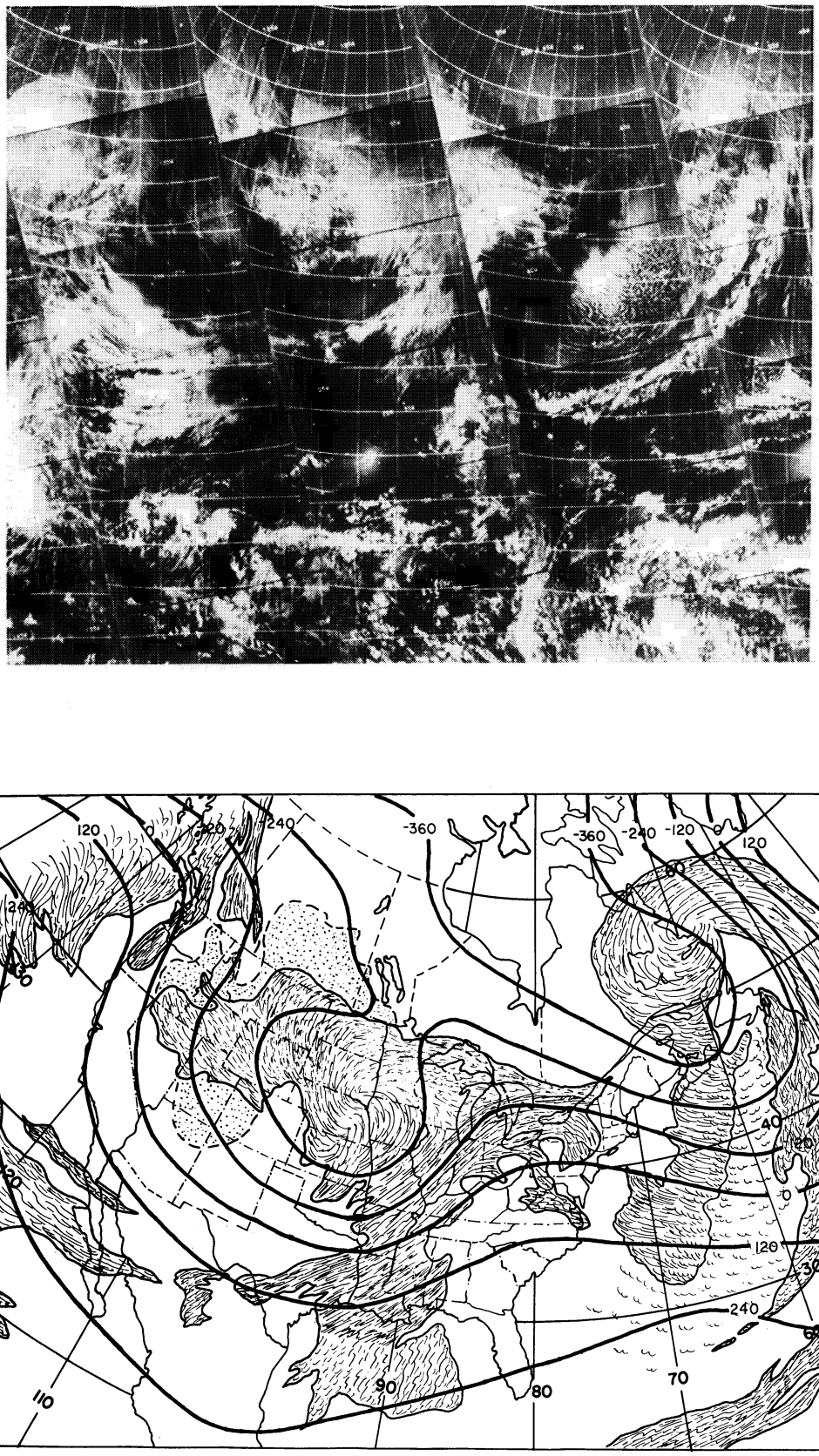

Fig. 4.2. Cloud montage and NMC 500 mb analysis for 00Z, 7 January 1967. (D values in meters.)

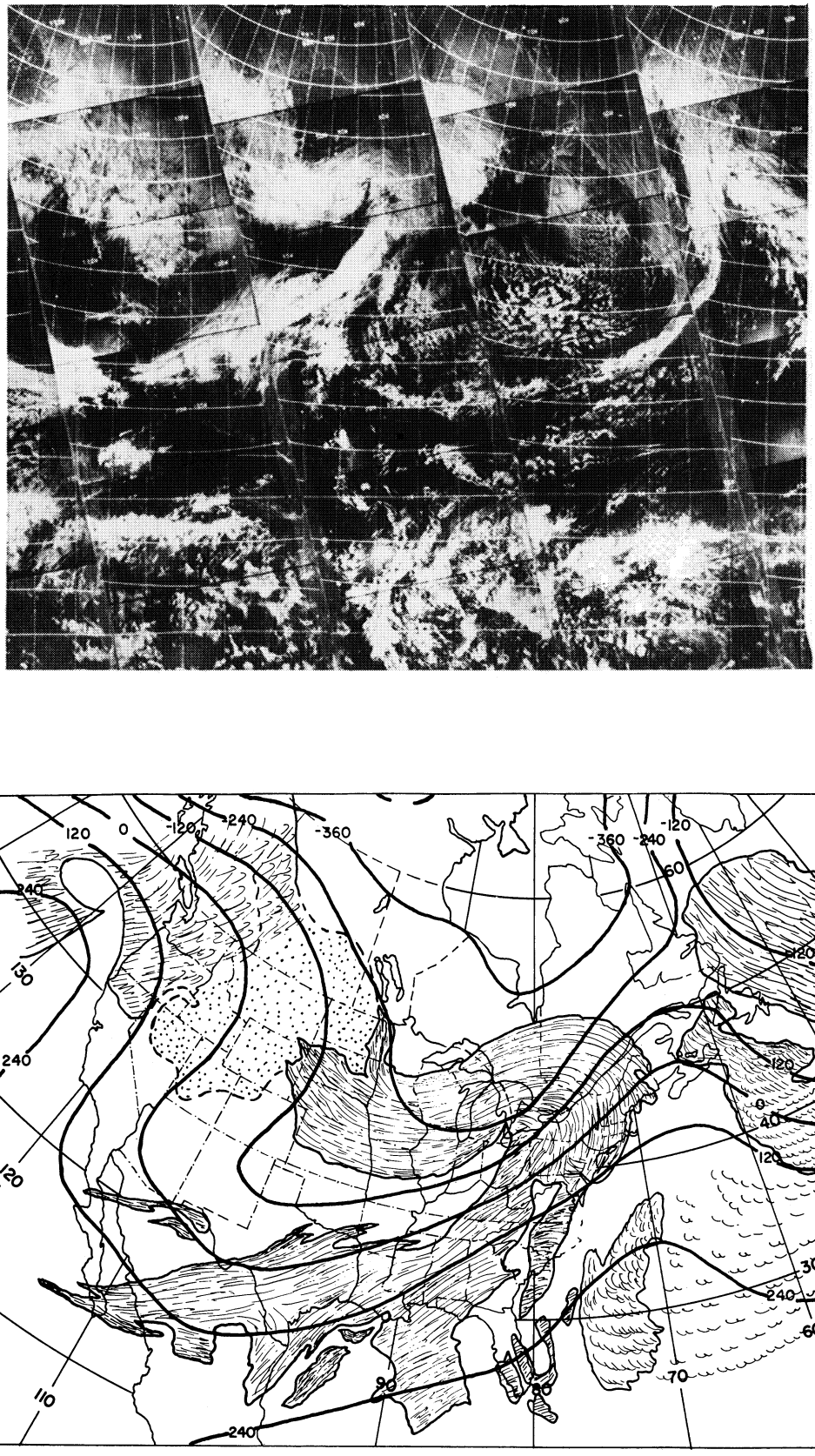

Fig. 4.3. Cloud montage and NMC 500 mb analysis for 00Z, 8 January 1967. (D values in meters.)

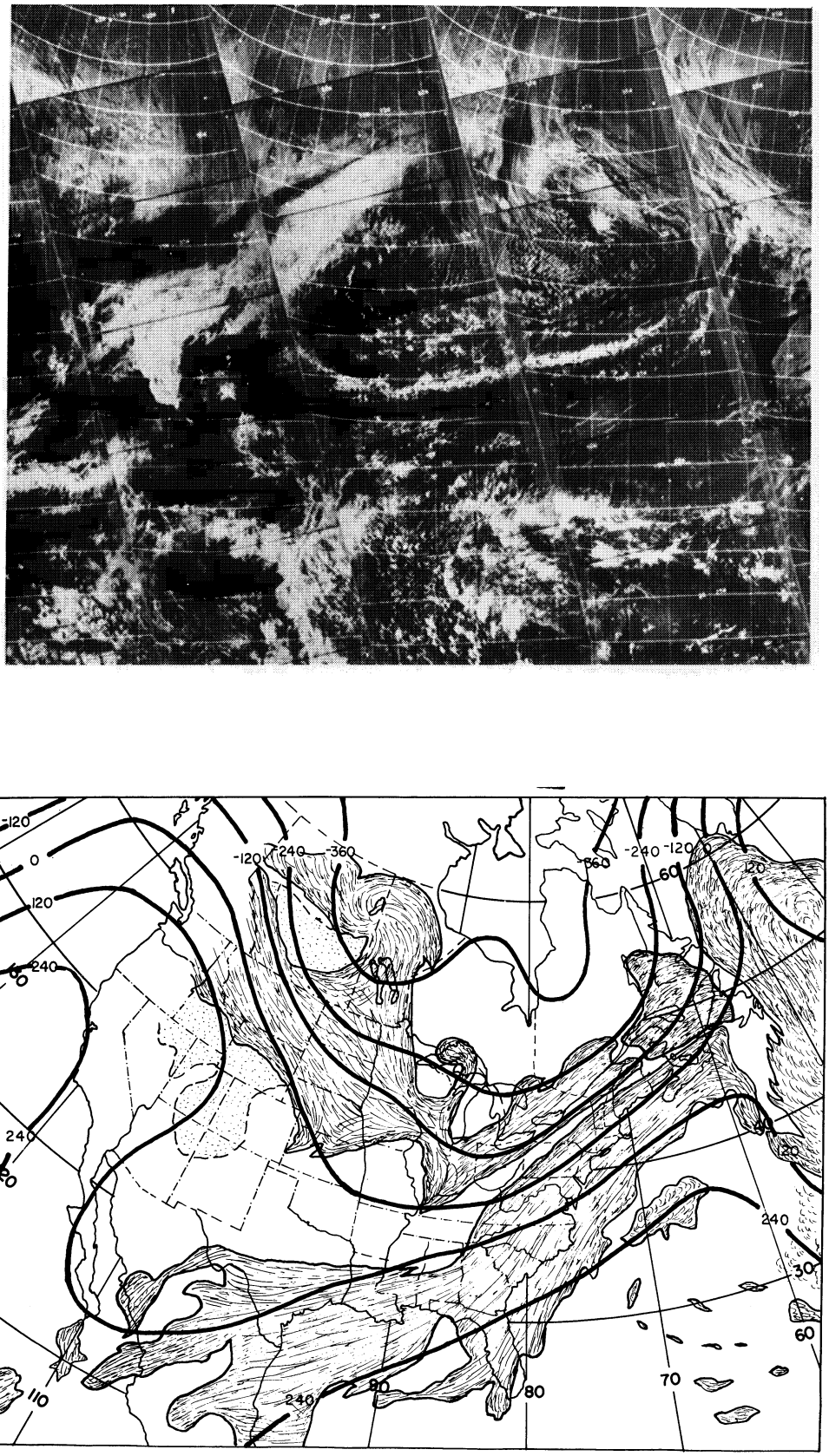

Fig. 4.4. Cloud montage and NMC 500 mb analysis for 00Z, 9 January 1967. (D values in meters.)

4.2.3 SINAP Analysis

The tendency fields derived with the thirty-six-hour forecast, the twelve-hour forecast, and the final NMC analysis are depicted for each date. The reanalysis' tendency fields are not shown, with the exception of the reanalysis of the twelve-hour forecast for six January (dashed contours, Fig. 4.5). This single example is included to demonstrate the delicacy of the SINAP modifications with a first-guess field of good quality. Alterations for other trials can be readily inferred from a comparison of the original tendency fields with the final NMC version. Areas of more significant change will be discussed in the text. The reanalysis subregions are outlined in the figures. For programming convenience these are rectangular, although in all trials only portions of the tendency field within the subregion were altered.

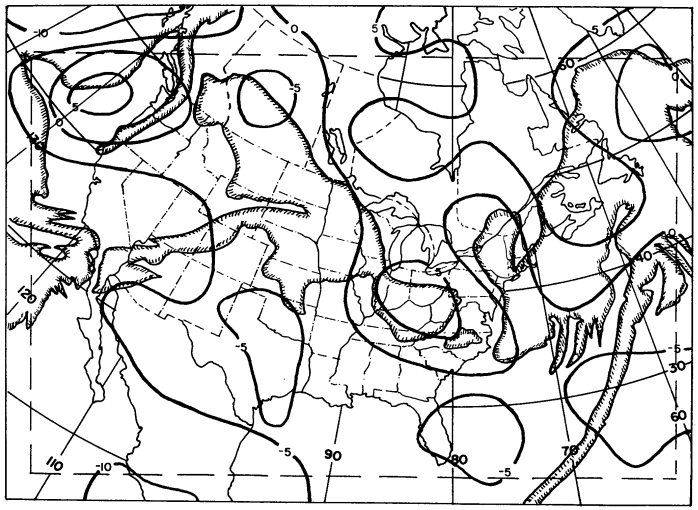

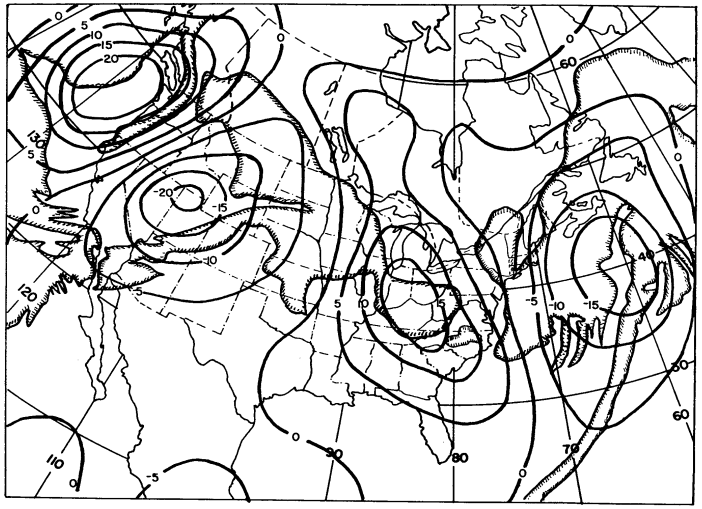

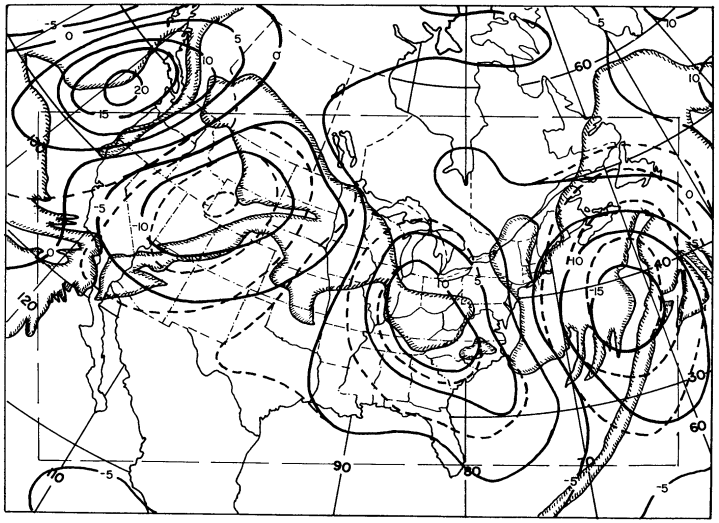

Fig. 4.5. Gross tendency fields for 00Z, 6 Janauary 1967. Upper left: Tendencies from thrity-six hour forecast. Lower left: Tendencies from twelve hour forecast. Above: Tendencies from NMC analysis. Units are decameters per twelve hours.

6 January

It is immediately obvious that the tendencies from the thirty-six-hour forecast correlate poorly with the observed cloud cover (Fig. 4.5). For the mature system off the East Coast, the center of negative tendency is not beneath the major cloud shield but to the south ahead of the cold front. Negative tendencies for the short wave in the northwest are also ill-defined. Largely because of the configuration of the jet, a closed negative center was entered for the latter although the system is over the mountains and the clouds are not well developed. Snow cover also provides a generous source of obfuscation. The large area of negative tendencies in the lower left-hand corner of the map was partially reduced to contrast with the system visible in the cloud photographs. This region is a desert of observational data, and the negative tendencies seem spurious. In all probability they are indicative only of the large uncertainty of both analysis and forecast in the Pacific. The ridging ahead of the jet stream present in the original tendency field was expanded in the reanalysis to penetrate farther in the direction of the frontal cloud band.

Very modest changes were made to the twelve-hour forecast first guess. The negative tendency maximum was extended to the north in the eastern system and the magnitudes ahead of the cold front were reduced. In the western vortex the negative values were slightly moderated over South Dakota and Nebraska while the center was extended to the southwest. Positive tendencies were introduced in the clear area over northern California. This reanalysis proved to be only a slight improvement on the original

guess field, largely because it considered mainly the orientation of the field. The NMC tendency field shows that the orientation of the first guess is quite good, but the magnitudes in all centers are low. In this sense the reanalysis technique is deficient. It cannot discriminate changes in magnitude of approximately forty percent, as indicated here. Day-to-day continuity of the tendency field is of some help in determining magnitudes, but the fields previous to this date were not available in this work.

Casual inspection of the NMC tendency field in Figure 4.5 shows that there is not a one-to-one correlation between clouds visible in the satellite photographs and areas of negative tendency. There is considerable cloud in the exact center of an area of positive tendency. It is most likely that this cloud is low level, generated orographically by the Appalachian chain. This type of abberation is unavoidable in working over continental areas.

For this one date the thirty-six-hour forecast height field and its associated instantaneous tendencies are given in Figure 4.6. These are included to further clarify the role of the previous analysis in the gross-tendency technique and also to point out that the thirty-six-hour forecast is not as poor as it may appear from its gross-tendency field. Although there is obviously room for improvement in this forecast, the correspondence of these fields with the observed cloud formations is distincly superior to that of the gross-tendency field (Fig. 4.5).

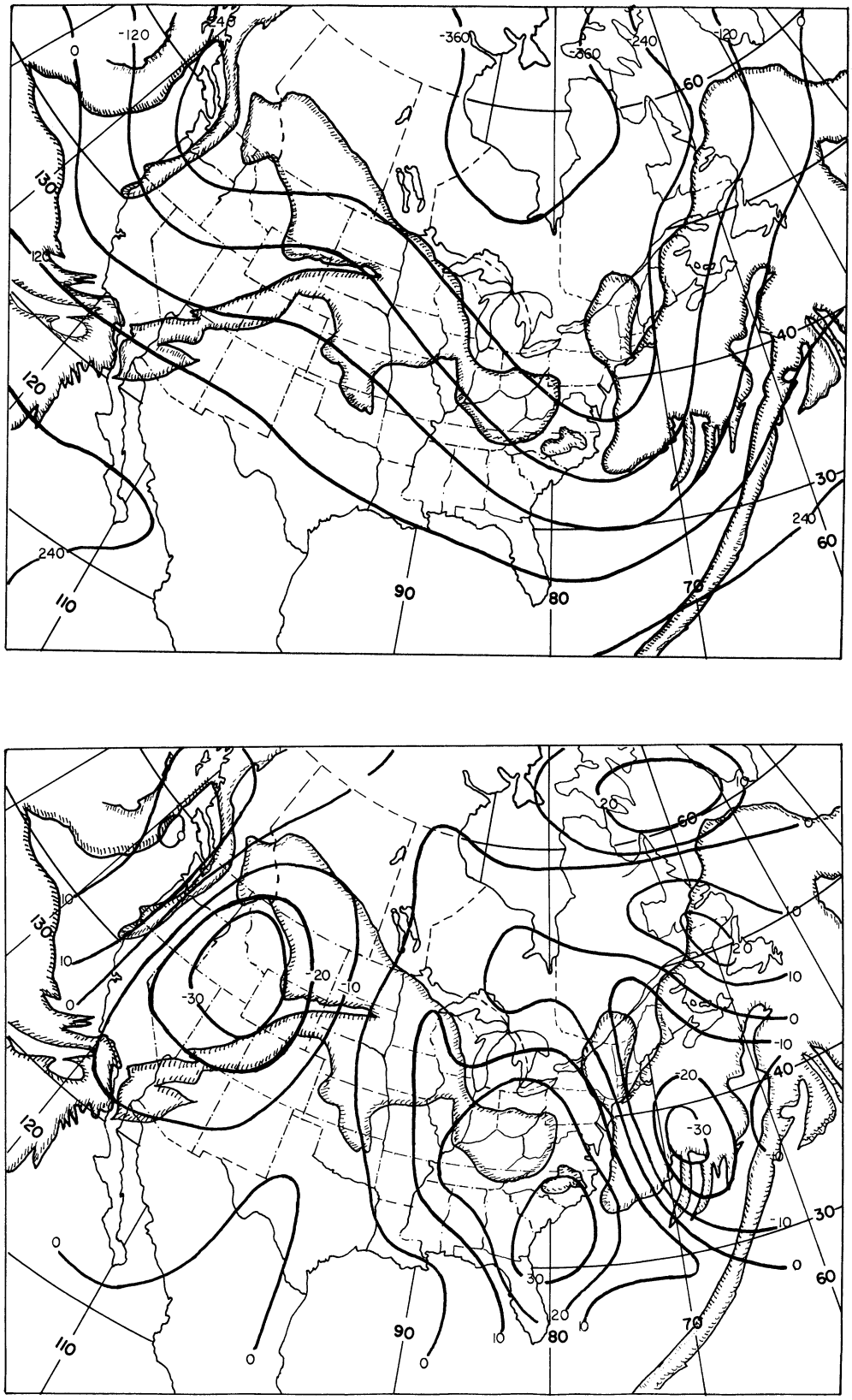

Fig. 4.6. NMC thirty-six hour forecast valid at 00Z, 6 January 1967 and associated instantaneous tendency field. Top: D value heights in meters. Bottom: Tendencies in arbitrary units.

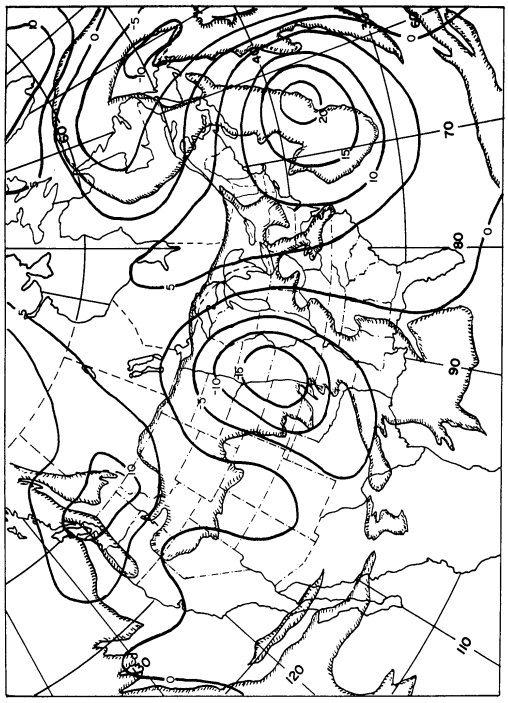

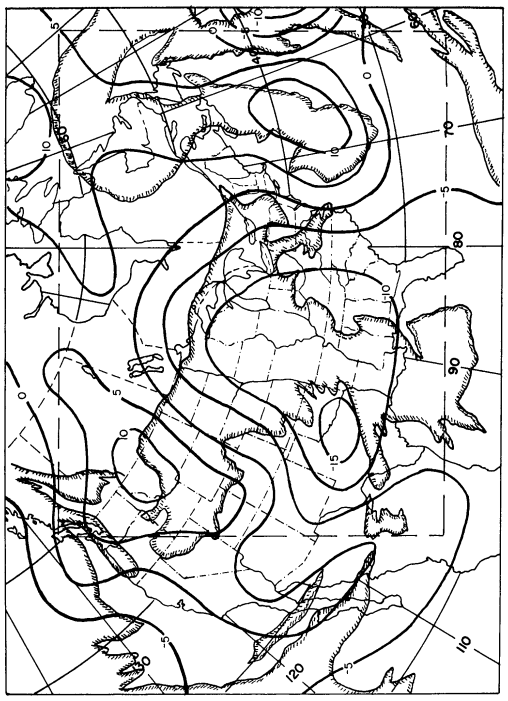

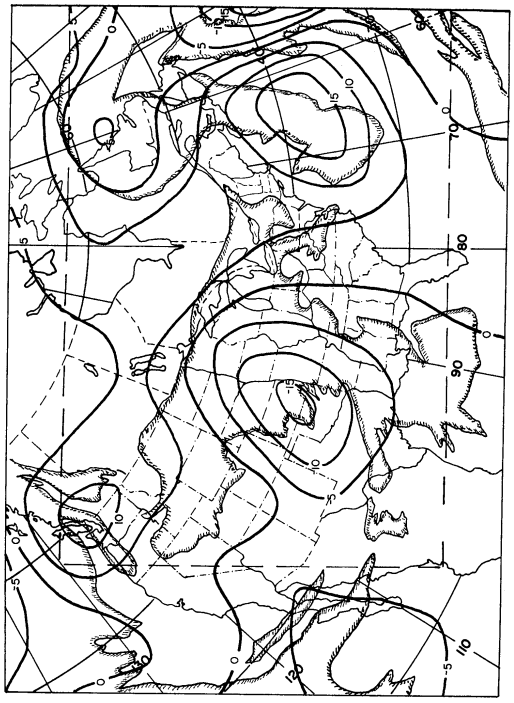

Fig. 4.7. Gross tendency fields for 00Z, 7 January 1967. Upper left: Tendencies from thirty-six hour forecast. Lower left: Tendencies from twelve hour forecast. Above: Tendencies from NMC analysis. Units are decameters per twelve hours.

7 January

Reanalysis on this date is concerned with both systems treated on the sixth. The thirty-six-hour forecast's tendency field (Fig. 4.7) fails to define the system centered over Newfoundland. A center of negative values was added in accordance with the cloud cover. The vortex over the Plains States is indicated in the original field but was reshaped to correspond to the cloud shield which has fully developed since the previous pictures. No modification was made in the area of positive tendencies off the Atlantic coast despite the presence of cloud here. The shapes of the two vortices require this to be an area of positive change. It is suggested by NESC that this cloud consists of cumulus caused by heating of the surface layer over the Gulf Stream.

The twelve-hour forecast field again offers little room for improvement. The major area of cloud over Newfoundland suggested intensification of the negative tendencies there with some moderation of the strong negative values along the eastern edge of the map. The negative tendencies were also slightly decreased over the Texas Panhandle, which lies in clear air. Due to the scarcity of observations west of the Baja Peninsula, no changes were made in what appears to be an area of erroneous negative values. This is again related to the difficulty of forecasting in the Pacific, and this maximum was reduced by all analysis systems.

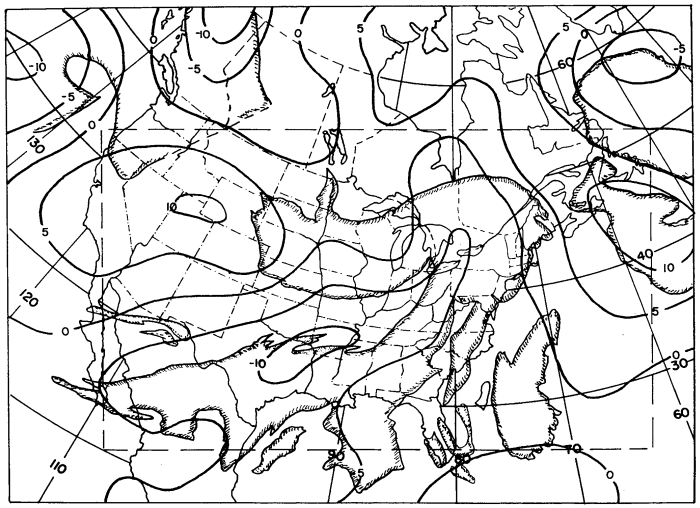

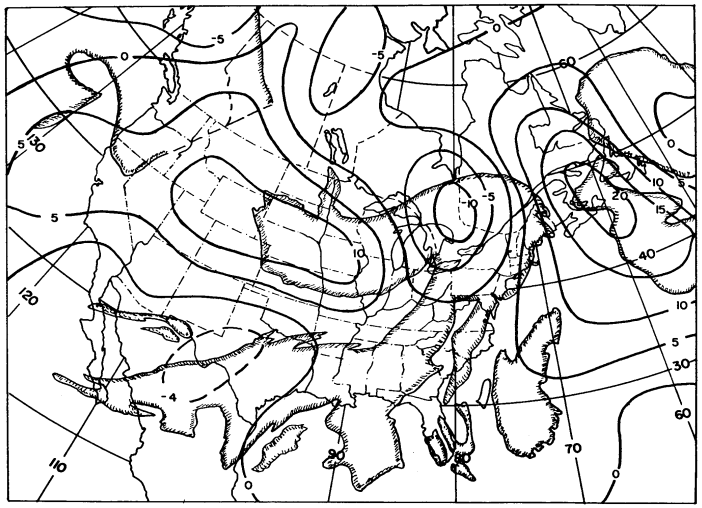

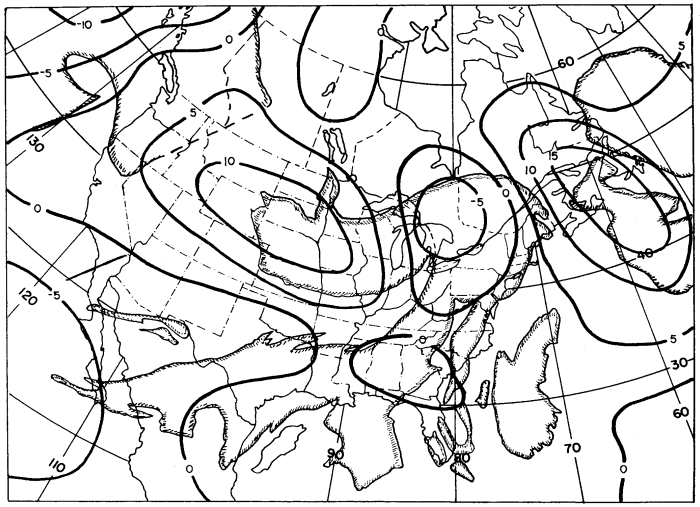

Fig. 4.8. Gross tendency fields for 00Z, 8 January 1967. Upper left: Tendencies from thirty-six hour forecast. Lower left: tendencies from twelve hour forecast. Above: Tendencies from NMC analysis. Units are decameters per twelve hours.

8 January

By picture time on this date the decaying cyclone in the Atlantic has moved east of the analysis area. The large storm over the Midwest has just passed maturity, although this is not well depicted in the photographs (note that the clear tongue which penetrates the central vortex in the classical model is not well defined here (Fig. 4.8)). In consequence, reanalysis of the thirty-six-hour forecast's tendency field was concerned exclusively with the Midwest cyclone, and the negative area south of Greenland was not altered. The most obvious changes were made in the center of the vortex. The positive tendencies ahead of the system were better defined and those present over Utah, Colorado, and Wyoming were extended to the southwest into the clear tongue, although not to the extent present in the NMC field. The bright clouds over Missouri are somewhat misleading, as is the heavy snow cover in the Western States. A modest wave was retained over Texas, with a corresponding decrease in negative values to the northeast, although the tendencies in the broad frontal area were nowhere changed to positive as depicted in the NMC field.

The twelve-hour forecast was not altered. Although there was some dissatisfaction with the treatment of the minor wave over Texas, and again with the area west of the Baja Peninsula, the cloud photographs did not seem to justify a reanalysis.

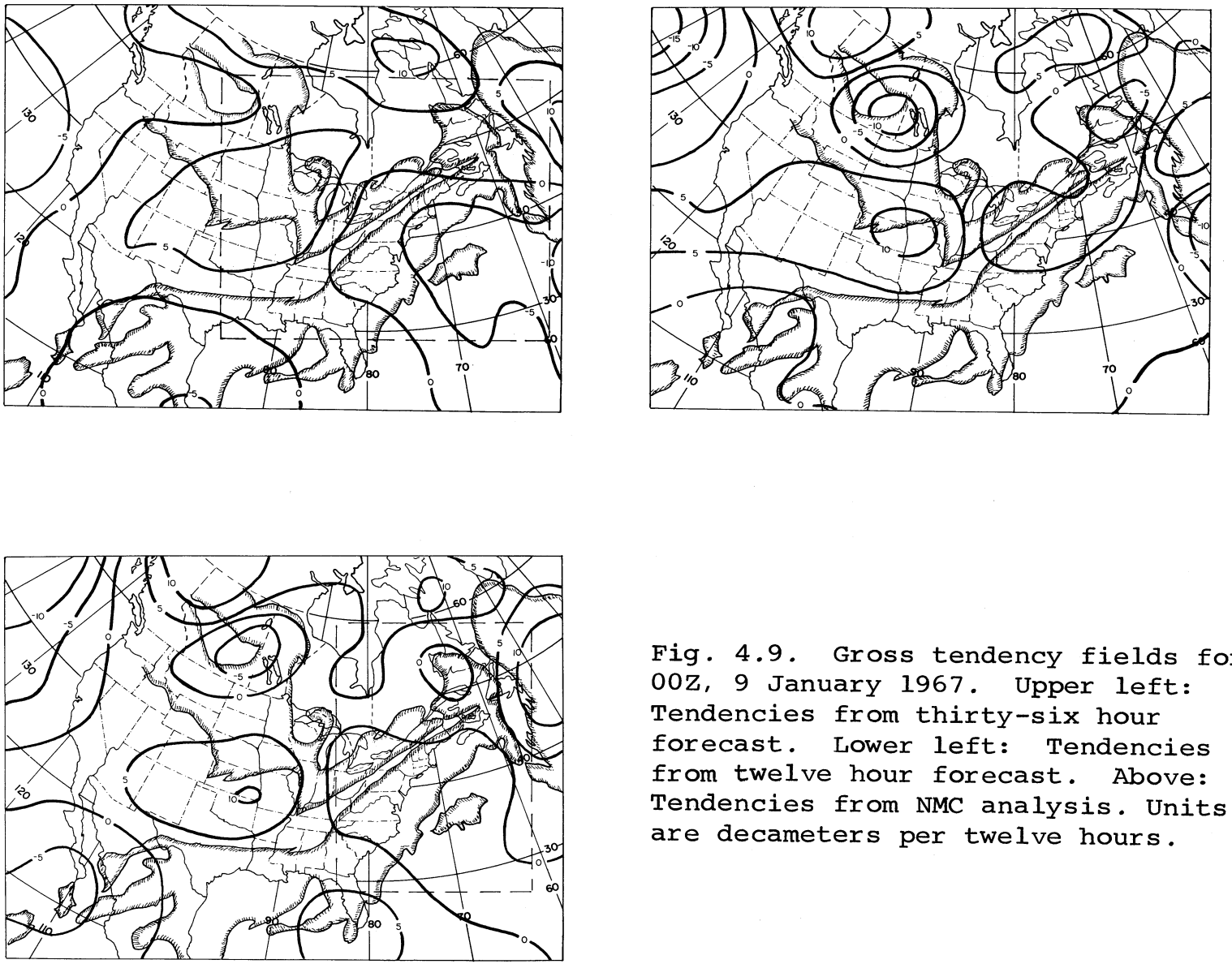

Fig. 4.9. Gross tendency fields for 00Z, 9 January 1967. Upper left: Tendencies from thirty-six hour forecast. Lower left: Tendencies from twelve hour forecast. Above: Tendencies from NMC analysis. Units are decameters per twelve hours.

9 January

By this date the short-wave system has crossed the United States and weakened noticeably. The major feature identifiable in the satellite photographs is the broad frontal cloud lying parallel to the axis of the deformed major trough (Fig. 4.4). The central vortex is not well defined, partly due to its filling and partly due to poor coverage in the cloud photographs. Alterations were made in the thirty-six-hour forecast's tendency field to reduce the area of negative tendencies east of the front and to introduce a negative center over the cloud vortex (Fig. 4.9). In addition, the negative tendencies west of Hudson Bay were extended to a center over Manitoba/ Saskatchewan to conform with the new vortex visible in the photographs.

Reanalysis of the twelve-hour forecast was very similar to that performed above. The negative center over Newfoundland was intensified and the negative area ahead of the frontal band eliminated. No changes were made in the western vortex.

4.2.4 Verification

Statistics

Although there is some day-to-day variation,[1] the

---

[1]The largest discrepancy is in the TCC for 9 January, twelve-hour forecast first-guess vs. NMC analysis. The value is 0.39 as compared with values over 0.90 for the other three days. This single value, which is computed over an area largely east of the continent, makes it appear that the first guess over the continent (Case I) is poorer than the first guess over the Atlantic (Case II). In actual fact the opposite is true.

verification statistics are sufficiently similar to permit presentation as a four-day average. They are subdivided according to the source of the reanalysis (36-hour forecast reanalyzed guess, 12-hour forecast reanalyzed guess, 36-hour forecast guess with bogus, 12-hour forecast guess with bogus) and the objective analysis system employed (A1-origional or A2-modified). Even with the averaging process there remains a burdensome quantity of numbers, which are presented in Tables C.1 through C.6 in Appendix C. The major features of these statistics are discussed below.

The effectiveness of the reanalysis technique in improving the guess field is best portrayed by a comparison of the original and reanalyzed guess fields with the final NMC product. The relevant statistics are given in Table 4.1. From this table it is possible to conclude that SINAP reanalysis is moderately successful, particularly with respect to the tendency itself. The twelve-hour change in the geostrophic wind (or the tendency gradient field) is more difficult to improve, especially in magnitude. This is almost certainly because the reanalyses stress the patterns rather than the magnitudes in the tendency changes. With this technique there is no way to reliably estimate the high gradients typical of the tendency centers, and errors here contribute greatly to the SRMS, SCC, and DCC. Precisely the same conclusions are indicated by the statistics which compare the final products of the analysis systems used here with their respective original and reanalyzed guess fields (see Appendix C).

The more challenging problem of verification is the effectiveness of the reanalysis technique in improving the final product, especially as a function of observation

TABLE 4.1

ORIGINAL AND REANALYZED GUESS FIELDS COMPARED WITH FINAL NMC ANALYSIS (JANUARY)

	36 ORIG	36 REAN	12 ORIG	12 REAN
SRMS	7.7	7.0	4.5	4.7
SCC	0.36	0.51	0.73	0.74
DCC	0.24	0.45	0.59	0.61
TRMS	66	40	31	23
TCC	0.48	0.80	0.75	0.88

density. As discussed previously, this aspect was investigated by the creation of artificially sparse-data networks. For this case, six objective analyses were made with each analysis model for each date. Requirements for data selection were constructed as follows:

i) Six observations were selected to give approximate coverage to the entire analysis area with a minimum of overlap for the first scan (R = 5.9 gridlengths).

ii) Thirteen observations were selected to give coverage without overlap for the second scan (R = 3.6 gridlengths).

iii) Twenty-eight observations were chosen to provide coverage without overlap for the third scan (R = 2.2 gridlengths).

iv) Forty-eight stations were chosen to provide coverage without overlap for the final scan (R = 1.5 gridlengths).

v) Fifteen additional stations (to total sixty-three) were added to (iv). The extra stations were picked to approximate the criterion of (ii) with the further requirement that each be well separated from the other

forty-eight stations.

vi) All reporting stations were utilized. The total number of observations on each of the four dates was 164, 167, 180 and 171 respectively.

For each of the above, all data used in sparser analyses are included. In addition, for (i) - (v), every effort was made to select only those stations which reported on each of the four dates, and no "wind-only" reports were accepted. Obviously it proved impossible to meet all of the imposed regulations. Observations are not universally dense over the analysis region, and the western and southeastern portions could not fully meet density requirements beyond (ii). Also, the seventh and eighth of January fall on the weekend when there appears to be a distinct propensity for absenteeism among the Latin American reports. The forty-eight-station distribution is depicted in Figure 4.10.

Figures 4.11 and 4.12 give height-tendency, root-mean-square error (TRMS) as a function of station density for both analysis systems operating on the original and reanalyzed guess fields. The final NMC analysis is used as the standard for comparison. With regard to the unmodified analysis system (A1; top figures), the most striking feature is the hump at low station densities. This instability in the analysis system makes it impossible to define a station density threshold at which the reanalysis procedure loses its effectiveness ("threshold of effectiveness"). Beyond the region of instability the reanalysis is of no consequence with a first-guess field as good as the normal twelve-hour forecast, and it is of only slight benefit for a considerably inferior guess field (viz. The thirty-six-hour guess).

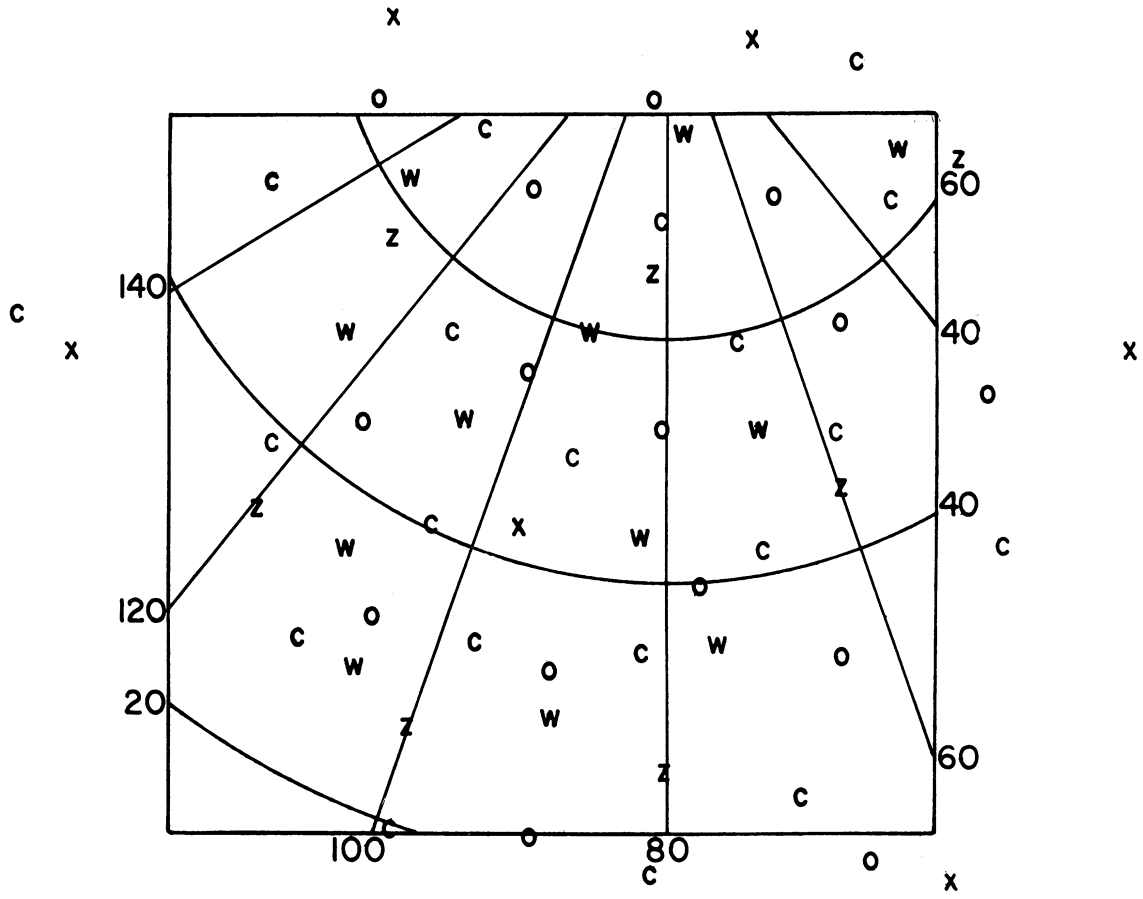

Fig. 4.10. Forty-eight station distribution for January case:

x - six station density
z - additions for thirteen station density
o - additions for twenty-eight station density
c - additions for forty-eight station density
w - stations withheld for ARMSE.

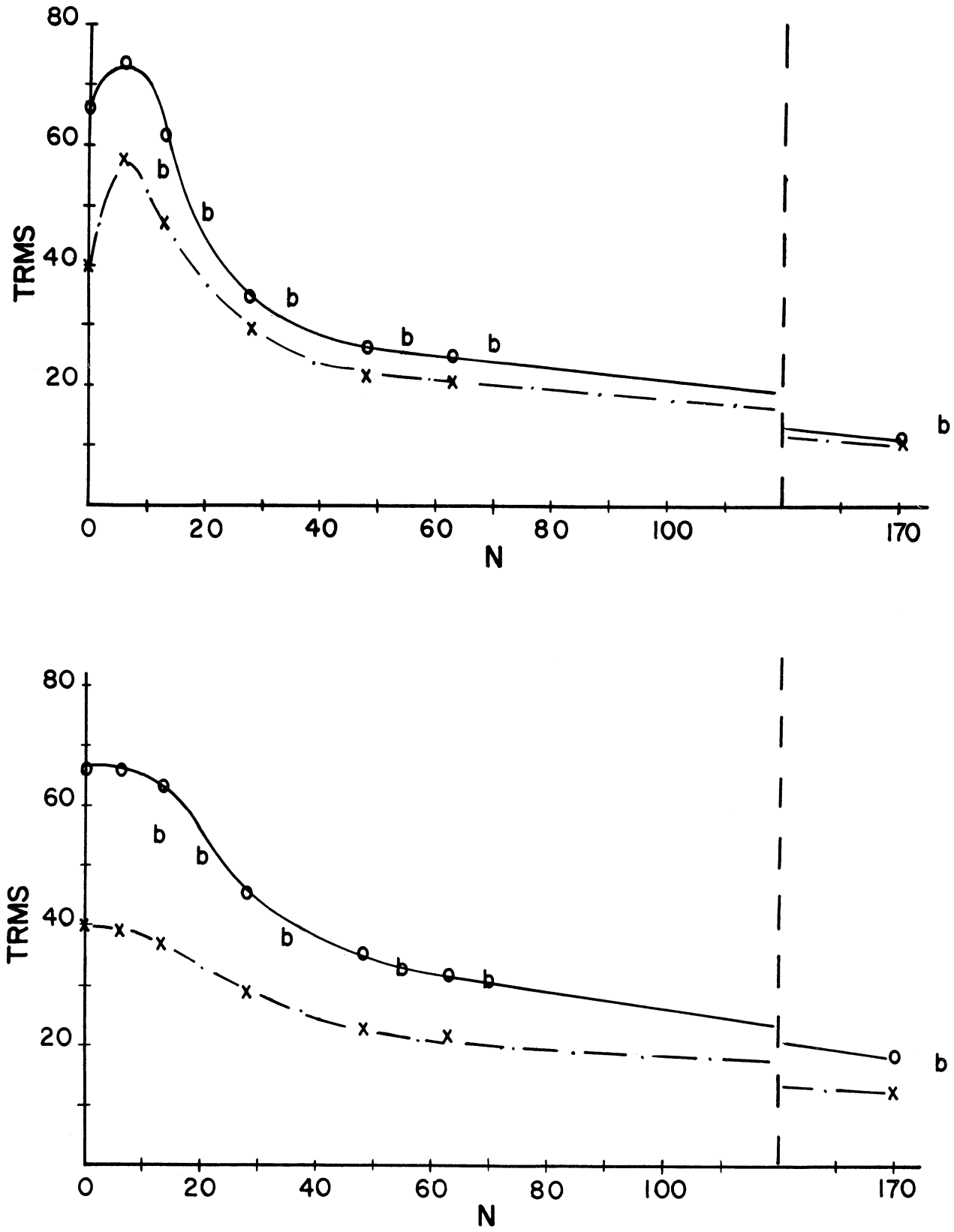

Fig. 4.11. TRMS for January case; thirty-six-hour forecast/reanalysis. Top: System A1. Bottom: System A2. o - original; x - reanalyzed guess; b - bogus input.

As discussed in Appendix B, the analysis system was tested and modified primarily to remove the instability at low station densities, but also to give more weight to the first-guess field. The statistics for the modified system (A2; bottom figures) show these results. Rather surprisingly, the quality of the first guess has quite limited influence on the reanalysis "threshold of effectiveness." For the normal twelve-hour forecast guess the twenty-eight-station analysis (approximately one report per fifteen gridpoints) is the obvious cutoff. For the thirty-six-hour forecast the point is less distinct though certainly not higher than the forty-eight-station analysis. This somewhat startling conclusion will be treated further at the end of this section.

Aside from the question of SINAP effectiveness the two analysis systems can be compared. With the normal twelve-hour forecast used as the guess field, beyond the instability the analyses are indistinguishable by this verification process. With the poor guess field, however, the modified system appears deficient at moderate station densities. (Fig. 4.11)[1] . The reason for this is that the modifications were designed only for good guess fields, primarily by the application of fairly stringent limits on the magnitudes permitted for individual corrections at a gridpoint (see Appendix B). Relaxation of these requirements would bring closer correspondence between the analysis systems operating

---

[1] The difference between the all-station A2 analyses from the 36-hour forecast and the reanalysis guess-fields (Fig. 4.11, bottom) comes from the southeastern portion of the analysis area where the density is rather low despite the inclusion of all reports.

with moderate data densities, but it would jeopardize the performance of A2 at low data densities. It is significant to note that the SINAP procedure removes the deficiencies of the modified system.

Reanalysis via the introduction of bogus station reports is still more difficult to assess by these verifications statistics. The mere presence of these reports destroys the uniformity which was constructed to evaluate the effects of station density. This difficulty not withstanding, the bogus station analyses are included in Figures 4.11 and 4.12. In general, this method is not effective. With the modified analysis system only slight improvement is obtained with the poor guess while no significant change is produced with the good guess fields. With the unmodified system the bogus stations appear to have a clearly negative effect on the poor guess field. This latter development is a good indication of the difficulty of working with pseudo station reports. For SINAP purposes these stations are necessarily chosen in active regions, usually in an area where the height-tendency field has an extremum. This in turn means that the stations are placed where the gradient of the height field is largest, and the inherent extrapolation error associated with "type-three" gridpoint corrections (see Appendix A) is certain to be maximum. The end result, except in regions of very dense data, is to unrealistically accentuate the height field such that the troughs are too deep and the ridges too sharp. Largely because of its careful attention to directional bias, the modified analysis system does not suffer these adverse effects to the same extent.

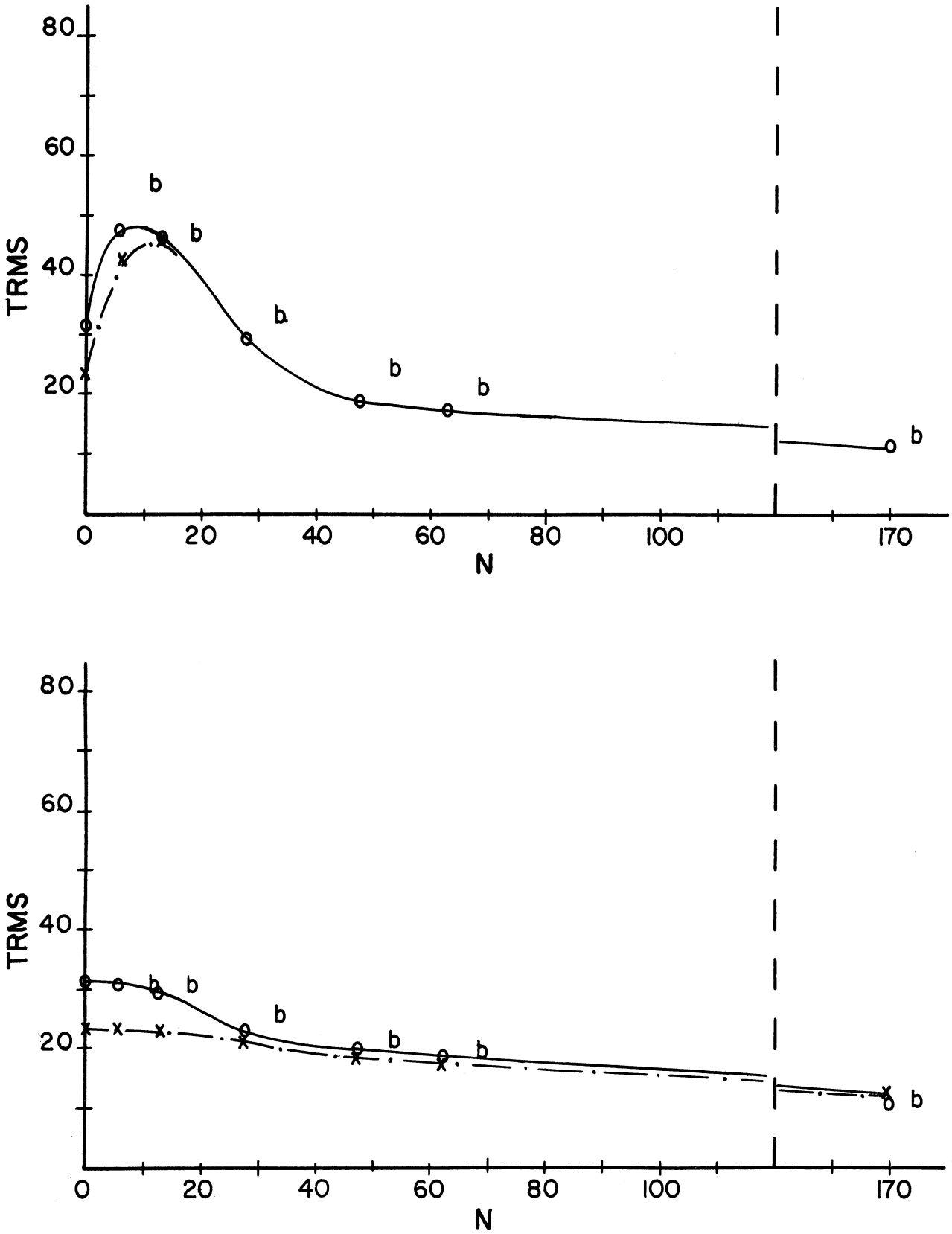

Fig. 4.12. TRMS for January case; twelve-hour forecast/ reanalysis. Top: System A1. Bottom: System A2. o - original; x - reanalyzed guess; b - bogus input.

The statistics computed for the gradient of the tendency field support the conclusions reached above. With respect to the effectiveness of SINAP, there appear to be no features which are sufficiently different from the results with the tendency field to merit special attention. Aside from the SINAP problem it is interesting to note that the gradient field is more sensitive to density changes than the tendency field itself. This aspect is common to both analysis systems.

It has been often said that statistics of the type used here are not necessarily meaningful. They can only compare two analyses, neither of which necessarily represents the true state of the atmosphere. This argument is irrefutable. It is only claimed here that the NMC analysis over North America is probably a fairly accurate representation of the actual 500-mb surface, and as such it has been used to establish a general evaluation of both the reanalysis procedure and the effects on the analysis system caused by varying the data density. It is of no consequence that the analyses performed here have not exactly duplicated the NMC product. There is a noise level associated both with the objective scheme and with the verification procedure which precludes perfect correspondence. A few statistics are reproduced in Table 4.2 to illustrate this point. The figures comparing the original guess fields with the final A1 analyses from these guess fields are practically independent of data density. Those which compare the final analyses to the NMC product indicate steady improvement with increasing density. A similar result can be found for the modified system in Appendix C. This seeming paradox suggests that the analysis or the verification procedure is approaching

TABLE 4.2.

12 HOUR FORECAST/REANALYSIS; SYSTEM A1; JANUARY CASE

	48 ST	63 ST	TOT
ANALYSIS FROM ORIG. GUESS VS. NMC ANALYSIS			
SRMS	3.7	3.5	2.6
SCC	0.84	0.86	0.91
DCC	0.64	0.72	0.75
TRMS	20	17	11
TCC	0.93	0.94	0.98
ANALYSIS FROM REAN. GUESS VS. NMC ANALYSIS			
SRMS	3.7	3.5	2.9
SCC	0.85	0.87	0.90
DCC	0.72	0.81	0.76
TRMS	19	17	11
TCC	0.93	0.94	0.98
ANALYSIS FROM ORIG. GUESS VS. ORIG. GUESS			
SRMS	4.4	4.5	4.6
SCC	0.75	0.76	0.76
DCC	0.59	0.59	0.55
TRMS	31	30	32
TCC	0.75	0.77	0.73
ANALYSIS FROM REAN. GUESS VS. REAN. GUESS			
SRMS	4.3	4.4	4.7
SCC	0.81	0.80	0.78
DCC	0.56	0.56	0.61
TRMS	25	25	25
TCC	0.85	0.86	0.85

the noise level at a density of only forty-eight stations. (approximately one station for 8 gridpoints). While it is not the purpose of this study to investigate the implications of this result with respect to the analysis or verification systems, it can be stated that the effects

of SINAP modifications can not be investigated by these statistics in regions with greater data density.

ARMSE

As discussed earlier, the areal-mean-error method of verification is an attempt to avoid the pitfalls associated with the more usual statistics. Tables 4.3 and 4.4 contain the results averaged over the four-day period for three sparse-data categories. The ARMSE is given for each scan of the analysis and is further broken down into the contributions from the stations used in an analysis (RETAINED) and from a selection of stations not used in the analysis (WITHHELD). (For the twenty-eight station category the analysis stations were too widely separated to permit an accurate estimate of their contribution.) The stations withheld in the case of the forty-eight and sixty-three-station analyses are shown in Figure 4.1.

The "original" and "final" columns in these tables measure respectively the improvement in the guess field and the effectiveness of the reanalysis in the final product. The results agree in general with those indicated by the verification statistics, although here reanalysis of the twelve-hour forecast appears inconsequential even at the first-guess stage. Reanalysis of the thirty-six-hour first guess improves the guess field but has varying impact on the final product depending on the analysis system used. With the unmodified system the improvement is negligible. With the modified system, the reanalyzed guess maintains the improvement in the final product. However, this final analysis from the improved guess is not better than the final

TABLE 4.3.

ARMSE FOR JANUARY CASE; 12-HOUR FORECAST (O), REANALYSIS (R), AND BOGUS WITH ORIGINAL (B)

ANALYSIS		ORIGINAL GUESS			SCAN 1			SCAN 2			SCAN 3			FINAL		
		O	R	B	O	R	B	O	R	B	O	R	B	O	R	B
A1	RETAINED	-	-	-	-	-	-	-	-	-	-	-	-	-	-	-
28 Station	WITHHELD	20	19	21	21	21	24	26	26	27	28	28	29	28	28	29
	ARMSE	-	-	-	-	-	-	-	-	-	-	-	-	-	-	-
A2	RETAINED	-	-	-	-	-	-	-	-	-	-	-	-	-	-	-
28 Station	WITHHELD	20	19	21	22	22	24	22	22	24	23	23	25	23	23	25
	ARMSE	-	-	-	-	-	-	-	-	-	-	-	-	-	-	-
A1	RETAINED	27	26	28	21	20	21	16	16	17	7	7	8	3	3	5
48 Station	WITHHELD	17	16	17	21	21	22	23	20	25	22	21	25	22	21	25
	ARMSE	33	30	33	30	29	31	29	28	31	24	22	27	23	21	26
A2	RETAINED	27	26	28	25	24	26	24	23	23	6	6	7	3	3	4
48 Station	WITHHELD	17	16	17	19	19	20	20	19	21	19	18	20	19	18	20
	ARMSE	33	30	33	32	31	33	31	31	31	20	20	22	19	19	21
A1	RETAINED	27	25	28	23	23	23	19	19	19	10	10	11	5	5	6
63 Station	WITHHELD	17	16	18	21	20	21	22	21	23	21	19	22	20	18	22
	ARMSE	32	30	33	31	30	32	29	29	30	23	21	24	21	19	23
A2	RETAINED	27	25	28	26	25	27	24	23	23	7	7	8	4	4	5
63 Station	WITHHELD	17	16	18	18	17	18	19	18	19	18	17	18	17	17	18
	ARMSE	32	30	33	32	20	33	30	29	30	19	19	20	18	17	19

analysis by the unmodified system on the unmodified guess. The introduction of bogus stations is again ineffective. These results are not especially surprising in the light of what has been discussed above. As with the statistics, the ARMSE is incapable of detecting SINAP modifications above the "saturation density" of forty-eight stations.

Close inspection of the scan-by-scan contributions of the withheld stations in the unmodified analysis system (A1) indicates that the early scans actually increase the errors in the twelve-hour forecast first guess. This conclusion must be viewed with some caution as these withheld stations were almost surely included in the analysis from which the first guess field was forecast, and so their errors are most probably not indicative of the largest errors in the guess field. However, the conclusion seems valid, since the destructive nature of the early scans was independently demonstrated by the test described in Appendix B.

Just as the verification statistics are not ideal, so too the areal-mean method has its drawbacks. Chief among these is its insensitivity to small-scale features. By definition the number of withheld stations must be kept small, and frequently the small, active systems, which are only poorly defined in an analysis, are not represented in the final statistic. The changes introduced by reanalysis of the twelve-hour forecast guess fields for this case are not as slight as the ARMSE would indicate. Furthermore, as discussed above, the verification statistics imply that the moderate density analyses from A2 operating on the thirty-six-hour guess are inferior to their counterparts obtained with the unmodified scheme. This difference is not clearly

TABLE 4.4.

ARMSE FOR JANUARY CASE; 36 HOUR FORECAST (O), REANALYSIS (R), AND BOGUS WITH ORIGINAL (B)

ANALYSIS		ORIGINAL GUESS			SCAN 1			SCAN 2			SCAN 3			FINAL		
		O	R	B	O	R	B	O	R	B	O	R	B	O	R	B
A1	RETAINED	-	-	-	-	-	-	-	-	-	-	-	-	-	-	-
28 Station	WITHHELD	35	28	35	29	28	32	30	27	32	31	28	33	31	29	34
	ARMSE	-	-	-	-	-	-	-	-	-	-	-	-	-	-	-
A2	RETAINED	-	-	-	-	-	-	-	-	-	-	-	-	-	-	-
28 Station	WITHHELD	35	28	35	31	28	36	31	27	33	30	26	31	30	26	31
	ARMSE	-	-	-	-	-	-	-	-	-	-	-	-	-	-	-
A1	RETAINED	37	29	38	30	25	28	20	19	21	8	8	10	4	4	6
48 Station	WITHHELD	40	30	41	31	25	32	27	24	28	25	22	25	24	22	25
	ARMSE	55	41	56	43	35	43	34	30	35	26	23	27	25	22	26
A2	RETAINED	37	29	38	31	25	35	26	19	24	6	6	8	4	4	5
48 Station	WITHHELD	40	30	41	36	25	37	32	24	32	29	22	27	29	22	26
	ARMSE	55	41	56	47	35	51	42	31	41	29	23	28	29	22	27
A1	RETAINED	38	28	38	29	24	27	21	19	20	11	11	12	6	6	7
63 Station	WITHHELD	41	28	42	30	20	32	27	24	28	27	22	25	23	22	24
	ARMSE	56	41	57	42	35	42	34	42	34	27	24	28	24	22	25
A2	RETAINED	38	28	38	35	27	38	26	20	24	8	8	9	5	5	5
63 Station	WITHHELD	41	28	42	29	29	41	33	25	33	28	23	27	27	23	26
	ARMSE	56	41	56	53	39	55	41	32	41	29	24	28	27	23	27

evidenced by the ARMSE.

4.3 Case II: Moderate Data Density, Atlantic, 10-16 May 1966

4.3.1 Introduction

This case was the first investigated during this work, and because of this some details of the January study were overlooked in the development. The discrepancies will be indicated in the following sections. The instantaneous tendency fields were used for all reanalyses performed during this period. In consequence almost every reanalysis required several trials, and it never proved possible to effect the precise changes that are straightforward with the gross-tendency technique. Since the period under consideration is in the spring, and also since the photographs are mainly over water, there is little confusion between snow and cloud cover. It will also be noted that the cloud systems in the photographs are better defined than those in the previous case. This difference is quite typical of the contrast in organization over oceans as opposed to that over land surfaces. All photographs have been rectified in time via the simple prediction model described earlier (Sec. 2.2).

4.3.2 Synoptic Discussion

The basic features of the circulation for this period are classical to meteorology. The long-wave features are virtually obscured by the rapid development and propagation of a series of cyclones along the polar front, much in the pattern of Bjerknes' (1951) original model. At the beginning of the period a minor surface wave is developing off

the East Coast in a region well known for cyclogenisis (Fig. 4.13). The development is reflected at the 500-mb level by a small thermal wave moving through the bottom of a major trough over the eastern half of North America. Farther to the east there is a second storm, just past maturity, which is associated in the upper levels with a typical depression northwest of Iceland. Between the eleventh (Fig. 4.14) and twelfth (Fig. 4.15) the western wave has reached maturity east of the Maritime Provinces. A deep and strongly baroclinic closed low is present at 500 mb over Newfoundland. The eastern system has filled considerably and moved to the southeast. By 00Z on the thirteenth (Fig. 4.16) the original wave has moved into the region of the Icelandic low replacing the original depression, which has lost its identity. The second system is still well defined but has also begun to weaken. A new thermal trough has developed at 500 mb over the Midatlantic States with an associated surface wave over the New England coast. For the next two days, the latter system develops as it moves up the front, (Fig. 4.17), but to a much lesser extent than its predecessor. At 00Z on the fifteenth (Fig. 4.18) the 500-mb trough has only a single closed isopleth. The previous system has stalled and filled in the Icelandic low. By the end of this period the second wave cyclone has replaced the first southeast of Greeland and begun to fill. Yet a third wave is developing off Cape Hatteras with a well-defined short wave aloft (Fig. 4.19).

Fig. 4.13. Cloud montage and NMC 500 mb analysis for 00Z, 10 May 1966. (D values in meters.)

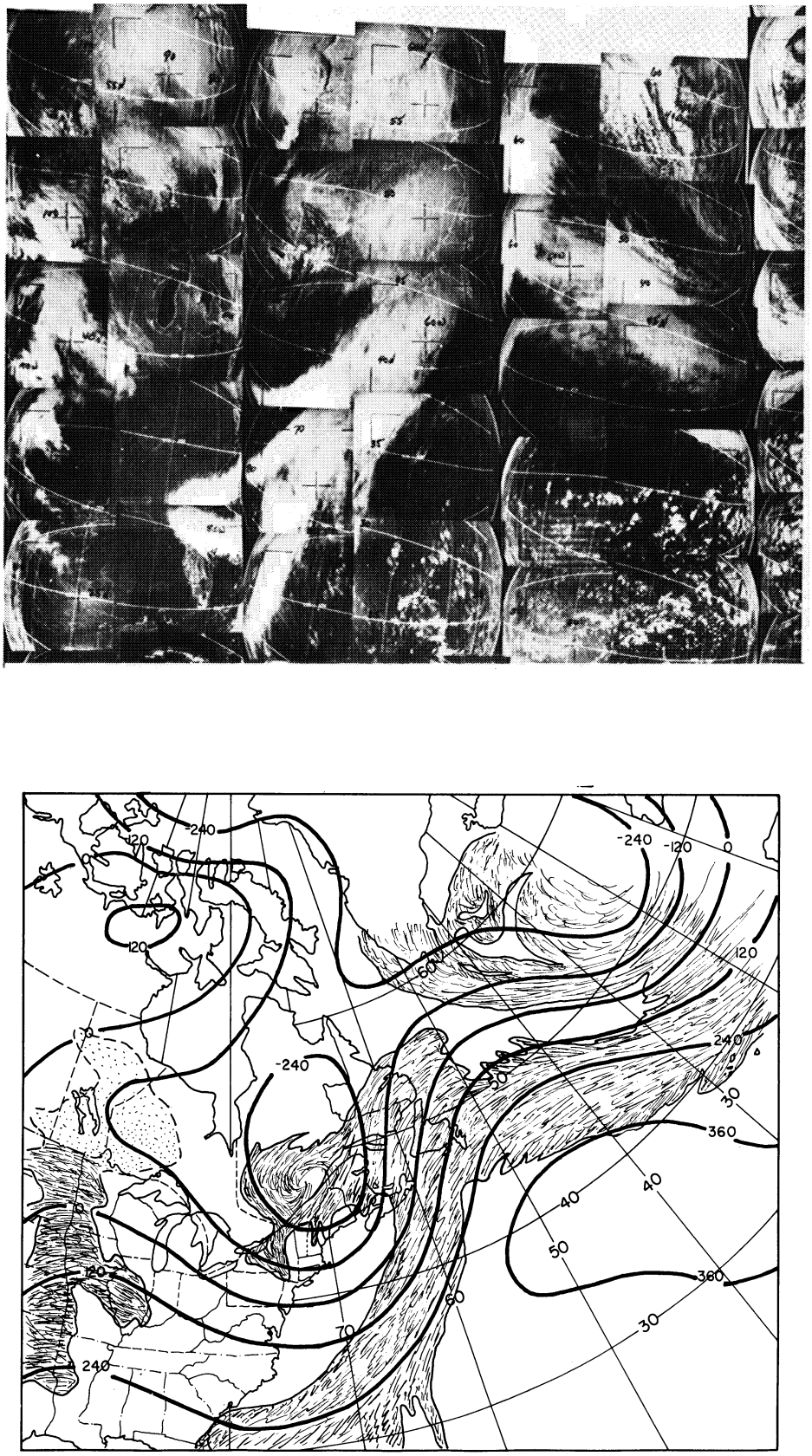

Fig. 4.14. Cloud montage and NMC 500 mb analysis for 00Z, 11 May 1966. (D values in meters.)

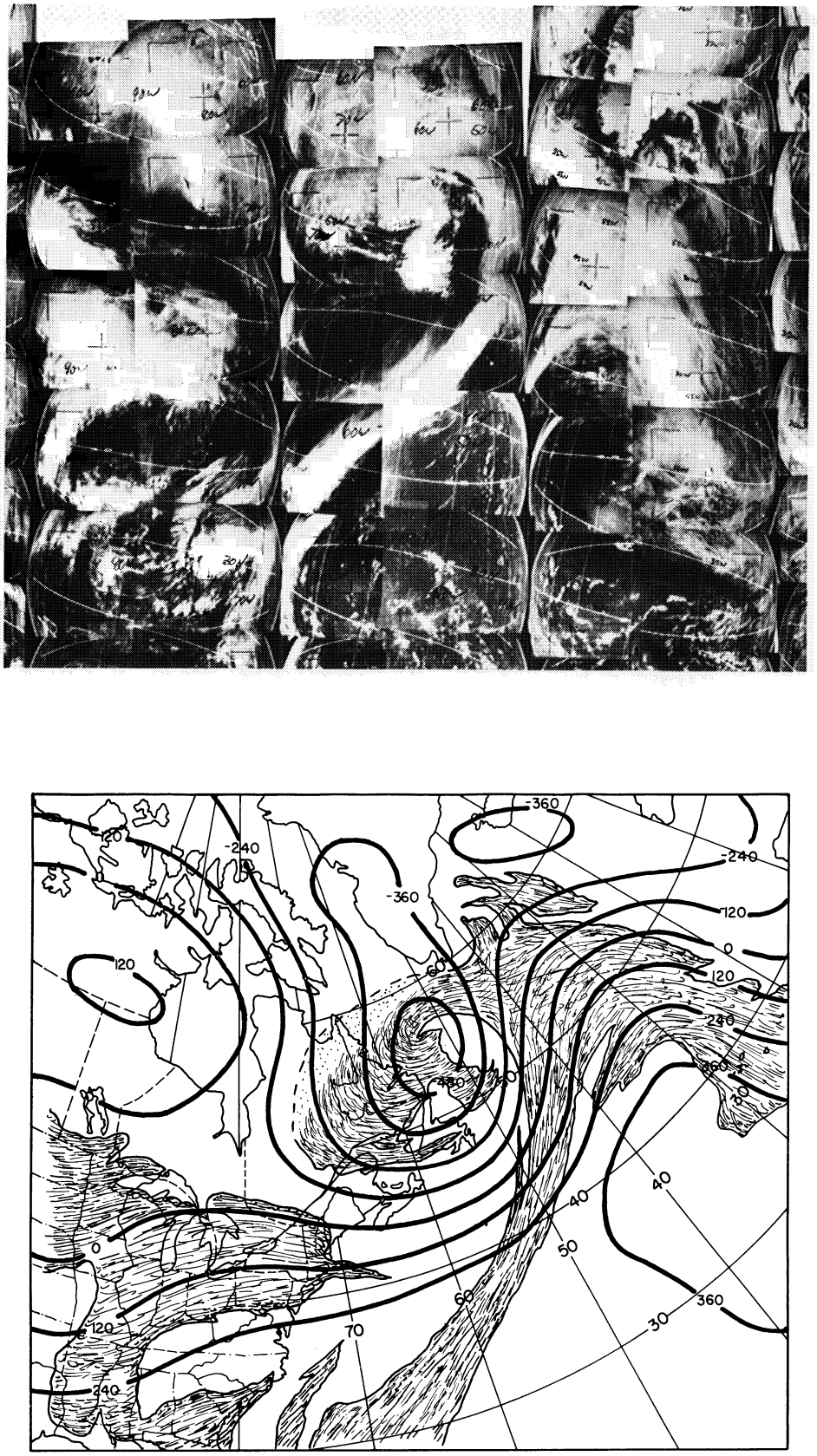

Fig. 4.15. Cloud montage and NMC 500 mb analysis for 00Z, 12 May 1966. (D values in meters.)

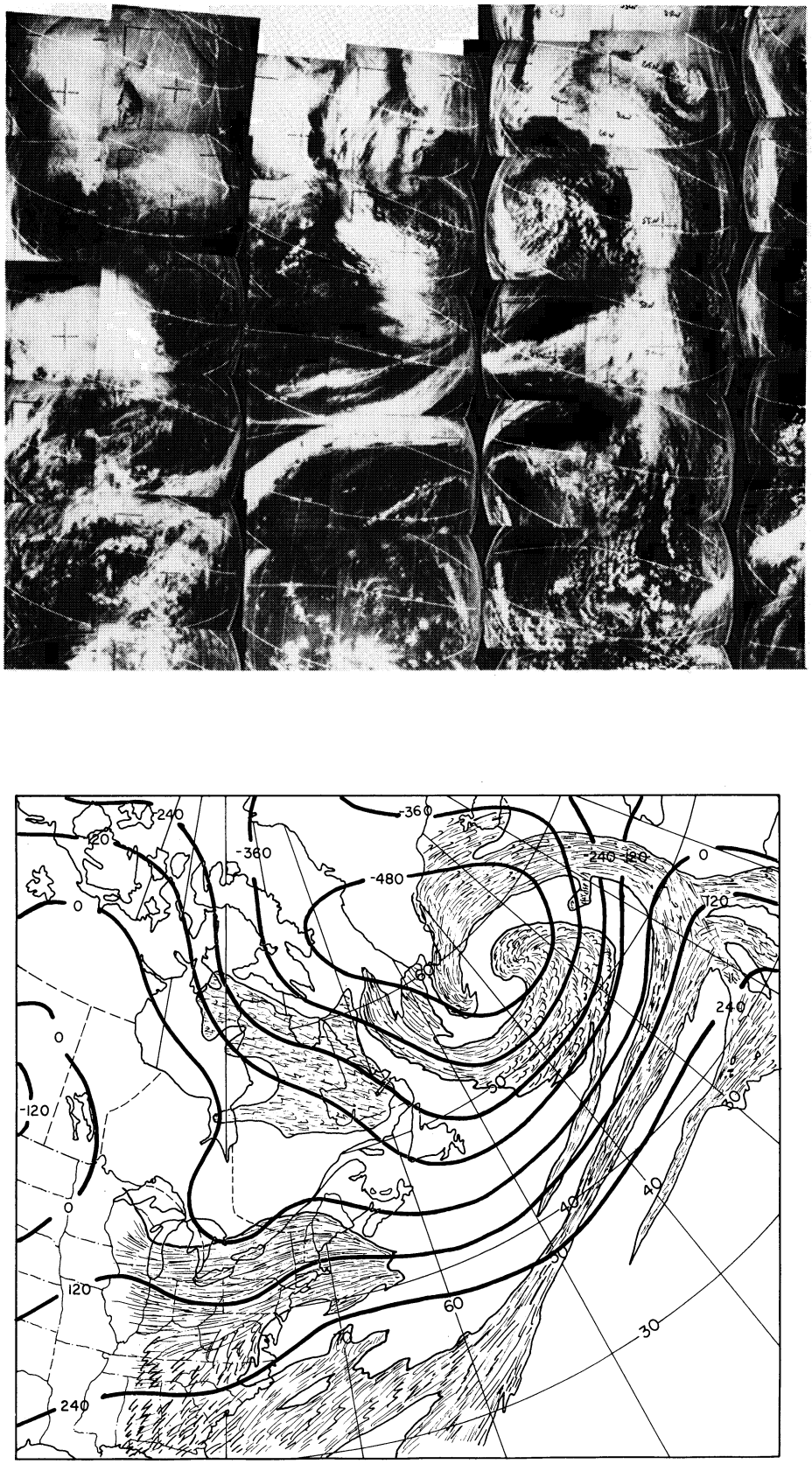

Fig. 4.16. Cloud montage and NMC 500 mb analysis for 00Z, 13 May 1966. (D values in meters.)

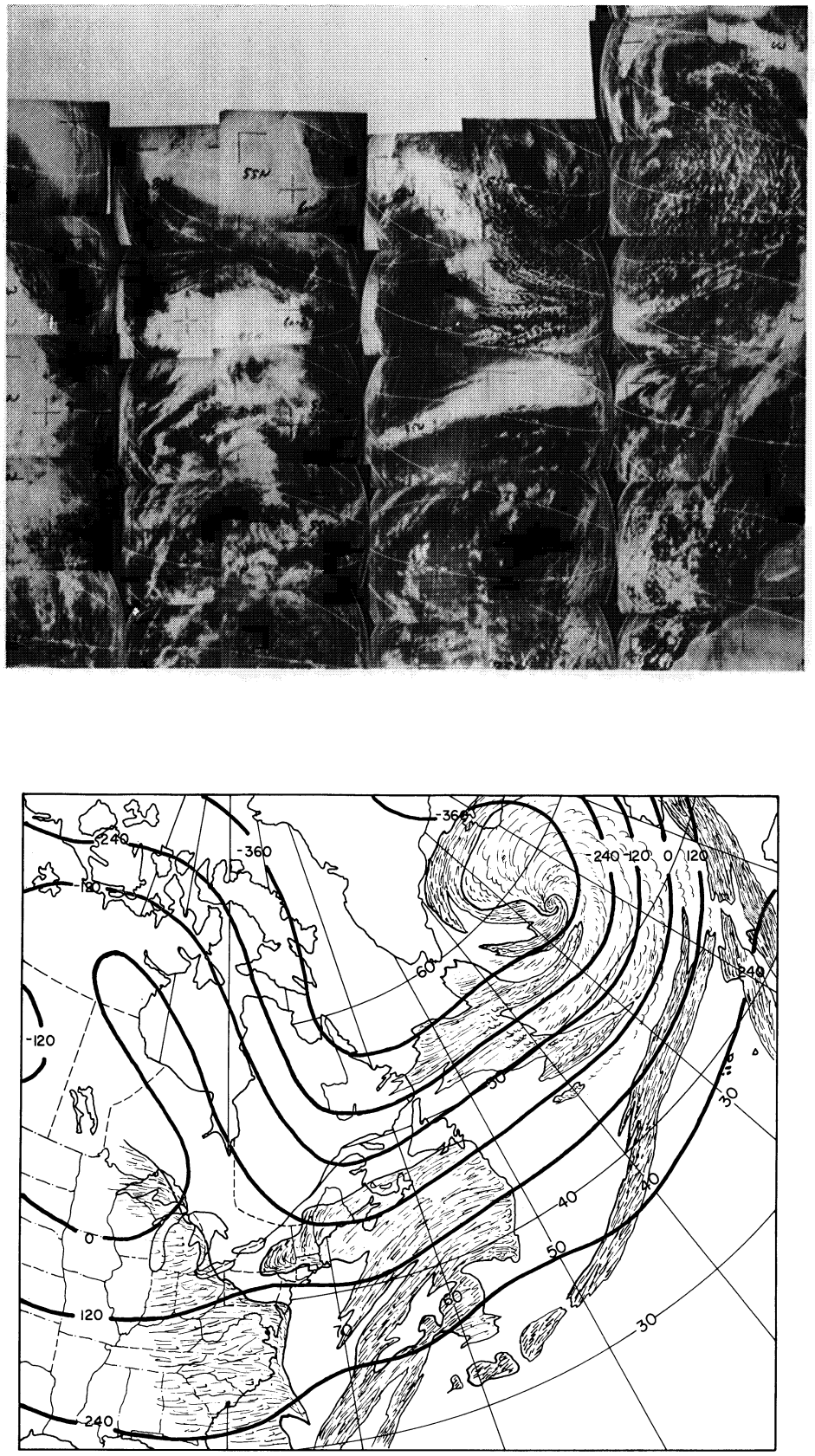

Fig. 4.17. Cloud montage and NMC 500 mb analysis for 00Z, 14 May 1966. (D values in meters.)

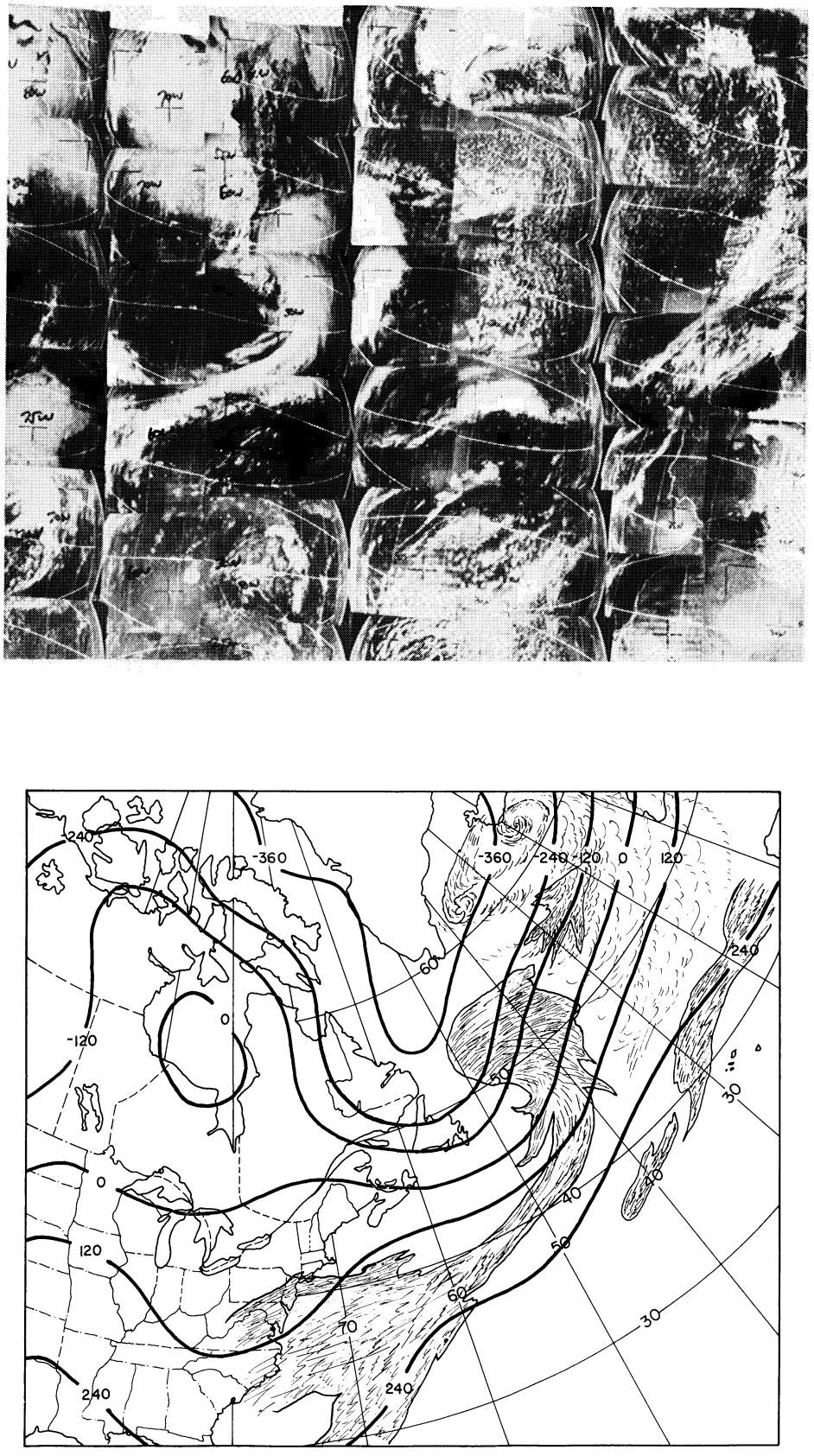

Fig. 4.18. Cloud montage and NMC 500 mb analysis for 00Z, 15 May 1966. (D values in meters.)

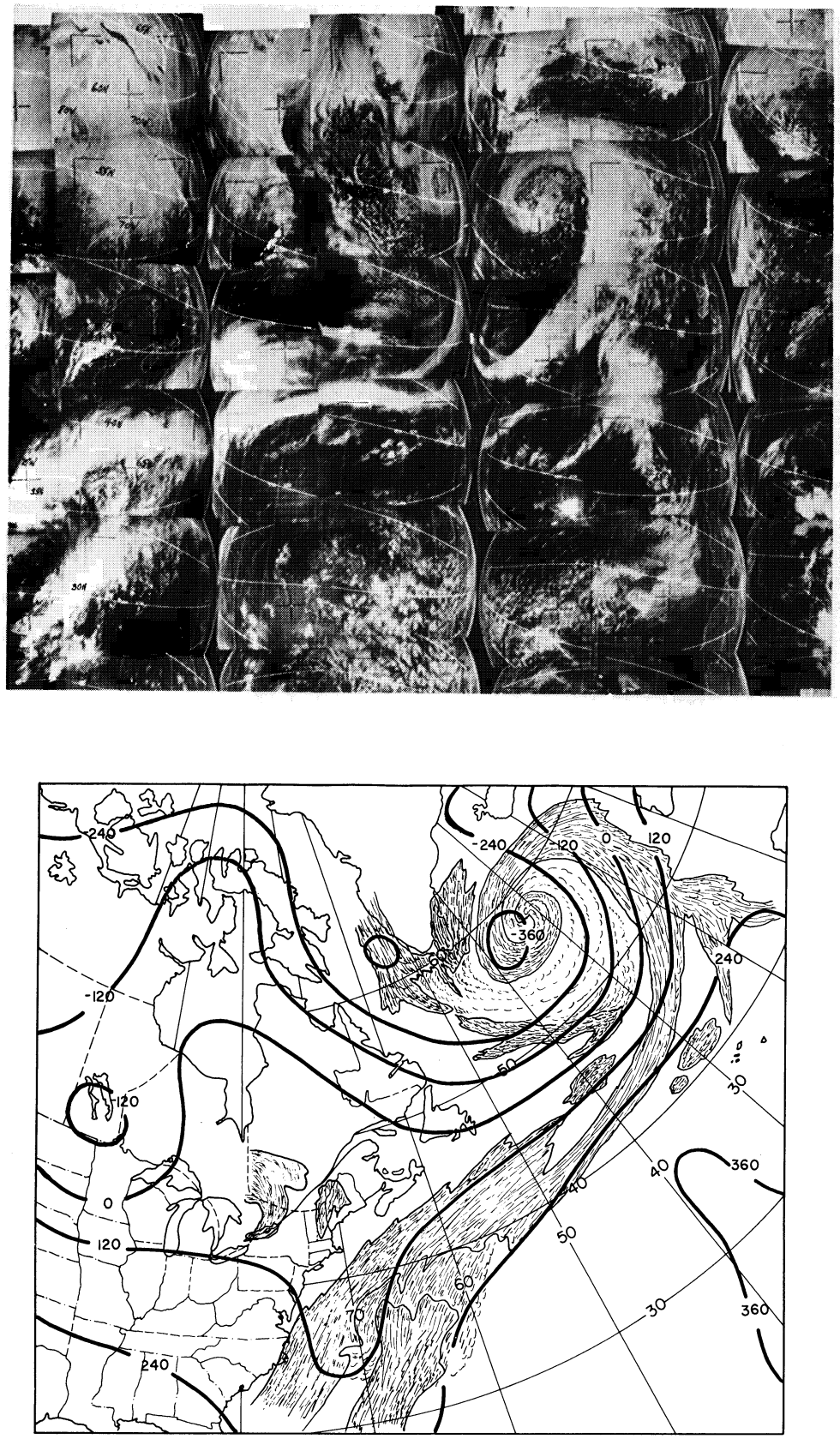

Fig. 4.19. Cloud montage and NMC 500 mb analysis for 00Z, 16 May 1966. (D values in meters.)

4.3.3 SINAP Analysis

The instantaneous tendency fields from the NMC twelve-hour first guess and NMC final analyses are depicted for each date. Again the reanalyzed tendency fields are not given but areas of major revision will be briefly described.

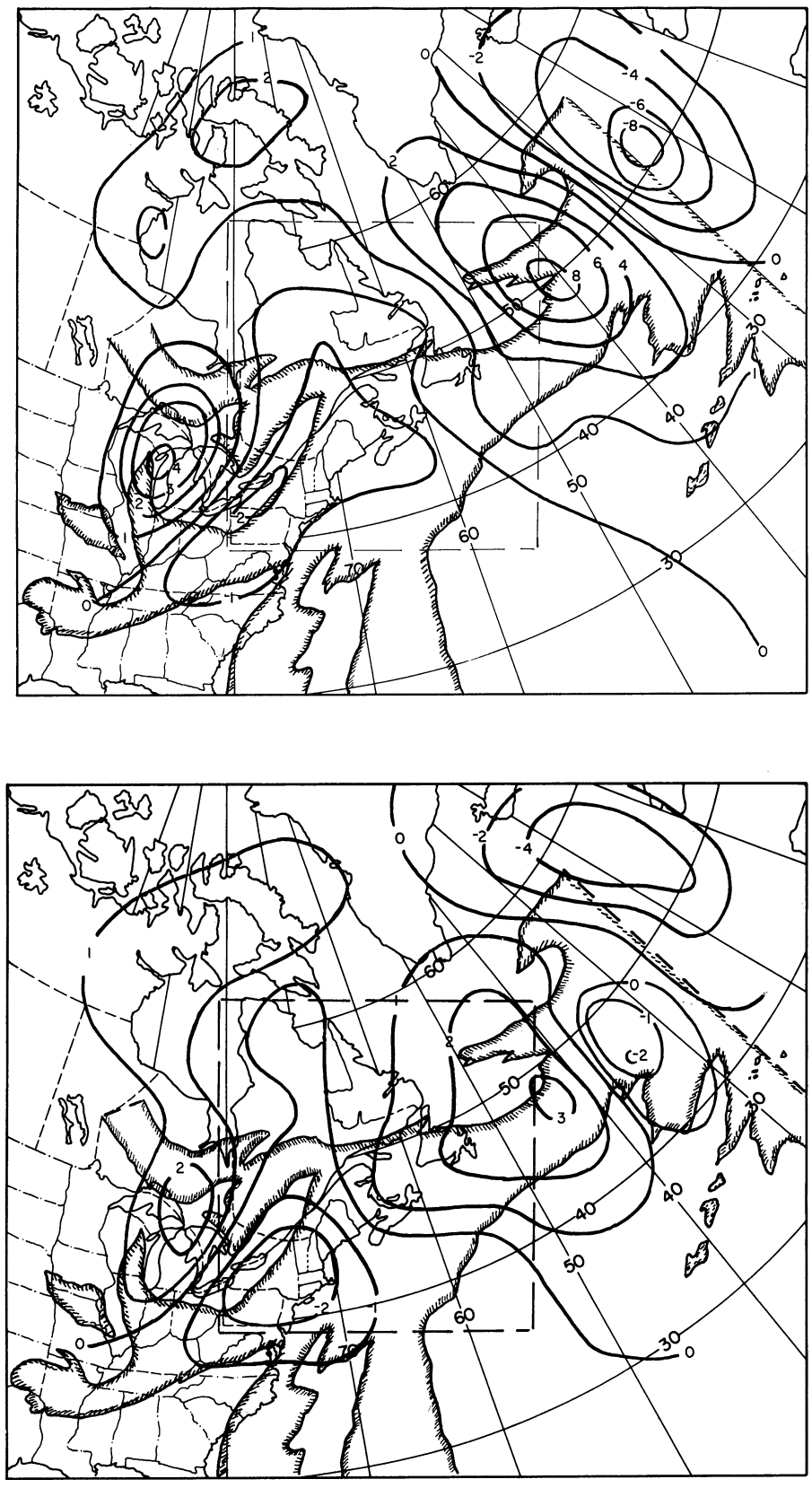

Fig. 4.20. Instantaneous tendency fields for 00Z, 10 May 1966. Top: From NMC analysis. Bottom: From twelve hour forecast. Arbitrary units.

10 May

The cloud system on this date is rather amorphous, although several features are distinguishable. The polar front can be followed across the photographs (Fig. 4.13). The center of the low over Quebec is visible, although the lack of cloud indicates that the region is inactive. The brightest clouds are found south of the St. Laurence River and are related to the developing surface wave. These features are in fair agreement with the tendency field computed from the twelve-hour forecast (Fig. 4.20). Moderate variations were made in the reanalysis (seven trials) to intensify the positive region behind the cold front and to extend the negative area to the northeast. The changes were not as severe as those depicted for the NMC analysis, which for this date appears to produce a particularly accurate tendency field in the region of the developing wave (as judged subjectively by the cloud cover). No attempt was made to alter the analysis of the mature vortex, since the available photographs provide inadequate coverage.

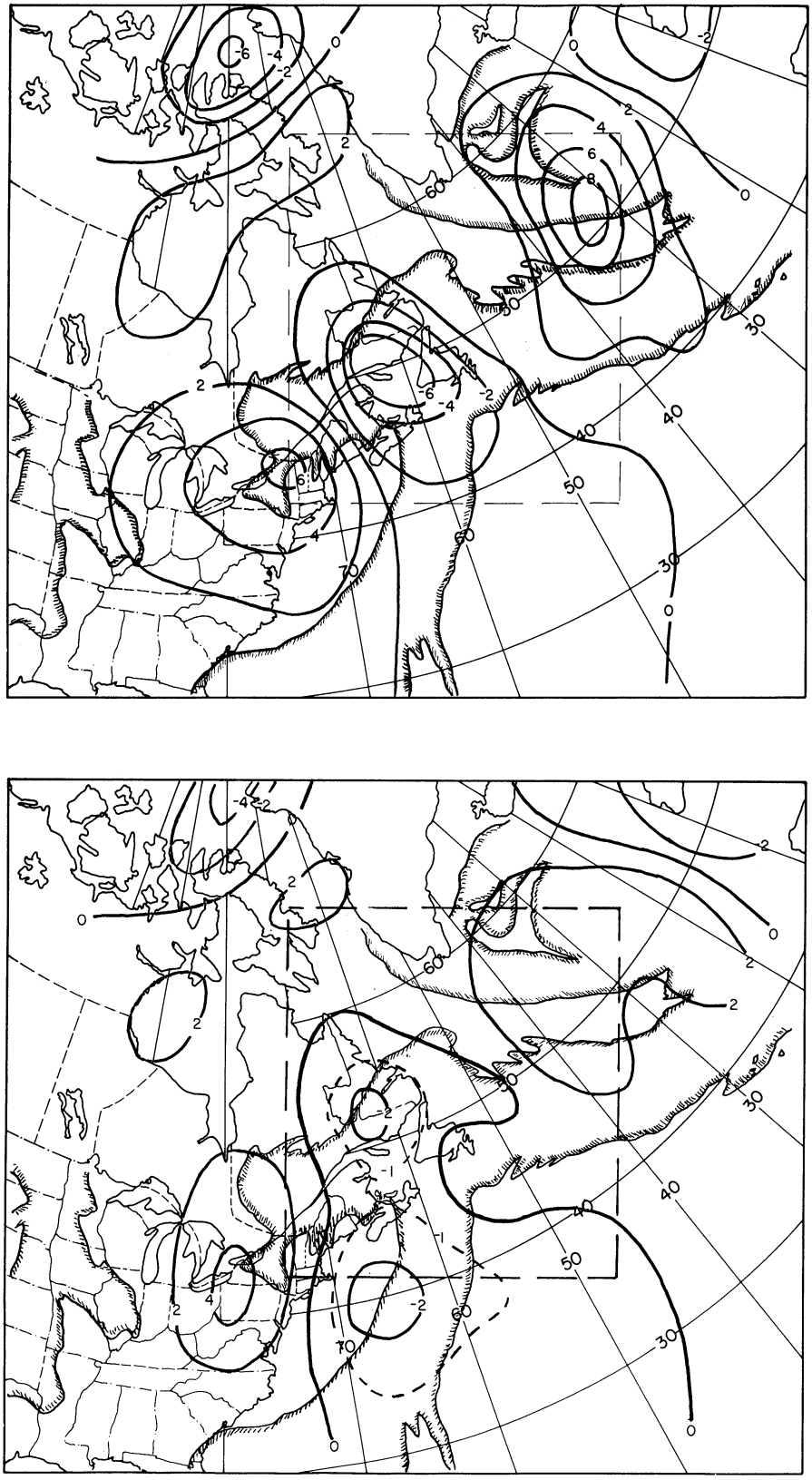

Fig. 4.21. Instantaneous tendency fields for 00Z, 11 May 1966. Top: From NMC analysis. Bottom: From twelve hour forecast. Arbitrary units.

11 May

The cloud photographs for this date show the wave approaching maturity (Fig. 4.14). The cloud shield has formed although the frontal band is still wide and indistinct; and the clear tongue has not yet entered the vortex. Clouds on the backside of the 500-mb low continue to be less well-developed than usual. As clouds in this sector are generally believed to be advective, it is possible that downward vertical velocities are unusually strong for this system. Modifications in the reanalysis (four trials) again expanded the area of positive tendencies in the clear area behind the storm, with some increase in magnitude (Fig. 4.21). The negative area in the main cloud shield was greatly intensified, whereas the maximum over the trailing front to the south was reduced. The positive area ahead of the system was also increased for contrast. These changes agree in general with the tendencies derived from the NMC analysis. The latter, however, show an extensive tongue of moderately high negative values extending to the southeast. This is unusual as the more typical configuration shows the tendency minimum tapering off along, or slightly ahead of the cold front. It appears likely that the analysis is in error here, particularly as this is a region with no data. It should be added, however, that the tendency fields generated fron the products of both analysis systems used here give very similar results.

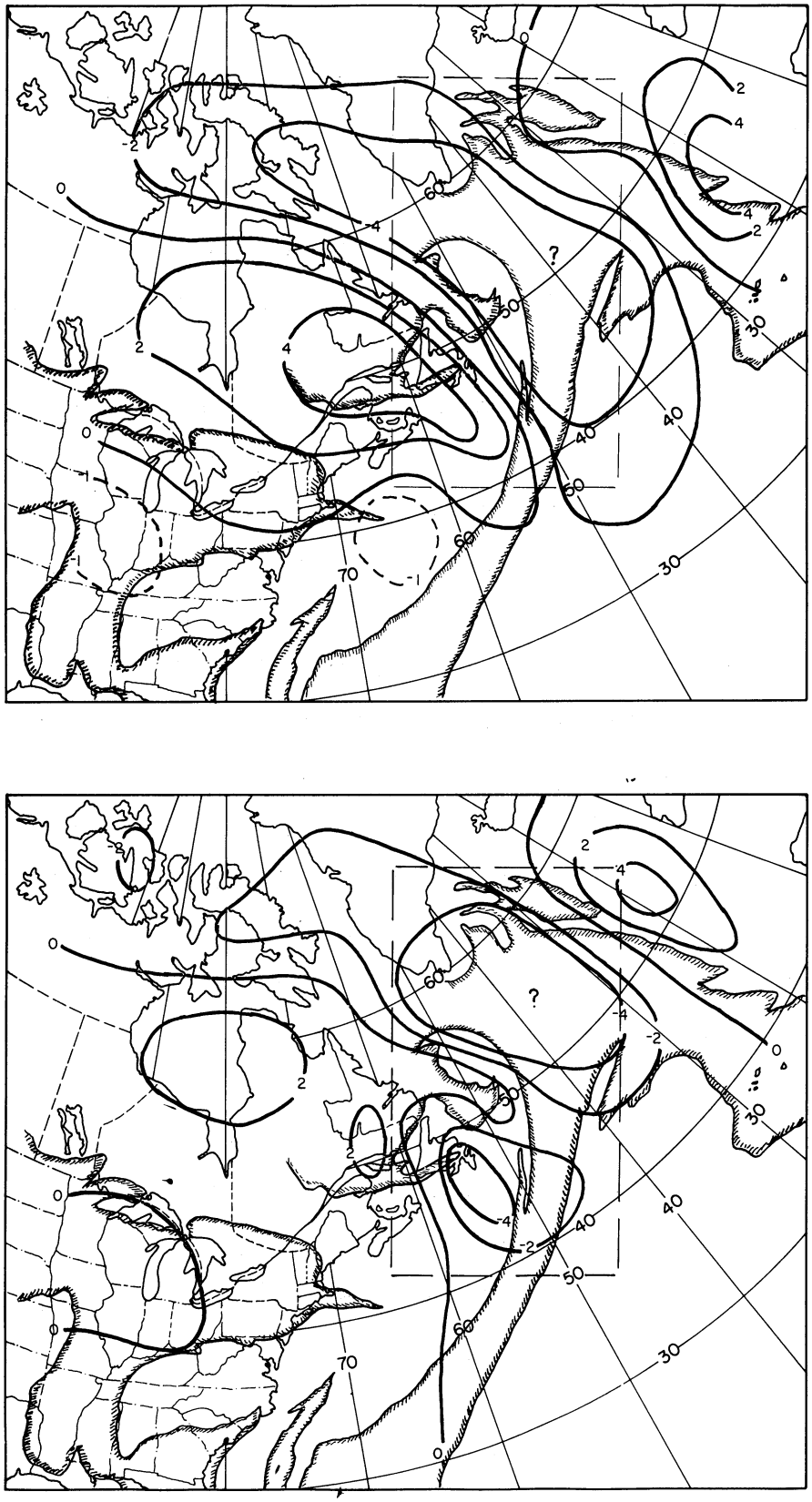

Fig. 4.22. Instantaneous tendency fields for 00Z, 12 May 1966. Top: From NMC analysis. Bottom: From twelve hour forecast. Arbitrary units.

12 May

By this date the initial wave is fully mature and has reached maximum intensity. The clear air intrusion has just been initiated (Fig. 4.15). The clouds associated with the second thermal wave, which develops later on the East Coast, can be seen in the Midwest. For the former system, the instantaneous tendency field computed from the twelve-hour forecast is a nightmare. Indeed it was one of the principal motivations for changing to the gross tendency technique. The general shape of the field correlates reasonably well with the visible clouds (Fig. 4.22) and the maximum negative values are coincident with the cloud shield. The values themselves, however, are extremely erratic. One row of gridpoint values (arbitrary units) across the cloud shield gives:

-432 -77 -428 -54 -563.

This field proved difficult to reanalyze (four trials). Changes were made to moderate the large positive area close to the vortex center and to smooth the interior values in the cloud shield, although the latter effort was not very successful. No attempt at reanalysis was made for the second system, since a negative center is already present in the initial guess field. In addition, the finite differencing method used in the computation precluded calculation of the tendencies at the edge or next-to-edge points, and much of the system lies in this area.

The tendency field computed from the NMC analysis is subjectively not a great deal better than the first-guess field. The corresponding row of gridpoint tendencies gives:

-572 -106 -410 -75 -565.

Also, the negative tendencies seem again to extend too far ahead of the cold front, though less so than on the previous date.

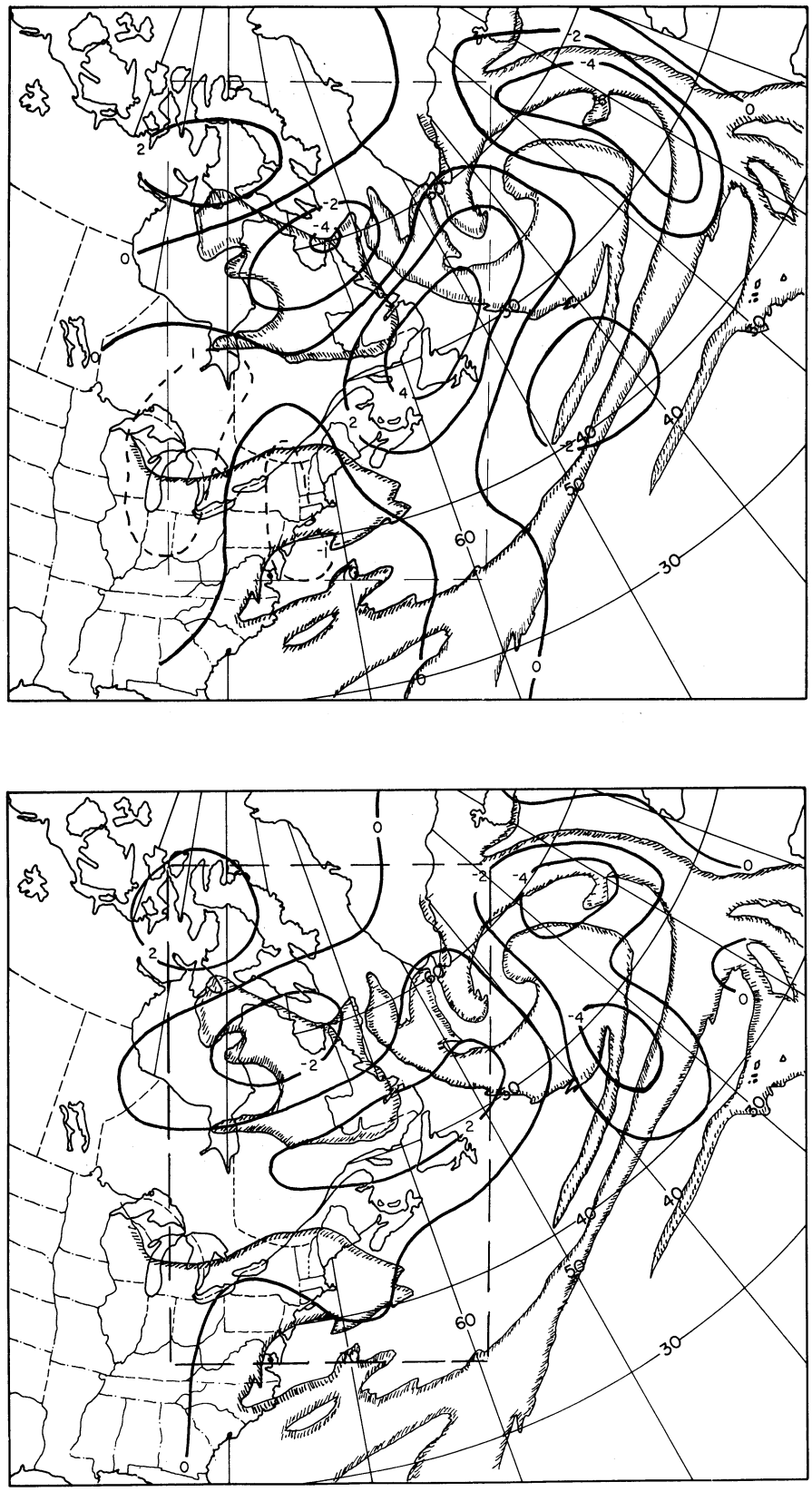

Fig. 4.23. Instantaneous tendency fields for 00Z, 13 May 1966. Top: From NMC analysis. Bottom: From twelve hour forecast. Arbitrary units.

13 May

Reanalysis (four trials) for this date was confined to the new system along the New England Coast and the short wave over Newfoundland. In accordance with the propensity of the forecast to underestimate the magnitudes of developing systems, negative tendencies were intensified for both systems and slightly reshaped to conform with the cloud cover. No attempt was made to alter the field associated with the older system now lying southeast of Greeland (Fig. 4.16).

The NMC tendency field for this date (Fig. 4.23) appears to agree well with the photographs. The local negative maximum along the cold front extending from the older system is somewhat questionable, although there is additional cloud in this area, and the same feature is duplicated by the products of both A1 and A2.

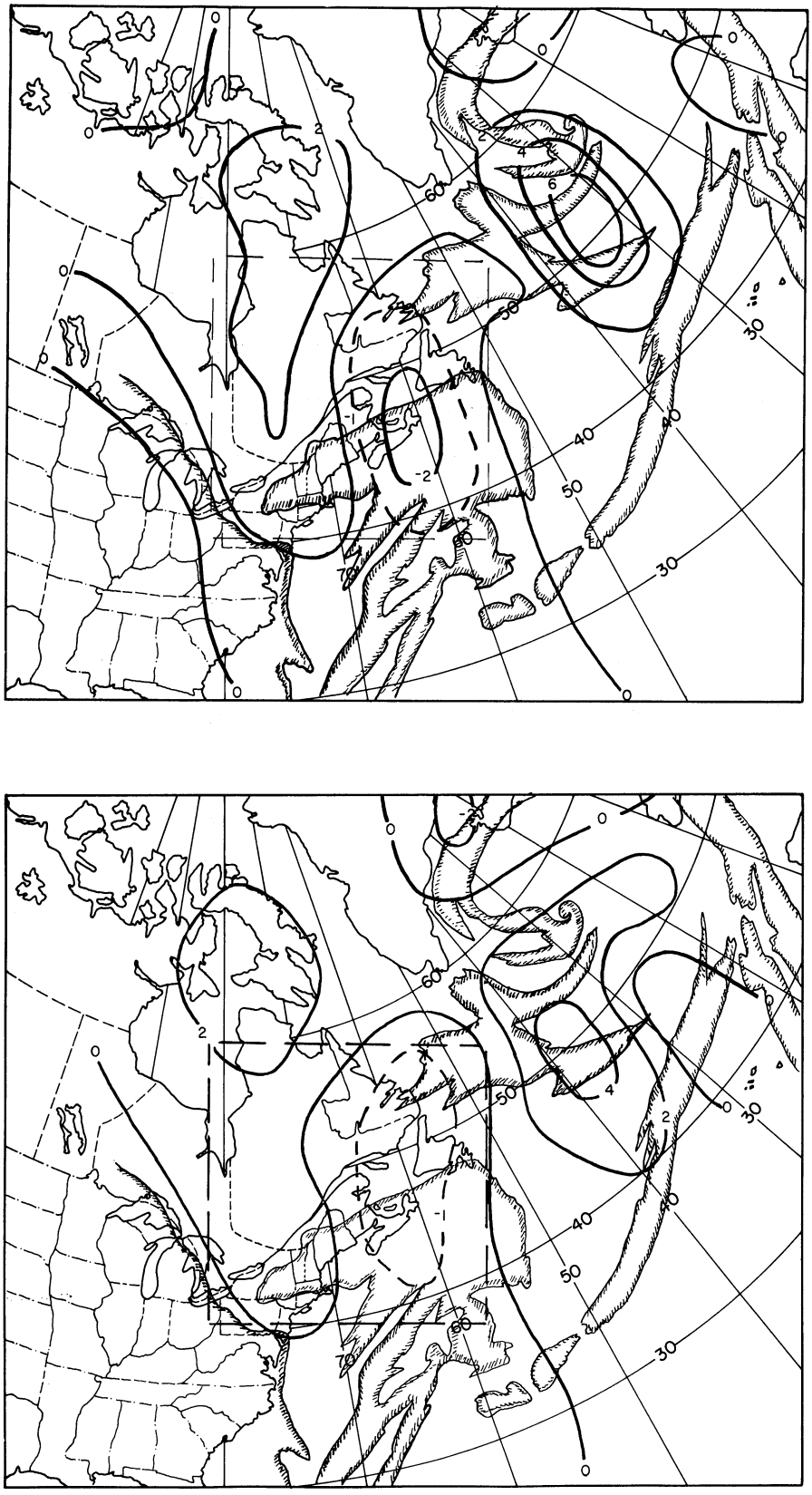

Fig. 4.24. Instantaneous tendency fields for 00Z, 14 May 1966. Top: From NMC analysis. Bottom: From twelve hour forecast. Arbitrary units.

14 May

The second wave is beginning to develop by this date, and some organization is visible in the cloud photographs (Fig. 4.17). Its presence is reflected in the tendencies derived from the first-guess field and consequently only minor alterations were made (Fig. 4.24). The magnitudes of the negative maximum were reduced in the northern portion and amplified in the region covered by cloud. Unfortunately, comparison with the NMC tendencies shows that the former adjustment was in error. In all likelihood the clouds are still low-level and so are displaced from the 500-mb tendencies by the usual vertical tilt. The disparity cannot be attributed to the analysis system, for the reanalysis is in a region of good data coverage.

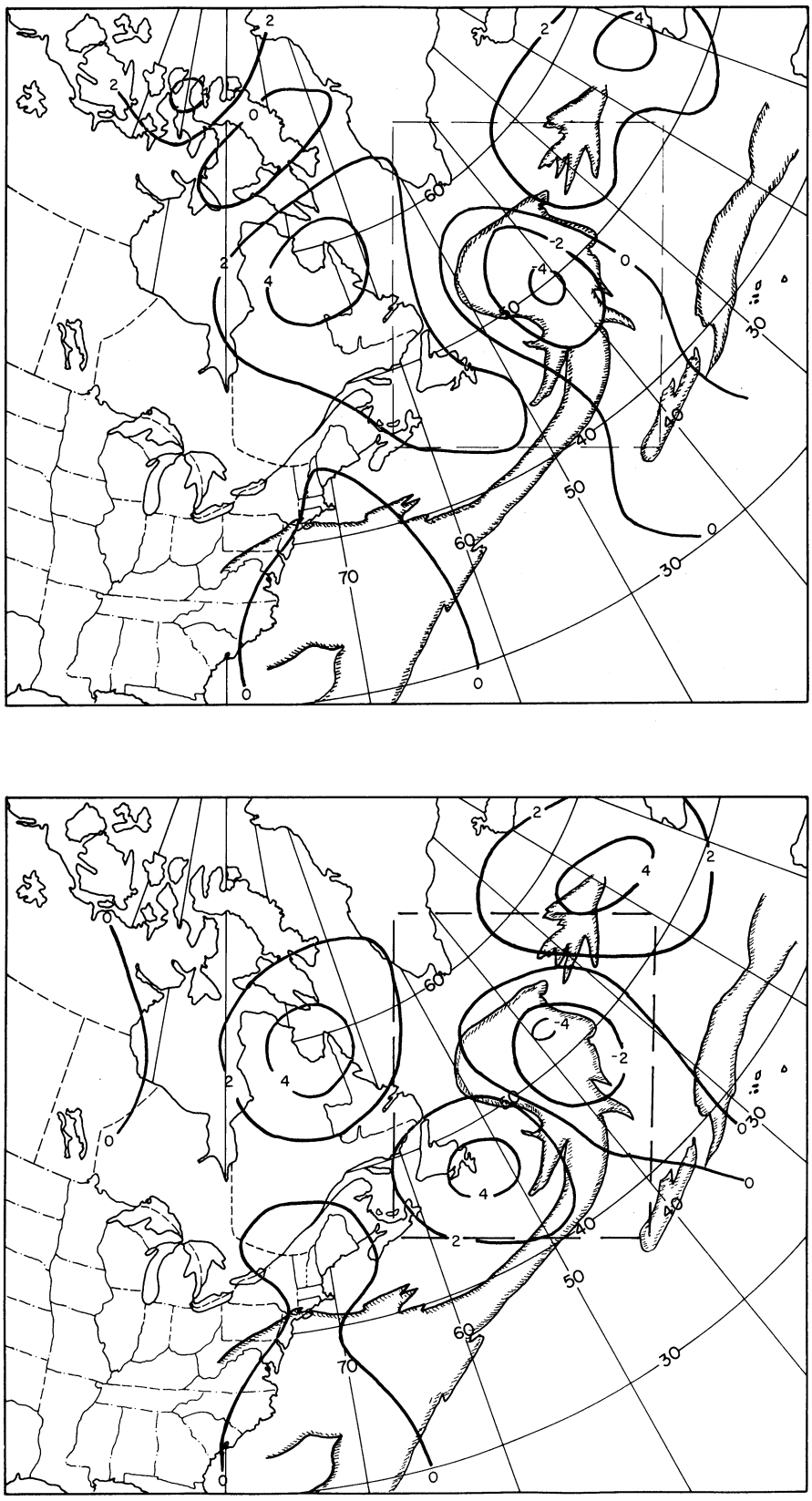

Fig. 4.25. Instantaneous tendency fields for 00Z, 15 May 1966. Top: From NMC analysis. Bottom: From twelve hour forecast. Arbitrary units.

15 May

By this date the second wave is approaching maturity, although clear air has not yet begun to enter the vortex (Fig. 4.18). The reanalysis (one trial) was concerned exclusively with moving the negative tendency maximum to a position coincident with the cloud shield (Fig. 4.25). The NMC tendency field shows excellent correspondence with the cloud cover for this date except that it again exhibits negative values rather far in advance of the cold front. These values were reduced somewhat in the tendency field associated with the modified analysis (A2).

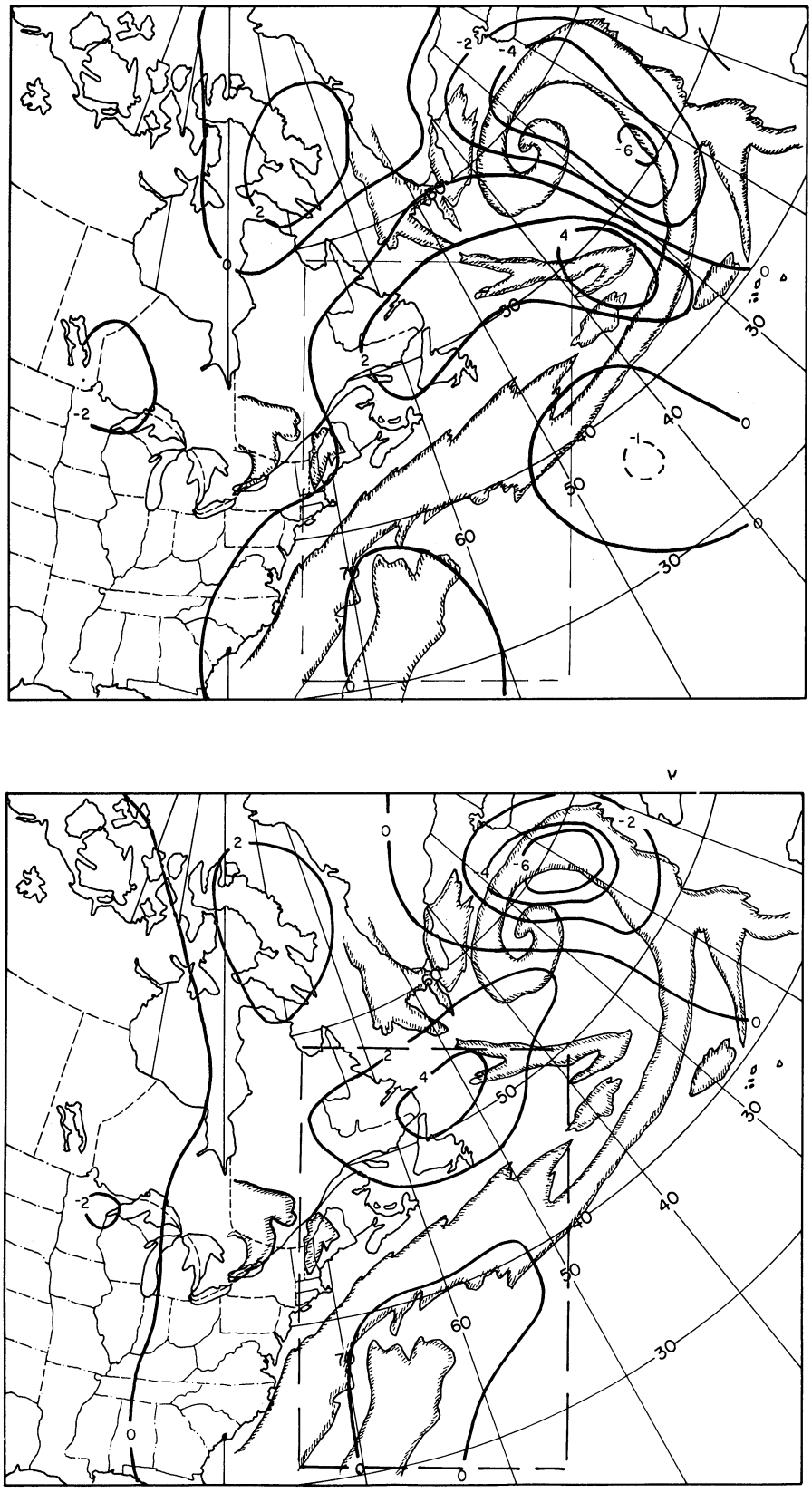

Fig. 4.26. Instantaneous tendency fields for 00Z, 16 May 1966. Top: From NMC analysis. Bottom: From twelve hour forecast. Arbitrary units.

16 May

The photographs for the final date in this period show that the second system is decaying in the Icelandic low. The new short wave has associated clouds, but they are not yet well organized (Fig. 4.19). No attempt was made to alter the guess field for the former system. The negative tendencies for the latter wave were intensified (two trials), whereas the leading positive tendencies were slightly decreased. It is comforting to note that for the occluded cyclone the trailing tongue of the negative maximum follows the shape of the cold front (Fig. 4.26).

After completing all reanalyses for this case, the gross tendency fields for both the original guess fields and the NMC analyses were computed. An examination of these fields suggested that reanalysis would be both easier and have greater probability of success if practiced on the gross tendency. Unfortunately these fields did not explain the questionable extension of the negative tendency maxima for the eleventh, thirteenth and fifteenth. For the first and last dates the final gross-tendency fields do not exhibit this behavior, whereas it is greatly amplified on the middle date.

4.3.4 Verification

Statistics

Because the observing stations are distributed rather inhomogeneously over the analysis area, the quality of the guess field is not constant over the grid. As a result, the verification statistics show considerably more day-to-day variation than those for the January case. However, the

seven-day averages which are presented here are quite representative of most dates. The major exception is the twelfth, but there is every reason to question all analyses for that date. The average statistics are tabulated in Tables C.7 through C.9 in Appendix C. The major features of the statistics are discussed here.

As with Case I, the effectiveness of the SINAP technique in improving the first-guess field can be estimated by comparison of the original and reanalyzed guess fields with the final NMC analysis. The accuracy of the latter as a standard should be sufficient despite the fact that most sub-areas are over the Atlantic. Except for the southeastern portions of the grid the available data exceeds what has been loosely described above as "saturation density" (one report per eight gridpoints). The relevant statistics which are given in Table 4.5 are in complete accordance with those for Case I (Table 4.1). Again it appears that it is more difficult to improve the gradient of the twelve-hour tendency field than the tendency itself, although modest improvement is made by this SINAP method. Not surprisingly, Tables 4.1 and 4.5 suggest that degree of improvement is dependent on the quality of the guess field. The values for May show this case to fall between the poorer (thirty-six-hour forecast) and better (twelve-hour forecast) guess fields of Case I.[1]

As with Case I, artificially sparse data networks were used to test the effectiveness of the reanalysis in the final product of the objective analysis. For this case five den-

---

[1] Note footnote to page 39.

TABLE 4.5

ORIGINAL AND REANALYZED GUESS FIELDS COMPARED WITH FINAL NMC ANALYSIS (MAY)

	ORIG	REAN
SRMS	5.6	4.3
SCC	0.75	0.80
DCC	0.55	0.56
TRMS	46	31
TCC	0.86	0.90

sities were tested with both modified and unmodified analysis systems. The densities were not chosen with the care exercised in the January case, since many of the difficulties of verification were not forseen at the beginning of this study. The main consideration was to ensure uniformity, although even this proved impossible for the lower right portions of the grid where observations are virtually non-existent. The selections were as follows:

i) Eight observations were chosen to cover all but the southeastern portion of the analysis area. None of these is located outside of the analysis area, so a definite bias exists at the edges of the grid. The density approximates the thirteen-station trial of Case I.

ii) Fourteen stations were selected. Again none lies outside the analysis area. The internal density falls between the thirteen and twenty-eight station-trials of Case I. Two stations used for (i) are replaced by neighboring stations (Portland for Stephenville and Topeka for Nashville).

iii) Twenty-nine observations were used, with two outside of the analysis area. This density approximates the twenty-eight-station trial of Case I but is slightly non-

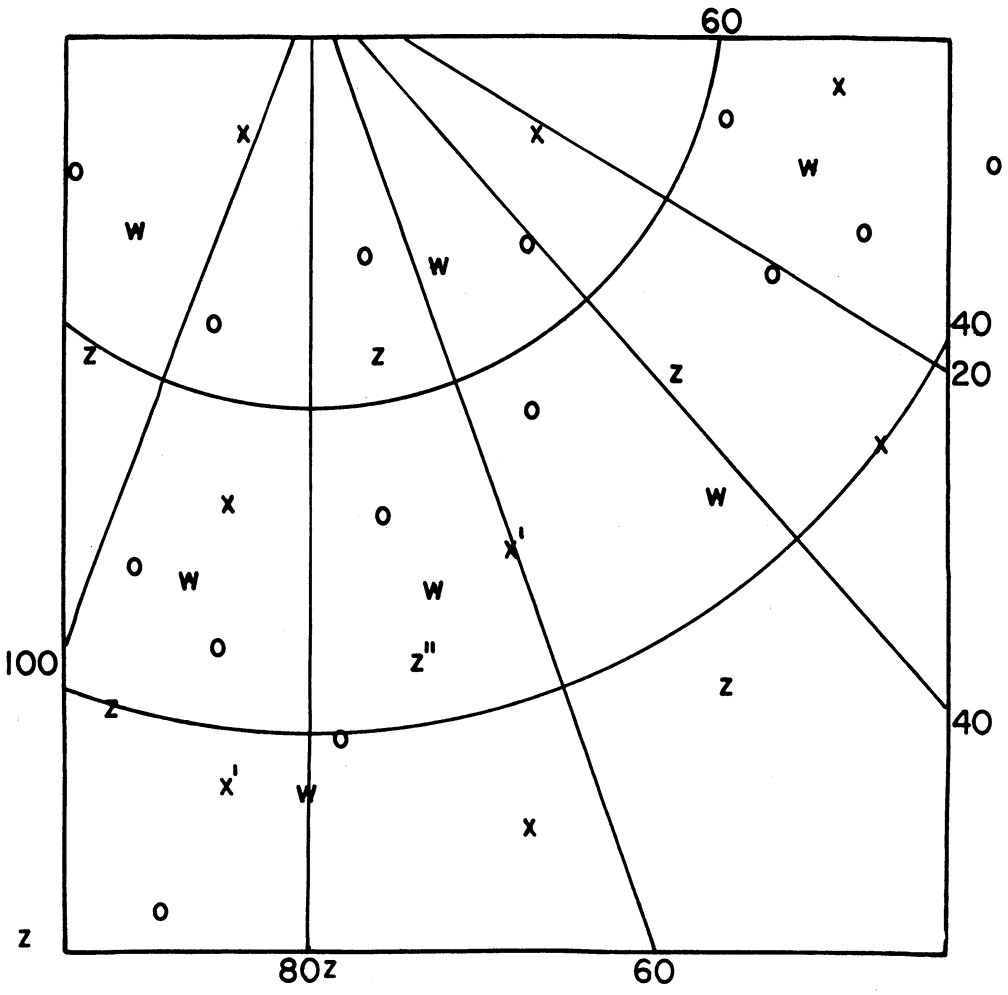

Fig. 4.27. Twenty-nine station distribution for May case:

x - eight station density
z - additions for fourteen station density
o - additions for twenty-nine station density
w - stations withheld for ARMSE

Prime: station not used in fourteen station trial.
Double prime: station not used in twenty-nine station trial.

uniform, with greater coverage over the continent. For this trial (as in (i)) Stephenville is used instead of Portland.

iv) Fifty-six stations were used. The coverage is quite non-uniform since no additional data have been added over the ocean. Both Portland and Stephenville are included in this selection.

v) All available reports within the analysis area, and a few to the right and left of the grid were used for this trial. The density over the ocean is slightly increased since one ship report previously withheld for the ARMSE is now incorporated in the analysis.

The twenty-nine-station density is depicted in Figure 4.27. Throughout the period only slight day-to-day variations were necessitated by missing reports.

Figure 4.28 is analagous to Figures 4.11 and 4.12. It gives the height-tendency, root-mean-square error as a function of station density for both analysis systems operating on the original and reanalyzed guess fields. The results for this case are in close agreement with those of Case I. The sparse-data instability of A1 is again apparent, and it is impossible to state where the reanalysis loses its effectiveness in this system's final product. With the modified system (A2) the reanalysis seems to lose effect between the twenty-nine and fifty-six-station trials. This is in general agreement with Case I.

A comparison of the analysis systems complements the discussion of the January results. It may be recalled that the modified system was deficient for moderate station density with a poor guess field. This feature is only faintly evident in the results for this case (see DCC in

Table C.8) suggesting that the normal first-guess field over the Atlantic is sufficiently accurate to permit the tighter rejection criteria of A2. A final feature which invites attention is the effect of exchanging Stephenville for Portland in the fourteen station trials. Although it is not clearly demonstrated in the averaged values of the statistics, the absence of the former station in the analyses at only this density caused abrupt discontinuities in the statistics for the unmodified system for the individual dates. This manifests the sensitivity of the unmodified system in sparse-data areas. As would be expected, the effect is greatly damped by the modifications of A2.

The input of bogus stations as a SINAP technique is unsuccessful in this case as it was with Case I. The results with the unmodified system suggest that these pseudo reports are erroneous (Fig. 4.28), but this is largely illusory. For the most part the bogus stations represent high gradients in sparse-data regions, and the biasing effect is overwhelming. This conclusion is substantiated by the reduced effect of these stations in the modified system.

ARMSE

Table 4.6 gives the results of this method of verification for two sparse-data densities averaged over the seven-day period. As with the statistics above, there was some, but not significant day-to-day variation, and these results corroborate those for Case I. The reanalysis here is a greater improvement of the normal first-guess field than in Case I, partly because the forecast is somewhat poorer and also because the cloud systems are better organized and more distinct. Once again, with the exception of the twenty-nine-station A2 analysis, the influence of the reanalysis is

TABLE 4.6.

ARMSE FOR MAY CASE; 12-HOUR FORECAST (O), REANALYSIS (R), AND BOGUS WITH ORIGINAL (B)

ANALYSIS		ORIGINAL GUESS			SCAN 1			SCAN 2			SCAN 3			FINAL		
		O	R	B	O	R	B	O	R	B	O	R	B	O	R	B
A1	RETAINED	21	20	20	28	27	28	21	22	21	7	7	9	3	3	3
29 Station	WITHHELD	27	21	26	28	25	30	31	29	31	30	28	30	29	27	29
	ARMSE	35	30	34	40	37	41	38	37	39	31	29	31	29	28	30
A2	RETAINED	21	20	20	19	19	20	17	17	17	5	5	7	3	3	5
29 Station	WITHHELD	27	21	26	27	22	27	26	21	27	25	21	26	25	21	26
	ARMSE	35	30	34	34	29	34	32	28	32	26	21	27	26	21	26
A1	RETAINED	22	20	21	24	23	24	21	21	21	13	12	13	7	7	8
56 Station	WITHHELD	24	21	23	29	28	28	29	28	27	27	26	25	26	26	24
	ARMSE	33	29	31	38	36	37	35	35	35	30	29	28	28	27	25
A2	RETAINED	22	20	21	22	20	21	17	16	16	10	10	10	6	6	7
56 Station	WITHHELD	24	21	23	23	20	22	20	18	19	19	18	19	19	18	19
	ARMSE	33	29	31	32	28	30	26	24	25	22	20	21	20	19	20

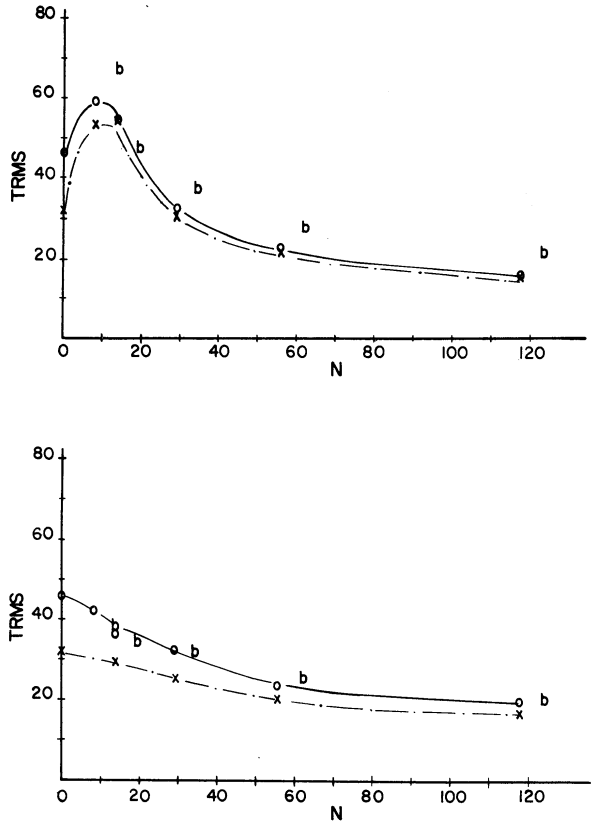

Fig. 4.28. TRMS for May case; twelve-hour forecast/ reanalysis. Top: System A1. Bottom: System A2. o - original; x - reanalyzed guess; b - bogus input.

lost in the final product.

The propensity of the early scans to increase the original guess field's error as represented by the withheld stations is very obvious here. As in the January case, the twelve-hour forecast, first-guess field seems more representative of these stations than the final product of the unmodified analysis system. This anomalous behaviour is mitigated by the de-emphasis of the early scans that occurs in the modified system.

4.4 Case III: Low Data Density, Pacific, 11-14 February 1967

4.4.1 Introduction

The final case study was selected in the Pacific where by dint of the scarcity of conventional data the cloud photographs should be of greatest value (Hubert, 1961; Oliver, 1962). However, this paucity of observation is a two-edged sword. Except for the northern region of the analysis area, the data density falls to a level where biasing is significant, and the unmodified analysis system becomes unstable. More importantly, the lack of observation destroys confidence in the verification procedures. It is impossible to execute a scheme of withheld stations for verification by the areal-mean method, and the accuracy of the NMC product must be viewed with suspicion. Obviously no program of artificially sparse-data analyses could be carried out for this case. These factors, together with the poor correlation of the cloud and tendency fields, and finally time commitments, precluded SINAP reanalyses for this case. But the outlook is not totally bleak. This case affords an opportunity to evaluate subjectively the NMC product by comparison of the implied tendencies (gross or instantaneous) with

the clouds visible in the satellite photographs. It is also possible to investigate the sparse-data correspondence of the NMC system with the objective analysis systems used here.

4.4.2 Synoptic Discussion

The synoptic situation chosen for this case undoubtedly challenges the analysis system to its utmost. Not only is it complex, but unlike the previous cases, the general circulation patterns in the nothern and southern portions are quite different. For the northern section, as in Case II, a series of wave cyclones evolves along a polar front extending southwest from the Aleutian Low. At the start of the study a surface wave is just developing southwest of Kamchatka (Fig. 4.29). A wave slightly past maturity lies ahead of this system, very close to the Aleutian sink area, which is itself clearly defined by a well-developed cloud vortex. The conglomerate is completed by yet another storm (in the decaying stage) northwest of the second wave. On the second day (Fig. 4.30) the first wave has reached the recognizable comma shape, while the second has become diffused with the Aleutian Low. A number of dying storms are discernible north of the main front, possibly associated with an old, indistinct arctic front. On the third day (Fig. 4.31) the first wave has reached maturity west of the Aleutian chain while the older system has filled and lost its identity. A third system is meanwhile generating to the west, again south of Kamchatka. On the final date of this case (Fig. 4.32) the initial wave has moved rapidly to the northeast and is beginning to decay. The trailing system has undergone explosive

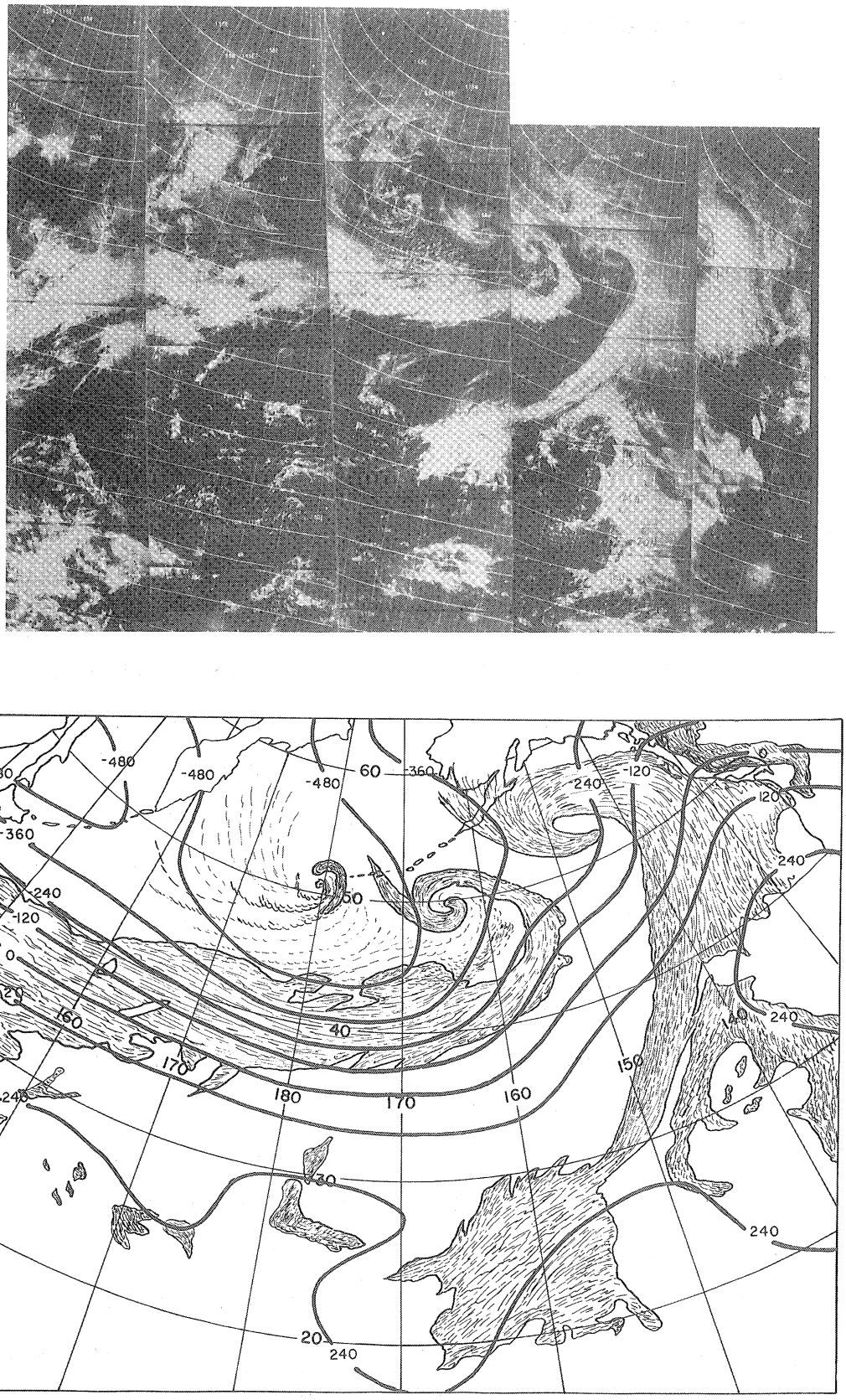

Fig. 4.29. Cloud montage and NMC 500 mb analysis for 00Z, 11 February 1967. (D values in meters.)

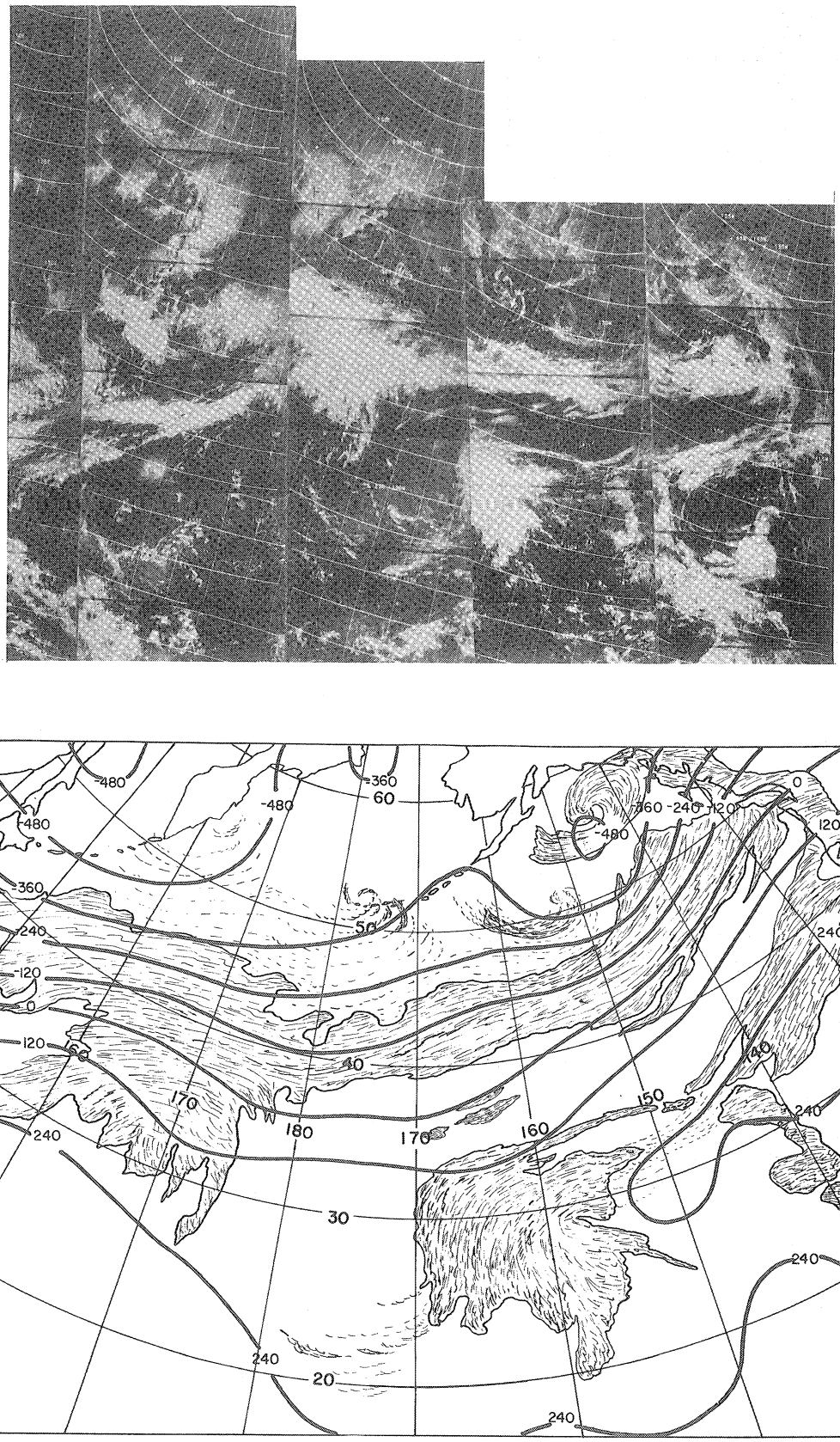

Fig. 4.30. Cloud montage and NMC 500 mb analysis for 00Z, 12 February 1967. (D values in meters.)

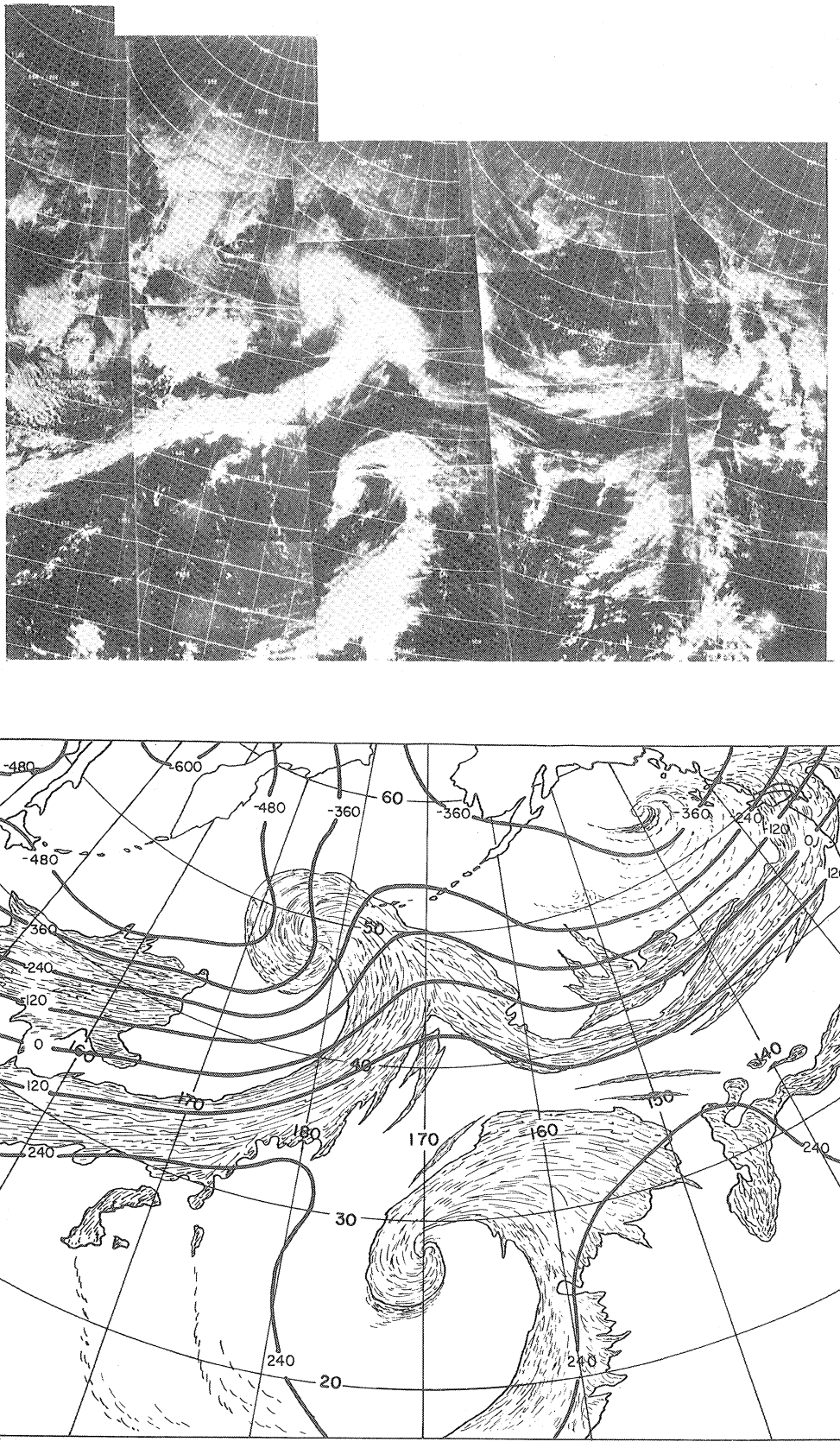

Fig. 4.31. Cloud montage and NMC 500 mb analysis for 00Z, 13 February 1967. (D values in meters.)

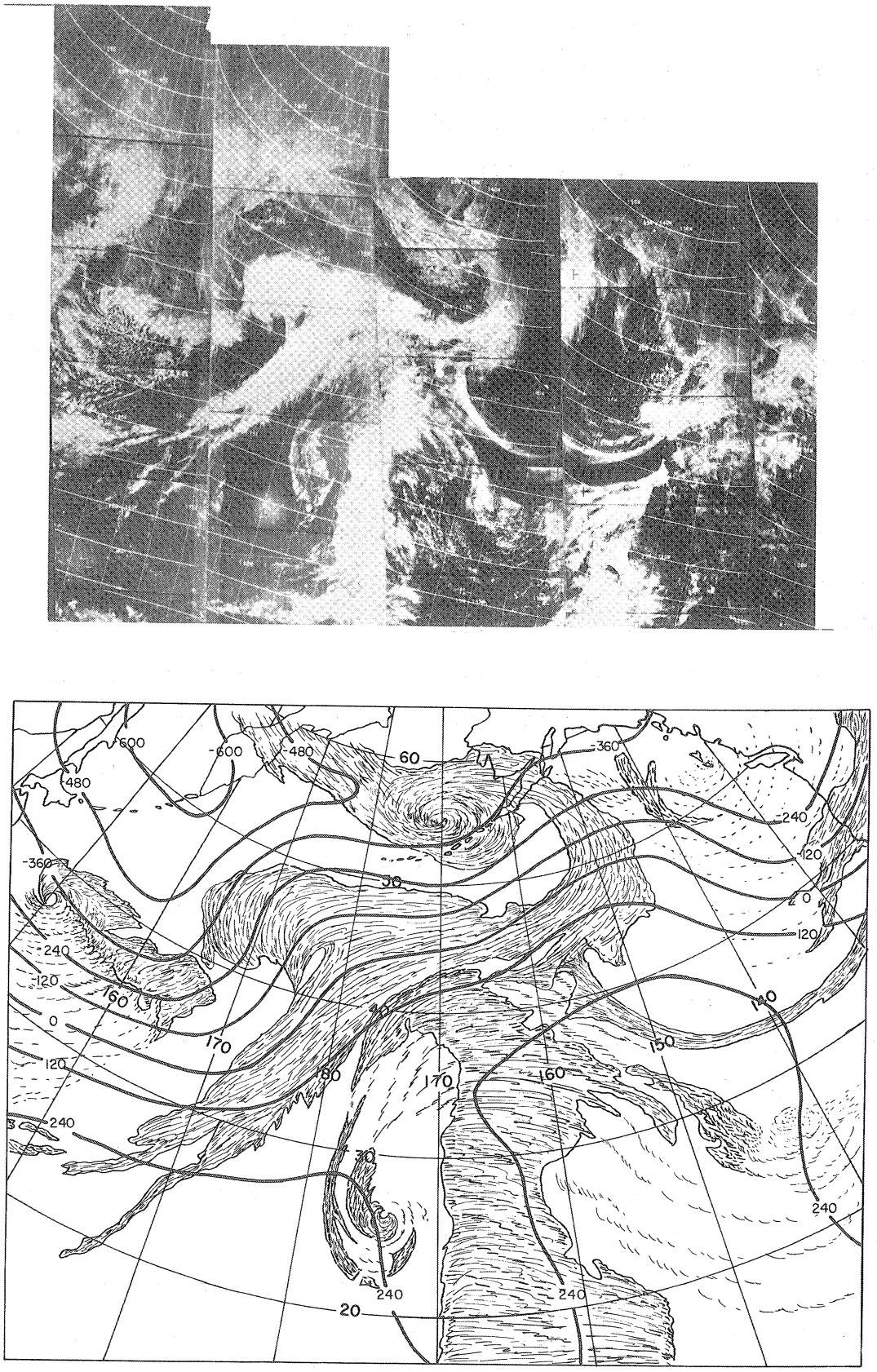

Fig. 4.32. Cloud montage and NMC 500 mb analysis for 00Z, 14 February 1967. (D values in meters.)

development and almost achieved maturity.

At the start of the period in the southeastern portion of the analysis area a disturbance is visible on what is possibly the old polar front. By the second day this storm has developed and moved to the west. On the third day (Fig. 4.31) it is fully mature and continues to move with an easterly-wave action. On the final day it appears to have almost completely filled but has become confused with the rapidly developing cyclone to the north.

4.4.3 SINAP Analysis

The instantaneous tendency fields, which are nearly simultaneous with the cloud photographs, for the NMC first guess and final product are depicted for each date. The tendencies for the products of the modified and unmodified analysis systems were computed but are not portrayed here. The major points of departure from the NMC versions will be discussed. It should be noted that the gross-tendency fields for all analyses were also computed, but with few exceptions these give very poor definition of the proposed correspondence with the satellite-observed cloud systems, and there seems little reason to present them here. It must be concluded that the gross tendencies offer little as a SINAP technique for this area, at least for modification of a single analysis, since both the previous and current fields are rather badly defined by conventional methods. This does not, however, preclude the utility of the technique for day-to-day changes with careful attention to continuity.

There is no trace of the easterly wave in any of the tendency fields produced for any date of this period. In consequence, all forecast (first-guess) fields in the

southern reaches of the analysis area are grossly inadequate. Each analysis attempts to define the system, but the scarcity of observation precludes definition sufficient to permit accuracy in the implied tendency field. Despite this lack of empirical evidence it is interesting to consider the possible correlation between cloud formations and the tendency field of an easterly wave. There is nothing in the theory discussed earlier to deny the same correspondence between tendency and vertical velocity that exists with the westerlies. The correspondence is dependent on geostrophicity, but there is no doubt that a well-developed easterly wave obeys this principle, particularly at the latitudes of the present case. Because of the reversal of the beta effect, vortex development in an easterly flow must differ from its westerly counterpart. As Riehl (1954) points out, the primary area of cyclogenesis may be on the upstream rather than the downstream side of the trough. Thus for initial development, the cloud configuration would probably not correspond well with the 500-mb tendency field.[1] In the same vein, storms on the leading edge of the inverted trough would tend to dissipate more rapidly than those in westerly flow.

---

[1] In the barotropic framework of this work the vertical tilt of the pressure systems has been ignored. For a developing surface wave in westerly flow this causes a modest displacement of low cloud formation from the 500-mb tendencies, although this error is generally below the resolution of the SINAP method. It is interesting to note that the tilt might help in the easterly case.

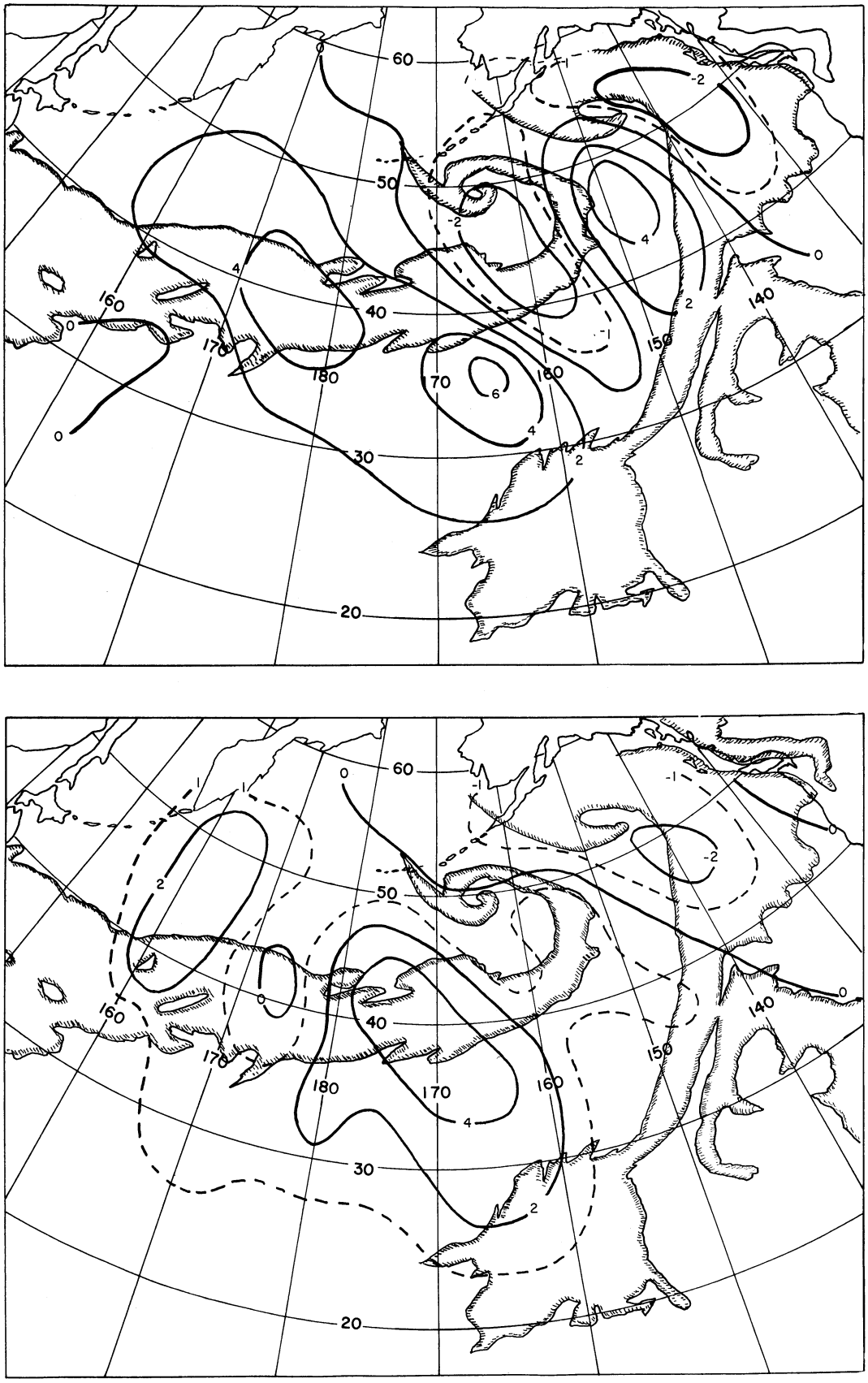

Fig. 4.33. Instantaneous tendency fields for 00Z, 11 February 1967. Top: From NMC analysis. Bottom: From twelve hour forecast. Arbitrary units.

11 February

With the exception of the major system near the coast of North America, the cloud structure visible in the satellite photographs is not reflected in the original tendency field (Fig. 4.33). The mature, well-defined vortex just to the west is totally absent, as is the wave formation south of Kamchatka (though the last is mostly west of the analysis area). The tendency field of the NMC analysis picks out the mature cyclone, but the center of negative values is displaced too far to the south and the orientation seems incorrect. The tendency fields of both A1 and A2 define this system, and both place the maximum negative values coincident with the vortex center. The unmodified analysis system gives a particularly good result. In addition, both tendency fields give negative centers along the front near the western edge of the analysis area, but these do not correlate well with the developing wave, and they are generally rather irregular and noisy. It is apparent that a great deal more smoothing has gone into the NMC product.

As previously mentioned, the tendency fields are incapable of defining the easterly wave. The NMC contour analysis (Fig. 4.29), however, does portray a very modest depression southwest of the cloud system, and the general synoptic pattern is not dissimilar to the fracture model described by Riehl (1954) as a mechanism for the creation of such waves. The large positive tendencies in the center of the analysis region would be associated with this process.

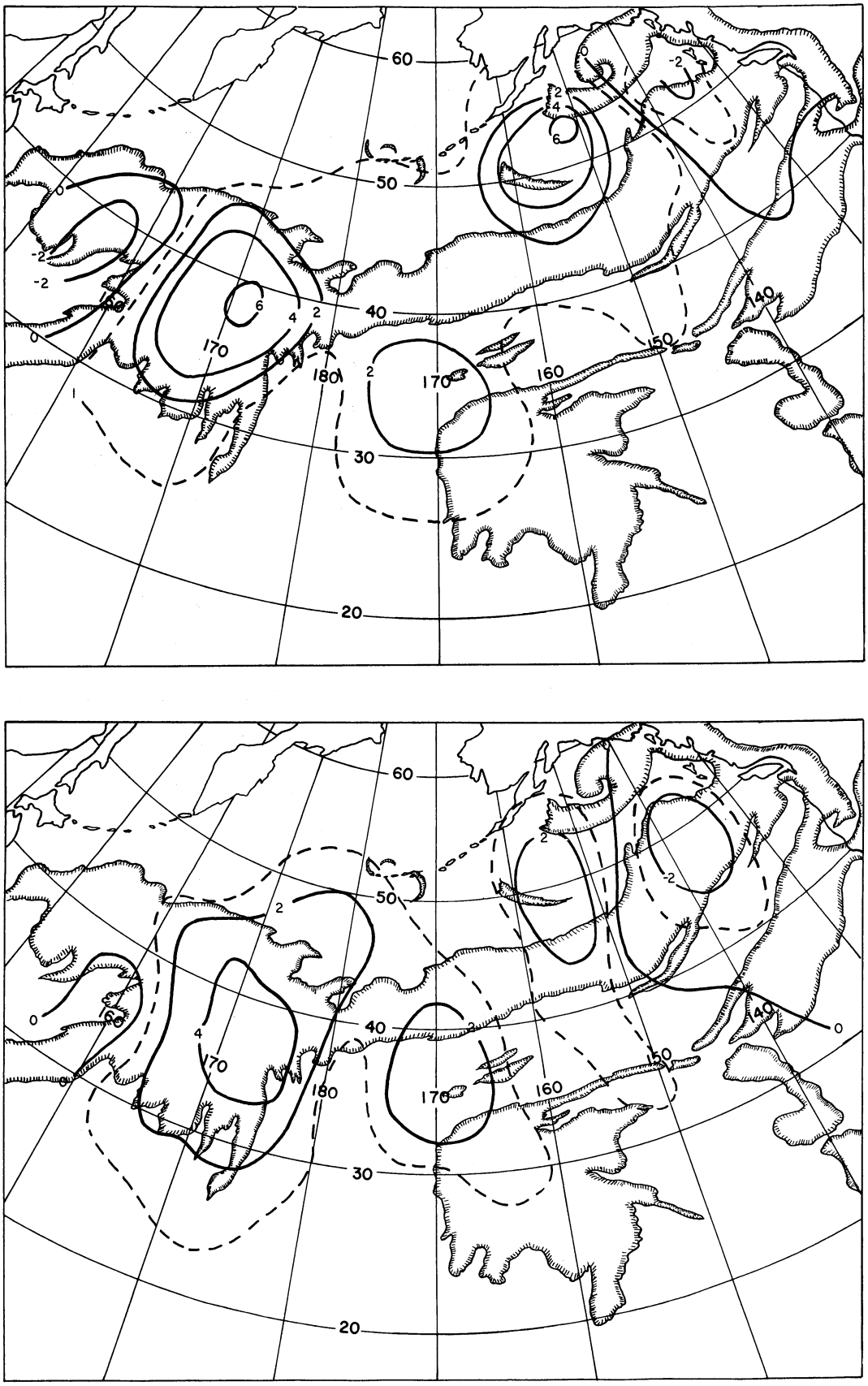

Fig. 4.34. Instantaneous tendency fields for 00Z, 12 February 1967. Top: From NMC analysis. Bottom: From twelve hour forecast. Arbitrary units.

12 February

The original tendency field for this date has a negative center associated with the dying vortex off the coast of North America and gives some indication of the emergent system south of Kamchatka (Fig. 4.34). Typically, the intensities of the latter are low, and they are greatly increased in the final analysis. The tendencies of the former storm are modified, although the orientation remains somewhat skewed.

The analyses produced by the different systems are not radically different for this date. The NMC analysis is again considerably smoother than the other two. The unmodified system produces an apparently spurious area of negative values northeast of the easterly wave. As this is not generated by the product of the modified system it would seem to be a further example of sparse-data instability.

Despite its development, the easterly wave is not shown in the NMC 500-mb chart (Fig. 4.30). Height values have lowered significantly since the previous analysis but without shape or continuity. The configuration of the field resembles a greatly extended mid-latitude trough rather than an easterly wave.

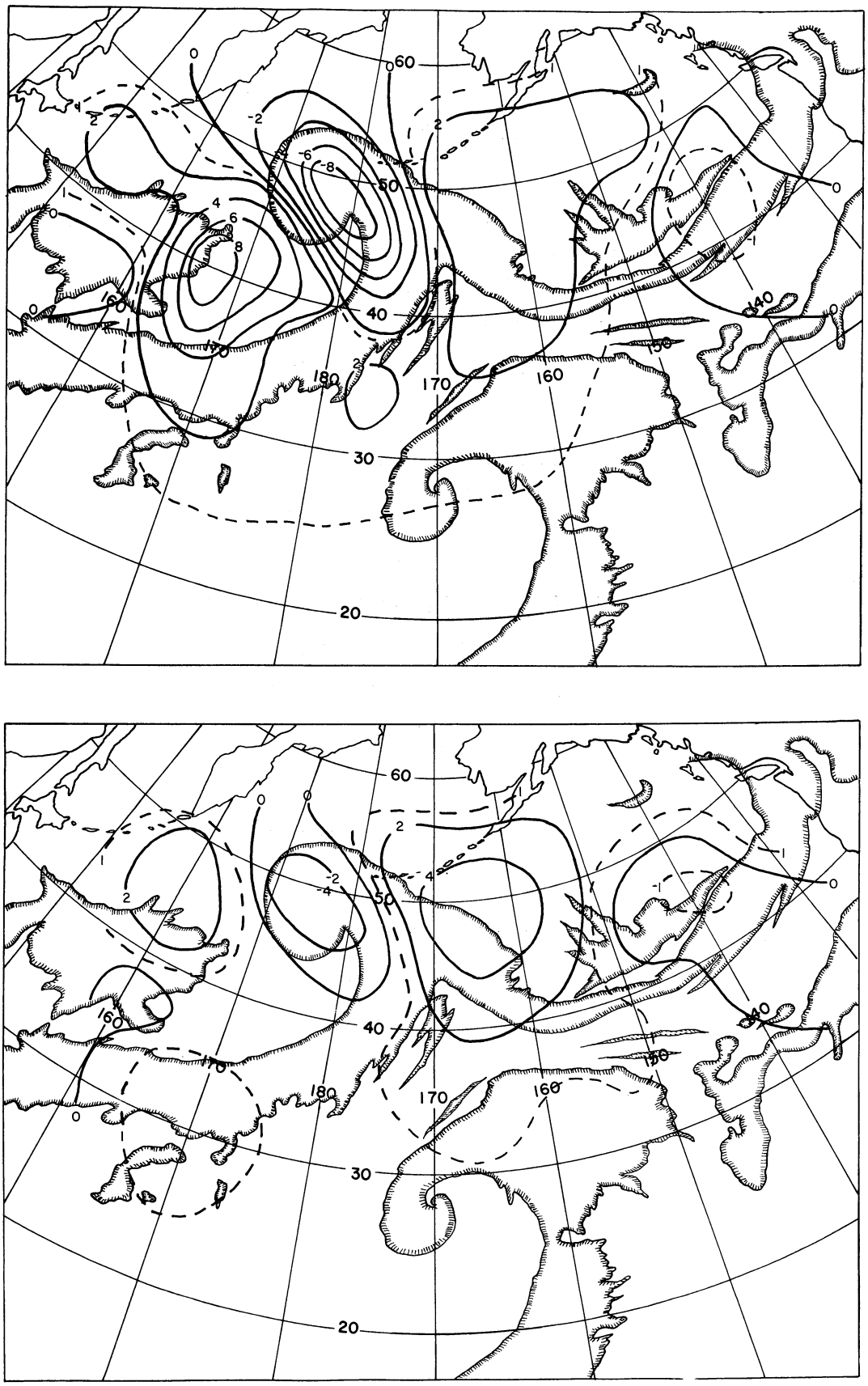

Fig. 4.35. Instantaneous tendency fields for 00Z, 13 February 1967. Top: From NMC analysis. Bottom: From twelve hour forecast. Arbitrary units.

13 February

Figure 4.35 for this date shows that the major storm is well represented even in the first guess, although the intensity is again too small. The developing wave to the west is likewise shown in both tendency fields. An area of negative values to the east is difficult to justify even though it is intensified in the tendencies computed from the final NMC analysis. The clouds do not appear to warrant this center.

The tendencies from the two analyses performed here agree generally with the NMC field. Both, however, intensify the developing system in the west, and neither agrees with the center in the east. Instead of the latter, a negative region coincides with the frontal cloud near the edge of the map. This would seem, subjectively, to be more reasonable.

By this date the easterly wave has reached full maturity, with the trailing front extending out of the vortex center to the northeast. There is a slight hint of a closed contour on the NMC 500-mb analysis coincident with the center. The contours of the easterly wave, however, are still not defined in the classical sense. A closed contour was also produced by the modified system, but it is displaced southeast of the vortex center.

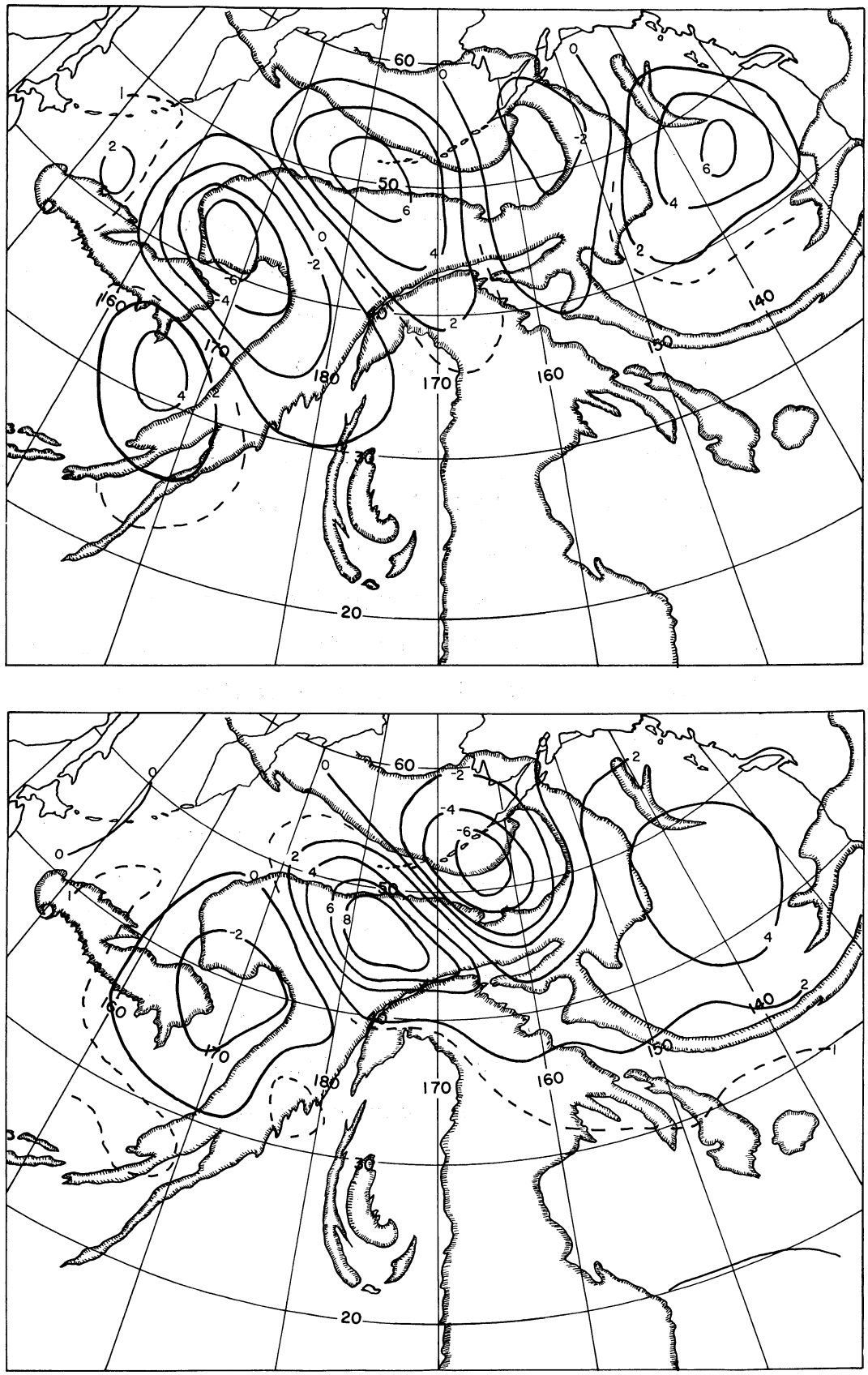

Fig. 4.36. Instantaneous tendency fields for 00Z, 14 February 1967. Top: From NMC analysis. Bottom: From twelve hour forecast. Arbitrary units.

14 February

The first-guess field for this date fails to estimate the speed with which the new system has developed. It is fairly well described by the tendencies computed from the NMC analysis. The previous storm has occluded more rapidly than indicated by the first guess, and its position remains somewhat questionable in the final tendency field.

The products of both the modified and unmodified analysis systems differ radically from the NMC analysis for this date. In view of the extreme confusion visible in the cloud photographs this is perhaps not surprising. However, there is some indication that the NMC tendency field yields the poorest correlation with the observed cloud systems.

The easterly vortex has completely decayed by this date. Perhaps its energy has been absorbed by the westerly system, which might account for the rapid development of the latter. For the first time the NMC 500-mb analysis shows an inverted trough extending from the southern edge of the analysis. The fact that the trough is weak and poorly defined is commensurate with the visible condition of the vortex (Fig. 4.32).

4.2.4 Verification

This section is perforce limited to a discussion of the objective analysis system rather than the effectiveness of the SINAP technique. The normal verification statistics for several combinations of the analyses are presented in Table 4.7.

The top row of the table gives comparisons of the final products of the three analysis systems with the original guess field. In general it can be stated that,

TABLE 4.7.

COMPARISON OF ANALYSIS SYSTEMS

	A1-GUESS	A2-GUESS	NMC-GUESS
SRMS	7.1	5.7	7.4
SCC	0,49	0.64	0.53
DCC	0.30	0.44	0.36
TRMS	39	25	55
TCC	0.69	0.85	0.64

	A1-NMC	A2-NMC
SRMS	6.6	7.2
SCC	0.66	0.58
DCC	0.54	0.46
TRMS	48	51
TCC	0.67	0.66

	A1-A2
SRMS	4.5
SCC	0.80
DCC	0.60
TRMS	24
TCC	0.89

as expected, the first-guess field of this case is considerably poorer than for either Case I or Case II (cf. Tables 4.1 and 4.5). This conclusion is based largely on the observation that the modified system effects far greater changes for this period than for the sparse-data trials of the other periods. Little reliance can be placed on the results for the unmodified system, as it has been shown to behave erratically at low data densities. The intentional emphasis of the modified system on the first guess is exemplified in these values.

The bottom row of statistics in Table 4.7 is a comparison of the two analyses performed here. The differences are significant but not formidable. It is likely the discrepancy would be greater if more of the reporting

stations fell in active regions.

The second row of statistics compares the analyses produced here with the NMC analysis. It is quite startling to see how little they correspond. The differences are so large that the effects caused by modification of the analysis system pale into insignificance. Unfortunately it is not possible to give reasons for this departure. It is, presumably, mostly due to the stability check included in the NMC model (see Appendix A), which permits data at lower levels to influence the 500-mb analysis. However, one would hardly anticipate this feature to exert such influence, barring an extremely inaccurate first guess. Difference charts formed by subtracting the NMC analysis from the A1 analysis are included as Figures 4.37 and 4.38. It is notable that the major sources of discrepancy are closely associated with active, no-data regions visible in the cloud photographs. This strongly suggests the utility of using the gross-tendency SINAP technique on a daily basis, particularly as systems move into the sparse-data area. Although this procedure has not been pursued in this study, it has been partially investigated by a check of the gross-tendency continuity in the twelve-hourly NMC analyses for this and the January case. As expected, the continuity is excellent over North America but poor over the Pacific.

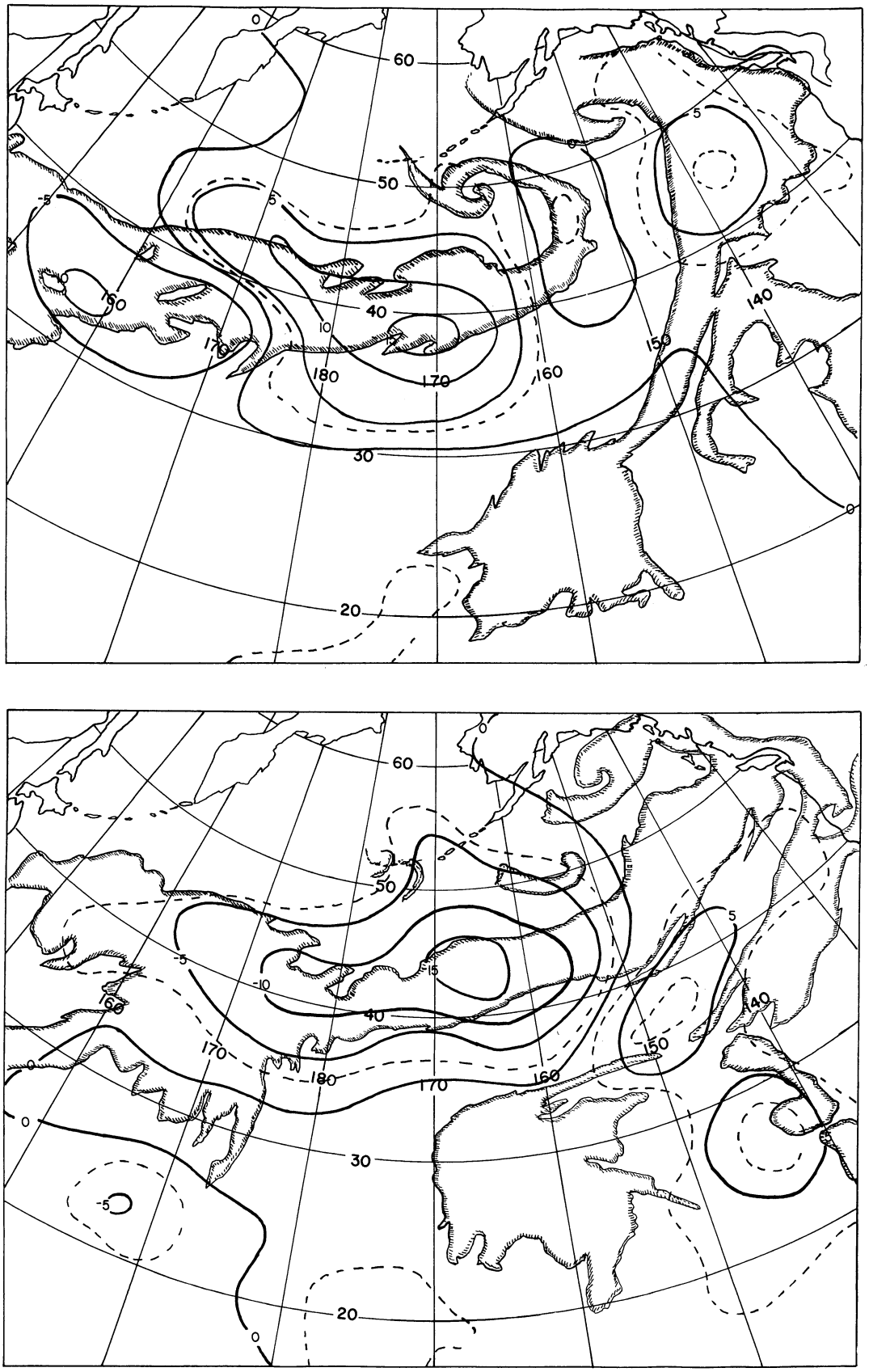

Fig. 4.37. A1 - NMC difference maps for 00Z, 11 and 12 February 1967. Units are in decameters.

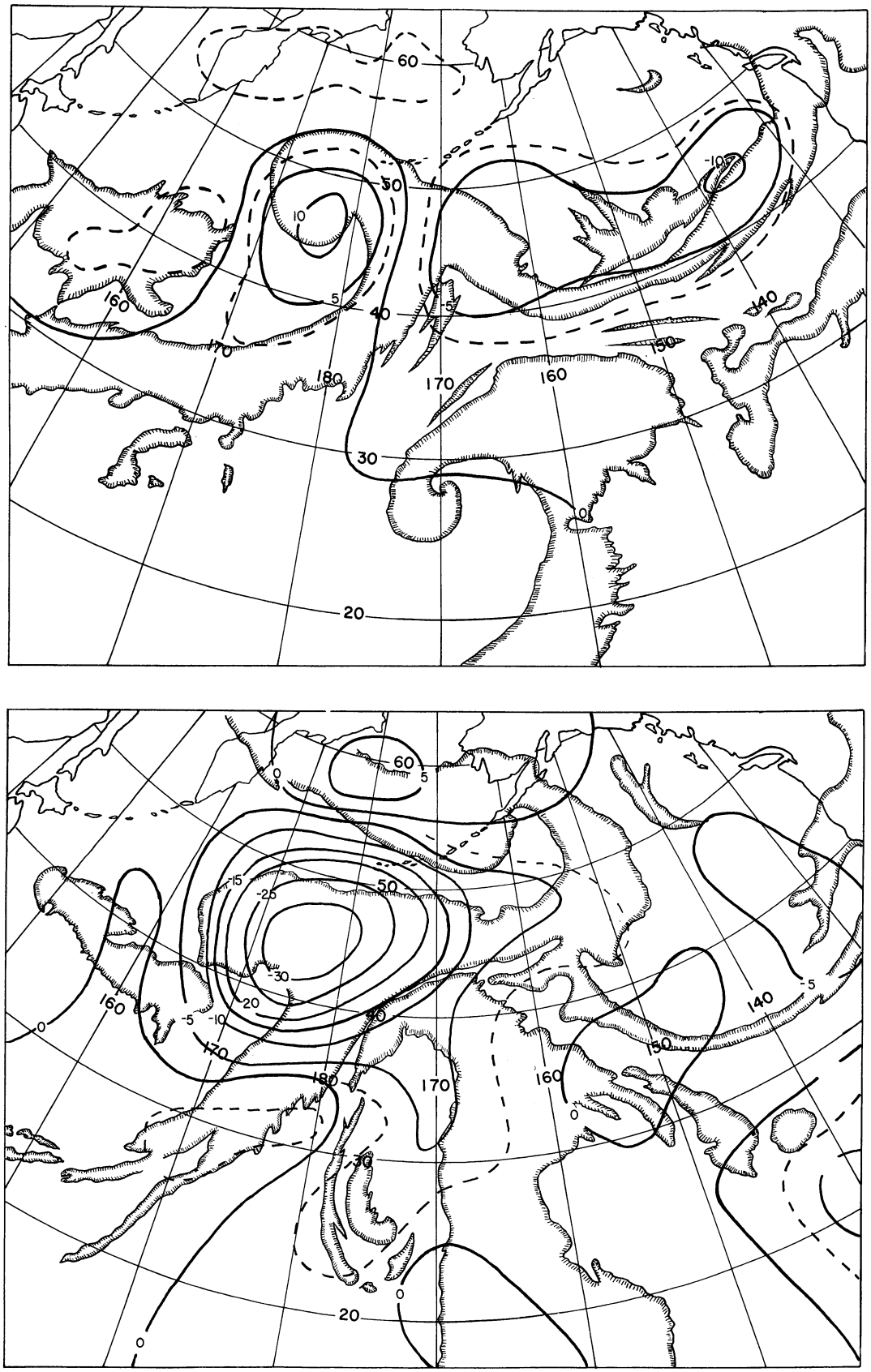

Fig. 4.38. A1 - NMC difference maps for 00Z, 13 and 14 February 1967. Units are in decameters.

5. CONCLUSIONS

Despite the limited sample of this study, it has been possible to elucidate several essental features of SINAP which have been previously only a matter of conjecture. Included in this realm are a reasonable technique for extracting information from the cloud photographs; an estimate of the circumstances under which SINAP can be routinely effective; and an investigation of the efficiency of input methods acceptable to an operational analysis/forecast procedure. In addition, as a byproduct of the SINAP investigations, it is possible to document several features of an objective analysis model that closely approximates the system currently operational at NMC (see Appendix A). Included in this category are the effect of the first-guess field; the problem of directional bias or uneven distribution in reporting stations; and the response of the system to variations in data density. The results are presented in tabular form below.

1. The shape of the 500-mb height-tendency field can be inferred easily and with fair accuracy from satellite-observed cloud formations. Estimation of magnitude is much less precise but can be approximated by continuity of both previous tendency maps and visible development in the cloud photographs. A differential of up to three hours between picture time and the time represented by the tendency field is acceptable for direct comparison. Reanalysis of the 500-mb height field can be done through either the instantaneous tendency field or a gross, twelve-hour tendency field. The two methods are equally effective, although the latter is simpler and more economical to perform.

2. Both SINAP tendency techniques have implicit limitations. Because of the relaxation procedure required for its computation, reanalysis via the instantaneous tendency values is limited to moderate alterations. The gross-tendency technique avoids this difficulty but requires that the previous (twelve-hour-old) analysis be highly accurate.

3. There is no utility in performing reanalysis in regions where the data density exceeds approximately one observation per ten gridpoints. In consequence, under normal circumstances, reanalysis in the Northern Hemisphere is limited to the Pacific and the South Atlantic; and effectiveness even in these areas is contingent upon increasing the weight of the first-guess field in the objective analysis scheme.

4. From a practical standpoint, only two methods of reanalysis input are acceptable to an operational analysis/forecast routine. These are input through a reanalyzed first-guess field or input via bogus data that may be processed exactly as regular station reports. Of these, the latter is simpler and therefore preferable, but from the standpoint of SINAP effectiveness, only the former is acceptable. The difficulties involved in conveying SINAP modifications by a few discrete points of information (pseudo stations) completely overwhelm the usefulness of the reanalysis.

5. For the major portion of the Northern Hemisphere the currently operational NMC analysis system gives too little weight to the first-guess field. The restricted use of this forecast debilitates the effectiveness of SINAP and may be harmful to routine analysis in sparse-

data areas.

6. Directional bias (uneven distribution) in the reporting network has a slight but systematic influence on the product of the objective analysis system. Under unusual circumstances (e.g. jet streams over coastal areas) the distortion may become extreme (see part iv of Appendix B).

7. The original analysis system used in this study performs erratically in areas of very sparse data. Instability is caused by excessive corrections to the first-guess field at gridpoints distant from any reporting station. As discussed in Appendix B, this can be reduced by restrictions on the permissible correction at a gridpoint, by control of the early scans' influence, or by a combination of both. It is not known if this difficulty exists in the multi-level system used at NMC. The effect would certainly be masked by vertical stability checks inherent in that system.

The primary conclusion of this study is straightforward. SINAP through cloud photographs is presently of limited utility. This result was not unexpected since the subjective, qualitative information available from the photographs is basically incompatible with the requirements of objective analysis and prediction. What was perhaps not anticipated prior to this study is that the deficiencies of SINAP are shared by both source and processor. Limited information is both available and obtainable from the photographs. It cannot be effectively utilized without adjustment of the objective analysis procedure, but such refinements are not difficult to introduce. Barring alteration in the system, the satellite photographs appear still to be useful, not as a source of additional data but for monitoring the quality of conventional analysis. In this

secondary role, the correspondence between cloud formations and the gross height-tendency field is informative, particularly in sparse-data areas.

6. SUGGESTIONS FOR FUTURE WORK

6.1 Height-Tendency Continuity

Although it appears that satellite photographs cannot at present be used to supplement conventional data in the analysis procedure, it is conceivable that alterations in the analysis program (similar to those discussed in Appendix B) could be effected at NMC. Even if this possibility is disregarded, the cloud/tendency relationship should not be overlooked as a subjective verification procedure, especially with regard to the development and continuity of systems in the Pacific. For either of these aspects to be fruitful a further study is indicated.

It has been stressed previously that the cloud photographs permit a good estimation of the shape but not the magnitude of the height-tendency field. However, even in the small sample considered in this work there is good indication that the magnitudes will correlate with the stage of storm development and the cloud intensity. Digital output of cloud cover and intensity which is derived from satellite data is now available at NESC. It should not prove difficult or expensive to perform a statistical investigation of the correspondence between these parameters and the gross-tendency field. It is reasonable to suppose that statistics derived from the relatively accurate analyses over the Atlantic would apply also to the Pacific.

6.2 Height-Tendency Analysis

From the SINAP standpoint it would be of interest to investigate an analysis system based on the height-tendency field rather than the height field itself. The mechanics of

the system could easily be patterned after the present system. For example, the gridpoint correction for a station reporting both height and wind (see Appendix A) becomes:

$$\frac{\partial}{\partial t}(\delta Z) = \frac{\partial}{\partial t}(C_k) = \frac{\partial}{\partial t}(Z_o + \frac{\partial Z}{\partial r} d_k - Z_g). \qquad 6.2.1$$

In finite difference form (introducing the geostrophic approximation):

$$\frac{C_k}{\Delta t} = \frac{1}{\Delta t}\{Z_o - Z'_g + \frac{f}{g}[(u - u')\Delta y - (v - v')\Delta x] - Z_g + Z'_g\} \qquad 6.2.2$$

where the primed terms refer to the twelve-hour-old values. If linear extrapolation in the old analysis is assumed correct, the primed quantities cancell and the equation reduces to the correction used in the present height-field analysis routine.

Apart from the obvious bias to SINAP there are advantages to an analysis scheme of this type. It would allow greater attention to continuity in that the final tendency field would be added to the previous analysis. There is presently no direct, internal check on the degree to which the forecast first-guess field diverges from the old analysis. It is anticipated that this system would also reduce the problem of extrapolating high gradients over large distances. The twelve-hour change in wind velocity (in the free atmosphere) is unlikely to be large, even if the velocity itself is large. The most apparent drawback to this scheme is that the analyzed field has high frequency components. This would increase the problem of aliasing, but should not be serious when the final output (tendency plus old analysis) is filtered in the usual manner. From the operational point

of view, a tendency analysis would pose another problem. Stations do not report tendencies and also occasionally miss a report. But these detractions are not sufficient to eliminate consideration of this scheme.

6.3 Tropical Disturbances

As previously noted, the satellite photographs used in Case III of this study depict the growth and development of a significant storm in the easterlies. On the other hand, the conventional 500-mb analyses for this period give very little indication of this disturbance. For various reasons no attempt was made during this study to modify the conventional analyses to reflect this system, but it is strongly felt that the problem should not be so ignored. Perturbations in the easterlies remain a source of some controversy (Sadler, 1963; Merritt, 1964). In view of the daily, global coverage of satellite television and the availability of extended periods of Nimbus high-resolution infrared radiation data, the time seems ripe for a concerted study of tropical disturbances. As a start, emphasis might be placed on the grosser features of the dynamics. The success of this study's simple advection model in predicting cloud formations suggests that successive satellite pictures could be used to estimate a mean horizontal wind associated with developing easterly perturbations. Radiation data could be used to estimate the level of this wind and also to investigate gross vertical motions within the systems.

APPENDIX A

THE ORIGINAL ANALYSIS SYSTEM

The analysis system originally written for this research was intended to conform as closely as possible with the one-level system operational at the National Meteorological Center prior to 1965. As such it is based primarily on the procedure devised by Bergthorssen and Döös (1955) and modification of this procedure described by Cressman (1959). The primary reference used in the development is an in-house summary of the NMC objective analysis system by McDonell. In order to enhance understanding of the modifications which were made on this system (Appendix B), it is appropriate to describe this scheme in some detail.

The objective analysis is an iterative, scanning procedure whereby successive guess fields are modified at regular gridpoints by observed data within the analysis area. For each scan, the guess value at each gridpoint is adjusted by all observations which lie within a radius of influence R from that gridpoint (Fig. A.1). The adjusted value at the gridpoint becomes the initial value for the succeeding scan. In total four scans are made with successively decreasing values of R (5.9, 3.6, 2.2, and 1.5 gridlengths). In this manner successively finer detail is introduced into the analysis.

The correction applied at each gridpoint depends on the number, proximity, and type of observational data within the radius of influence. If height-only is reported by a station, a correction C_i is computed:

$$C_i = Z_o - Z_c \qquad \text{A.1}$$

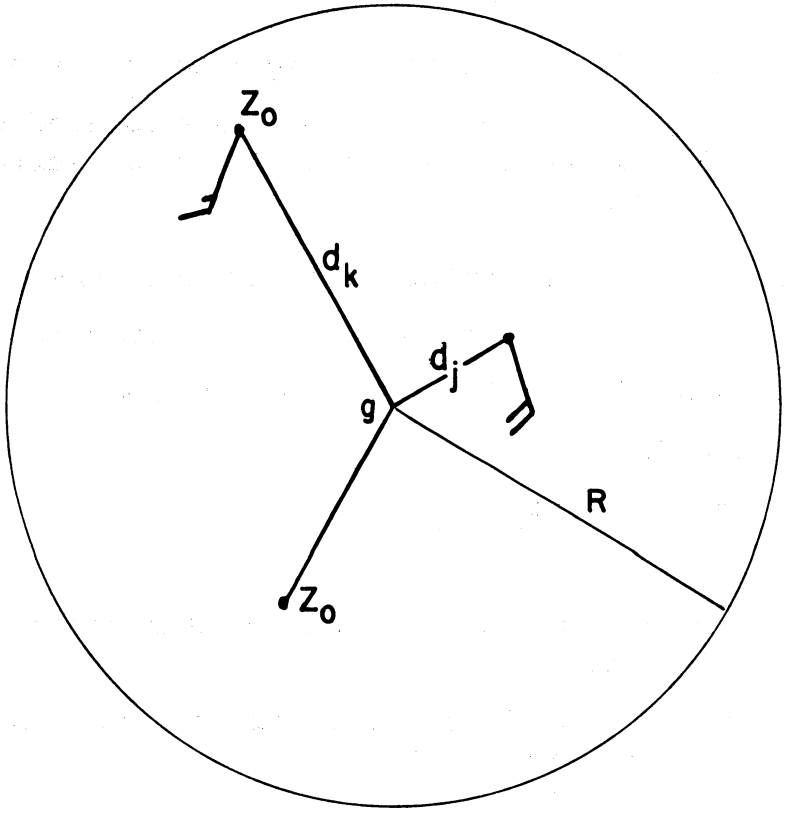

$$C_i = (Z_o - Z_c)_i$$

$$C_j = (Z_c + \frac{\delta Z}{\delta r} d_j - Z_g)_j$$

$$C_k = (Z_o + \frac{\delta Z}{\delta r} d_k - Z_g)_k$$

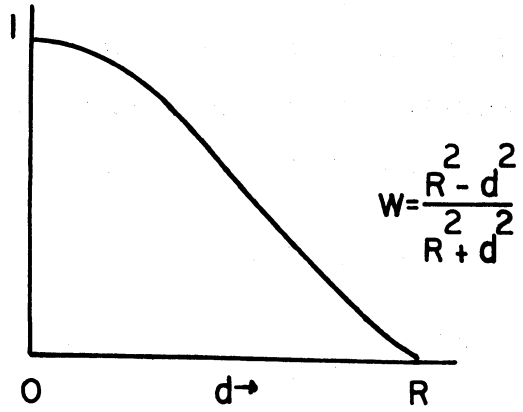

$$W = \frac{R^2 - d^2}{R^2 + d^2}$$

$$C_g = \frac{A\sum_{i=1}^{\ell} W_i C_i + B\sum_{j=1}^{m} W_j C_j + \sum_{k=1}^{n} W_k C_k}{A\ell + Bm + n}$$

Fig. A.1. The original analysis system.

where Z_o is the observed height at the station and

Z_c is the guess height interpolated bilinearly to the station from the four surrounding gridpoints.

If wind-only is reported by a station, the guess height at the station is extrapolated to the gridpoint by means of the observed gradient (the geostrophic wind). A correction C_j is computed:

$$C_j = Z_c + \frac{\partial Z}{\partial r} d_j - Z_g \qquad \text{A.2}$$

where $\frac{\partial Z}{\partial r}$ is the height gradient derived from the wind report;

d_j is the distance separating the observation from the gridpoint;

Z_g is the guess height at the gridpoint.

If both wind and height are reported by a station, the observed height is extrapolated to the gridpoint by the geostrophic wind. A correction C_k is computed:

$$C_k = Z_o + \frac{\partial Z}{\partial r} d_k - Z_g \qquad \text{A.3}$$

where d_k is the distance between the station and the gridpoint.

Each correction is weighted according to the distance separating the observation from the gridpoint:

$$W = \frac{R^2 - d^2}{R^2 + d^2} \qquad \text{A.4}$$

where R is the radius of influence.

All individual corrections are further weighted according to type and summed to give the total correction C_g at the gridpoint for the scan. Thus:

$$C_g = \frac{A \sum_{i=1}^{\ell} W_i C_i + B \sum_{j=1}^{m} W_j C_j + \sum_{k=1}^{n} W_k C_k}{A\ell + Bm + n} \qquad A.5$$

where $A = 1/8$,

$B = 0,\ 1/8,\ 1/4,\ 1/2$ on the four successive scans.

The additional weighting coefficients are imposed to guard against poor guess fields. The height-only report is lightly weighted throughout the analysis, whereas the wind-only report is given increasing weight with the reduction of the maximum distance over which the guess height may be extrapolated. On the final scan if $(\ell + m + n) \geqslant 3$, the correction C_g is increased by replacing the denominator in A.5 by

$$A = \sum_{i=1}^{\ell} W_i + \sum_{j=1}^{m} W_j + \sum_{k=1}^{n} W_k \ . \qquad A.6$$

The observational data are checked prior to each scan; they are rejected if they do not meet certain criteria. For each station report a mean error Q_m is computed from the difference between the guess heights and the observed heights for that station and all neighboring stations within two gridlengths of the report.

$$Q_m = \sum_{i=1}^{N} (Z_c - Z_o) \qquad A.7$$

where N is the number of stations within two gridlengths (including the original station).

According to the disparity between the observed value at the station and Q_m, the station may be rejected as indicated in Table A.1. All data used in the analysis are obtained from the Raob file of the NMC B-3 data tapes where all station reports have been prechecked for hydrostatic consistency.

TABLE A.1

REJECTION CRITERIA FOR OBSERVED STATION-HEIGHTS

N	$E = \lvert Q_m - Z_o \rvert$	Minimum Scans Report Retained
Any	$120 \leqslant E$	0
<3	$E \leqslant 120$	1
3	$75 \leqslant E < 120$	1
3	$E < 75$	2
>3	$75 \leqslant E < 120$	2
>3	$E < 75$	3

In addition to the smoothing implicit in the scanning technique, a smoother is applied to the field after the third and fourth scans. This smoother is identical to the nine-point smoother developed by Schumann (1957) and currently used at NMC.

The first-guess field used to initiate the analysis procedure is either the 500-mb twelve-hour forecast from the previous analysis time (the field used at NMC), the thirty-six-hour forecast field valid at analysis time (used to simulate poor twelve-hour forecasts), or a reanalysis

field based on the satellite photographs.

As mentioned in the text, because these analyses are performed for only one level, the procedure is somewhat different from that employed at NMC (Gustafson and McDonell, 1965). In Washington the analysis is done in two three-scan stages. Large influence radii are used in the first stage; smaller radii with tighter tossout criteria are used in the second stage. After the first stage, the 850 and 700-mb levels are analyzed. On completion of the latter a stability check is made at each gridpoint by computing:

$$S_7 = D_7 - .539D_5^* - .461D_{10} \qquad A.8$$

where D_7 is the analyzed 700-mb D value,

D_5^* is the 500-mb analyzed D value after the first stage,

D_{10} is the analyzed 1000-mb D value.

If the stability at any gridpoint exceeds predefined limits, it is brought within those limits by adjusting the preliminary value of the 500-mb field. The second stage of the 500-mb analysis is then performed on the modified D_5^* field.

APPENDIX B

A MODIFIED ANALYSIS SYSTEM

As indicated in the main text, a decision was made to modify the analysis system to permit a greater role for the initial guess field and to alleviate the erratic results obtained with very sparse data fields. Without altering the basic framework of the NMC system, there are essentially five ways in which such modifications can be made. These are: the number of scans used; the radius of influence used with each scan; the form of the weighting factor; the filtering procedure; and the criteria for acceptance of an observation. Three of these methods were dismissed at the outset. Alteration of the radius of influence for a given scan, as distinct from an alteration in the number of scans, can be of only modest importance. There seemed little prospect of determining a selection more effective than that presently employed without exhaustive testing beyond the scope of this work. The same reasoning applies to modification in the weighting function, although there is no doubt that this can be improved. Experiments by Gandin (1963) and Eddy (1967), among others, show that weighting factors which are statistically more realistic will lead to better analysis, particularly in sparse-data areas. Finally, the filtering procedure presently used has won acceptance in numerical prediction and there seemed little reason to tamper with it. As a result, the scope of the modifications was limited to the number of scans and the acceptance/rejection criteria.

To gain further insight into the performance of the unmodified system, a test program was written and executed on data fields available for eight days. One field taken from each data tape was assumed to represent the exact state of the atmosphere. Pseudo reports of station-heights and height gradients (corresponding to station-winds) were

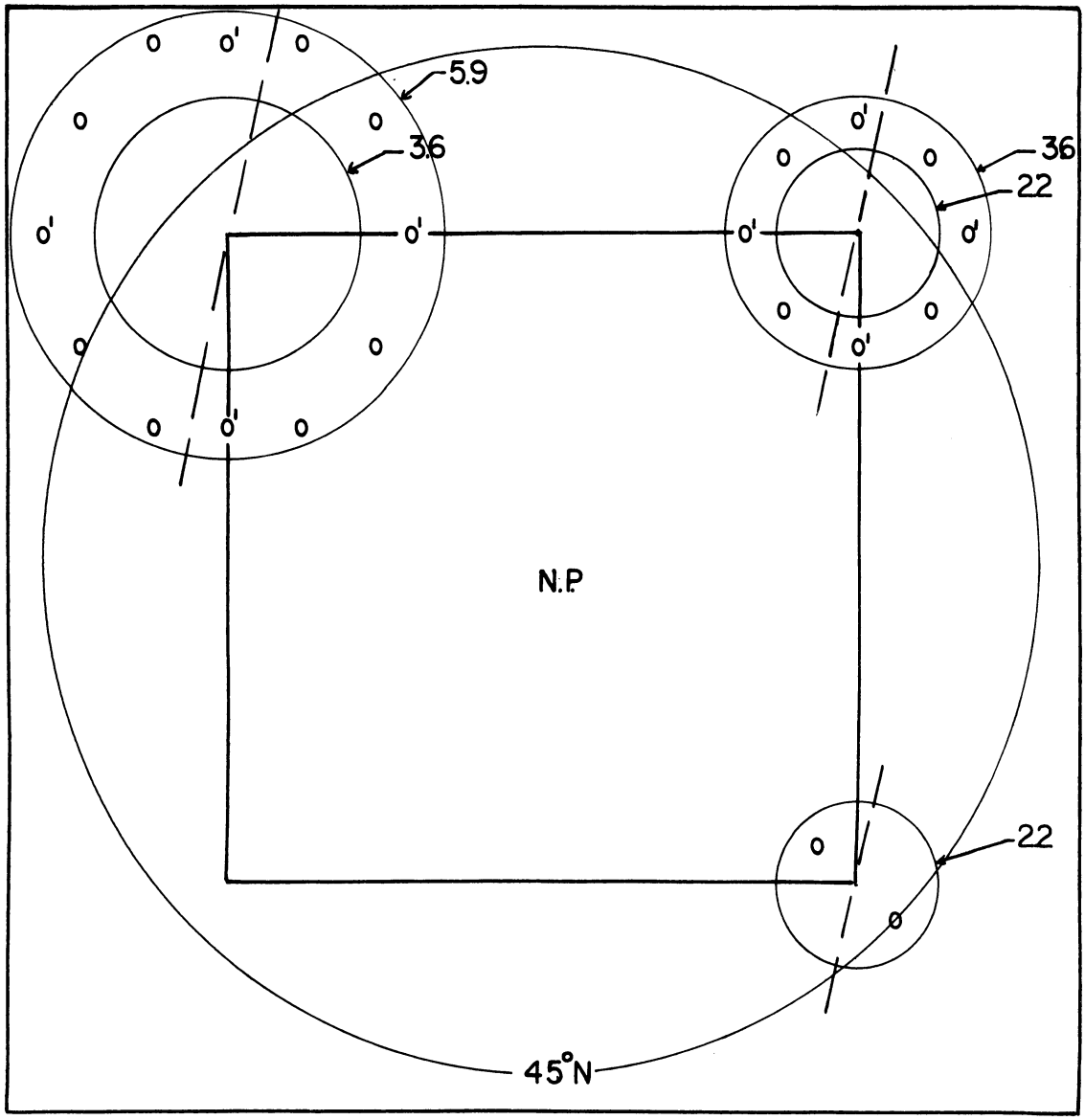

Fig. B.1. Station distribution for analysis test. Primed stations are those used in four-station trials. Stations to right of dashed lines are those used for biased distribution.

interpolated from this field and used to modify various guess fields. This field itself was used to simulate a perfect guess. Other guess fields were obtained from the twelve-hour-old analysis, the twelve-hour and the thirty-six-hour forecasts valid at the time of the "report." In this manner it was possible to obtain a wide spectrum of quality in the initial guess. The analysis were performed over a sub-grid which is at all points farther from the edge of the data than the largest scanning radius (Fig. B.1). Verification statistics computed by the test programs correspond to those used in evaluating the effects of SINAP; namely the root-mean-square errors and correlation coefficients for the twelve-hour height tendency and the twelve-hour wind change (speed and direction.) The test program was designed to investigate four specific questions which will be discussed individually.

i) Contribution of the individual scans

The initial question regards the effectiveness of the individual scans. To investigate this feature three one-scan analyses were executed for each data set using the 5.9, 3.6, and 2.2 gridlength of influence. In order to eliminate as much as possible the influence of the weighting factor, all reports influencing each gridpoint were selected approximately equidistant from the gridpoint. In addition the stations were chosen at distances greater than the next smaller radius of influence (Figure B.1). Results of this part of the investigation are given in Table B.1 and Figure B.2. The statistics imply that the first two scans are useful only if the quality of the first-guess field is sufficiently low (Cases 3 and 4). Stated another way, it is doubtful

TABLE B.1.

DENSE DATA ONE-SCAN ANALYSIS WITH VARIABLE R AND FIRST GUESS QUALITY

CASE		NO. OF SAMPLES	ORIGINAL GUESS	R=5.9 12 ST/ACT	R=3.6 8 ST/ACT	R=2.2 2 ST/ACT
	SRMS		0	1.4	1.3	0.7
	SCC		1.00	0.93	0.95	0.98
1	DCC	8	1.00	0.75	0.82	0.88
	TRMS		0	19	17	9
	TCC		1.00	0.97	0.97	0.99
	SRMS		3.1	3.1	3.3	2.1
	SCC		0.69	0.66	0.66	0.86
2	DCC	2	0.52	0.43	0.50	0.73
	TRMS		37	38	37	21
	TCC		0.86	0.84	0.86	0.95
	SRMS		6.4	6.0	5.7	3.8
	SCC		0.33	0.35	0.36	0.63
3	DCC	8	0.20	0.19	0.26	0.49
	TRMS		73	69	65	41
	TCC		0.43	0.46	0.52	0.77
	SRMS		8.9	8.0	7.8	4.7
	SCC		0.31	0.38	0.38	0.59
4	DCC	2	0.08	0.10	0.13	0.33
	TRMS		118	107	105	66
	TCC		0.11	0.16	0.19	0.52

that the first two scans are useful for the normal first-guess field composed of the twelve-hour forecast (Case 2) but may be useful if persistence (Case 3) is used for the first-guess field. It will be noted that the two samples considered in Case 2 hardly constitute a fair trial; however, a careful investigation of station errors (interpolated value minus observed value of the 500-mb height), which were printed out after each scan of the regular analyses performed in

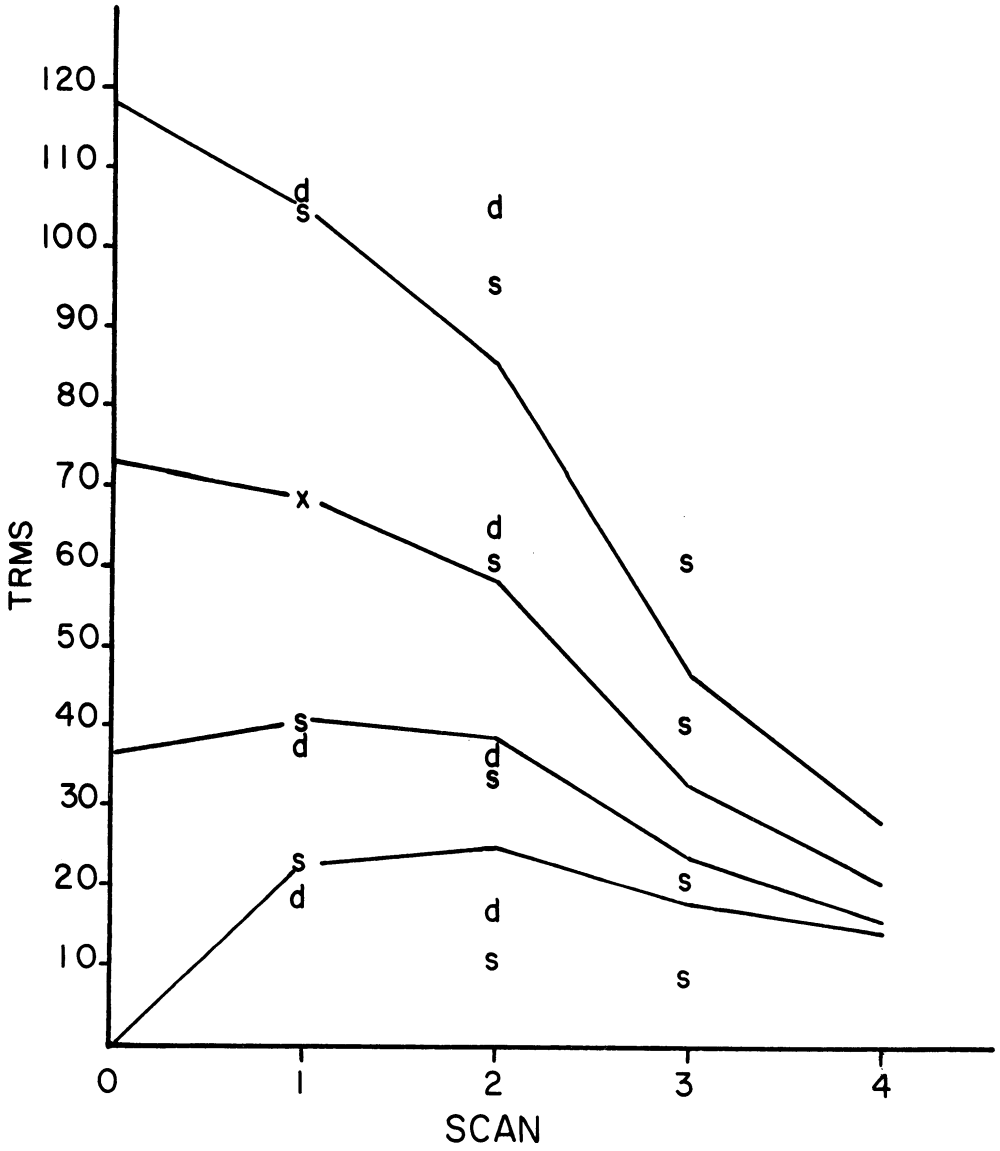

Fig.B.2. Tests of unmodified analysis system. Lines represent complete four-scan analysis. Letters represent one-scan analysis with radius of influence appropriate to indicated scan.

s - sparse data
d - dense data
x - s and d coincident.

TABLE B.2.

MODERATE DATA DENSITY ONE-SCAN ANALYSIS

WITH VARIABLE R AND FIRST GUESS QUALITY

CASE		R=5.9 4 ST/ACT	R=3.6 4 ST/ACT	R=5.9 4/12	R=3.6 4/8
	SRMS	1.9	0.9	0.9	1.1
	SCC	0.87	0.97	0.97	0.96
1	DCC	0.69	0.84	0.83	0.83
	TRMS	23	11	9	16
	TCC	0.95	0.99	0.99	0.98
	SRMS	3.4	3.1	1.3	1.2
	SCC	0.59	0.67	0.94	0.95
2	DCC	0.35	0.52	0.75	0.72
	TRMS	41	34	11	15
	TCC	0.80	0.88	0.99	0.97
	SRMS	6.0	5.5	1.0	1.1
	SCC	0.36	0.39	0.97	0.95
3	DCC	0.21	0.27	0.84	0.88
	TRMS	69	61	7	12
	TCC	0.47	0.55	0.99	0.97
	SRMS	7.8	7.0	1.0	1.4
	SCC	0.38	0.42	0.99	0.99
4	DCC	0.10	0.15	0.91	0.91
	TRMS	105	96	7	15
	TCC	0.18	0.24	0.99	0.99

this research, fully corroborate the results of this test.

ii) Station density

A second question concerns the effect of station density on the analysis system, particularly with regard to the earlier scans. To clarify this effect, one-scan analyses for R = 5.9 and R = 3.6 were repeated for all four cases given in Table B.1. The only change was to replace with four directionally

TABLE B.3.

INFLUENCE OF SCANS IN COMPLETE FOUR-SCAN ANALYSIS ON VARIABLE FIRST GUESS QUALITY

CASE		SCAN 1 4 ST	SCAN 2 4 ST	SCAN 3 2 ST	FINAL 1 ST
	SRMS	1.9	2.0	1.2	0.9
	SCC	0.87	0.87	0.95	0.97
1	DCC	0.69	0.67	0.80	0.80
	TRMS	23	25	18	15
	TCC	0.95	0.94	0.97	0.98
	SRMS	3.4	3.3	2.3	1.6
	SCC	0.59	0.59	0.83	0.93
2	DCC	0.35	0.41	0.68	0.81
	TRMS	41	39	23	16
	TCC	0.80	0.83	0.95	0.97
	SRMS	6.0	5.3	3.18	1.95
	SCC	0.36	0.39	0.70	0.88
3	DCC	0.21	0.28	0.53	0.71
	TRMS	69	59	33	21
	TCC	0.47	0.57	0.84	0.94
	SRMS	7.8	6.3	3.6	2.4
	SCC	0.38	0.44	0.70	0.87
4	DCC	0.10	0.14	0.40	0.61
	TRMS	105	86	47	29
	TCC	0.18	0.32	0.72	0.91

balanced reports the twelve-station density used with the larger scan radius and the eight-station density used with the smaller. The results of this test are given in Table B-2 and Figure B.2. Direct comparisons of the dense and sparse analyses (the right hand columns of Table B.2) indicate very little difference with the possible exception of the magnitude of the TRMS for the smaller scanning radius. Furthermore, the differences appear to be independent of

the quality of the first guess. Comparisons of these analyses with the correct field are more difficult to interpret (Fig. B.2). Again the changes associated with data density are small. For the larger scan radius the sparser network appears slightly worse for good guess fields and slightly better for poor guess fields. With the smaller radius the sparse network is in all cases a slight improvement. Because all changes are so modest it would appear unnecessary to include large numbers of station reports in the early scans.

iii) Contribution of the early scans to the complete analysis

It seemed advisable to repeat the four cases with complete four-scan analyses in order to investigate the effects of earlier scans on the results for R = 3.6 and R = 2.2. In view of (ii) above, only four reports were used to correct the gridpoint values on the early scans. Verification statistics computed after each scan are given in Table B.3 and may be compared with those obtained for one-scan analysis in Tables B.1 and B.2. The results for the TRMS are depicted on Figure B.2. These values give further evidence that the first two scans are ineffective for the normal twelve-hour forecast, first-guess field. Indeed there is some indication that they are injurious. With the poorer guesses (Cases 3 and 4), the early scans do have a beneficial effect, although it is perhaps not as great as one would anticipate

It might be noted that the complete analysis on the perfect guess (Case 1) gives some indication of the noise level associated with the analysis scheme (although there are data networks which are more dense than that utilized

TABLE B.4.

BIAS DATA, ONE-SCAN ANALYSIS WITH VARIABLE R AND FIRST-GUESS QUALITY

CASE		R=5.9 6/ACT	R=3.6 4/ACT	R=5.9 6/12	R=3.6 4/8	R=2.2 1/2
	SRMS	1.8	1.3	1.1	1.2	1.3
	SCC	0.90	0.96	0.95	0.96	
1	DCC	0.68	0.77	0.79	0.79	0.78
	TRMS	27	16	19	16	13
	TCC	0.94	0.98	0.97	0.98	0.99
	SRMS	3.2	3.1	1.0	1.4	1.5
	SCC	0.63	0.68	0.96	0.93	0.94
2	DCC	0.42	0.48	0.72	0.67	0.69
	TRMS	41	34	17	16	12
	TCC	0.82	0.87	0.97	0.97	0.99
	SRMS	6.2	5.5	1.1	1.2	1.4
	SCC	0.32	0.38	0.97	0.94	0.92
3	DCC	0.20	0.25	0.81	0.82	0.79
	TRMS	72	61	14	12	10
	TCC	0.43	0.55	0.97	0.97	0.98
	SRMS	8.6	7.0	1.4	1.5	1.6
	SCC	0.34	0.42	0.99	0.99	0.96
4	DCC	0.10	0.15	0.88	0.87	0.82
	TRMS	111	96	15	14	10
	TCC	0.16	0.25	0.99	0.99	0.99

here[1].) There appears to be particular difficulty with regard to wind direction. This gives some support to those who advocate that the wind and height fields should be analyzed separately and then combined (Ghandin, 1964).

---

1 Alaka and Lewis (1967) find a minimum RMSE of 4.4 meters for the saturated NMC analysis system.

iv) Directional bias in reporting stations

A final test was conducted to at least partially examine the effects of directional bias in the reporting stations, a situation which exists naturally in all oceanic regions close to a continent. In order to investigate this aspect one-scan analyses were repeated for the three, large scanning radii. All factors are similar to those discussed in (i) except that the reports in the first and second quadrants have been ignored (Fig. B.1). As a result, six instead of twelve and four instead of eight reports were used for the R = 5.9 and R = 3.6 analyses respectively. Results of this test are given in Table B-4, and may be compared with Tables B-1 and B-2. The statistics indicate that biasing is of very minor importance, though there is a slight trend towards increasing significance as the first-guess field improves. In this instance the statistics are somewhat misleading. The difference maps (analysis heights minus verification heights) representing the three right-hand columns of Table B-4 show a very regular pattern of positive and negative areas which are oriented perpendicular to the direction of bias. This suggests that even though the bias effect is small in the test cases, it produces a systematic error in the wind field. Furthermore, regular analyses over the Atlantic Ocean demonstrate severe biasing errors quite distinct from the problem of low station density. By coincidence, for several of the days investigated, the stations in the coastal regions are situated in or close to the jet stream. These stations necessarily contribute importantly to the analysis of the mid-Atlantic region. Since the observed winds are representative of the height gradient only in the near vicinity of the reporting stations, the corrections extrapolated to distant

gridpoints cause major and rather dubious modification of guess field. This problem is accentuated by the sparseness of the data, and more than any other factor it causes instability in the analysis of sparse-data networks.

Modifications to the analysis system were based on the above tests and also on investigation of the regular analyses. However, there is obviously no definitive solution to all the idiosynchracies encountered, and a considerable period of time was spent juggling the modifications with tests on real data. The final product, which is detailed below, is clearly not an optimum system, but does appear to be an improvement over the unaltered version. The changes are listed in what is felt to be the order of their relative effectiveness.

The first change was designed to limit the magnitude of an individual correction affecting a gridpoint. Inasmuch as all station reports are checked for consistency with the guess field prior to each scan (see Appendix A), it seems only reasonable that each gridpoint correction derived from these reports should likewise be checked and bounded. Printouts of high individual corrections obtained in the course of test runs show that during the first two scans corrections frequently exceed two hundred meters even with the weighting factor included. In view of the general quality of the guess field, such values are unreasonably high and although the effect is greatly reduced where a large number of reports influences a gridpoint, it becomes critically important in sparse data regions. Unfortunately, as in all data-rejection schemes, beyond the very crude guidance of climatological variance the selection of

acceptance limits is entirely subjective. The procedure described below was devised to roughly conform with the data-rejection method currently utilized at NMC, but the precise limits imposed on the corrections have been only briefly tested.

In the course of a scan, the mean value of all corrections applicable at each gridpoint is computed. Each correction is compared to this mean, and if it exceeds it by a fixed value (Table B.5) it is rejected. The mean is then recomputed without the rejected value and the procedure continued until all corrections are accepted. Experiments have shown that rejections are legion of the first scan, moderate on the second scan, and virtually non-existent on the final two scans.

In addition to the rejection of the individual corrections, if the toal correction exceeds the limit given in Table B.5, it is reduced to the limiting value. It should be emphasized that these criteria have been selected for use with good guess fields, as is apparent from a comparison of the early scan limits with the original TRMS of the four cases in Table B.1.

The test results associated with data density suggested that equivalent analyses could be obtained without using all station reports which fall within the radius of influence in the early scans. Consequently, a five-station limit is imposed for the correction of each gridpoint. The stations are chosen such that the two closest are automatically included, but the final three are selected with the condition that at least one station must lie in every quadrant about the gridpoint. This means that more distant stations may be preferred because of their directional relationship with

TABLE B.5.

LIMITS (METERS) IMPOSED ON GRIDPOINT CORRECTIONS

SCAN	LIMIT
1	50
2	75
3	120
4	120

the gridpoint. This is not felt to be disadvantageous since the modifications are intended to deemphasize the role of the early scans, and two stations have been shown to be quite effective for the third scan (see Tables B.1, B.4). The requirement obviously limits the effect of biasing. A further discrimination is made regarding the type of report. All wind-only reports at a distance greater than 2.2 gridlengths from a gridpoint are ignored. If such a report is within this distance and is the closest report in the quadrant, it is accepted unless an ordinary raob in that quadrant is less than one gridlength more distant from the gridpoint. This provision becomes important only in the Pacific where aircraft reports outnumber the raobs and are frequently clustered in the vicinity of the regular reporting stations.

After selection of the influencing stations, provision is made to reflect the prevailing data density by skipping early scans when all data are sufficiently close to the gridpoint. All gridpoints are tentatively flagged as shown in Table B.6. As indicated in the table, where the full complement of reports does not exist (especially at low latitudes and in the Pacific), the first two scans are ignored. This puts special emphasis on the first-guess

TABLE B.6

INITIAL SCAN DETERMINATION FOR GRIDPOINTS

NO. STATIONS	MAX. STATION DISTANCE (GRIDLENGTHS)	INITIAL SCAN	MIN. NO. STATIONS FOR RETENTION
5	$3.6 < D \leqslant 5.9$	1	4
5	$2.2 < D \leqslant 3.6$	2	3
5	$\leqslant 2.2$	3	1
<5	5.9	3	1

field for sparse-data regions, which have proven to be the places where the analysis scheme breaks down. In addition, the number of rejected corrections is checked and the scan skipped whenever the number of retained reports falls below NMIN in the table. As part of the output, a field of the initial scan for each gridpoint is produced. Early experiments showed that this field was occasionally discontinuous and a smoother was added whereby the initial scan at each gridpoint is the average of the tentative value for that point and the four surrounding points.

In the case where a correction is rejected it would be reasonable to include, if possible, another report in the same quadrant. In the system used, however, sorting and storing of the influence stations and selection of the initial scan for each gridpoint is done prior to the actual analysis. In this manner a number of first-guess fields can be analyzed quickly and efficiently. If the station reports were not presorted, the replacement approach could be considered.

APPENDIX C

VERIFICATION STATISTICS

TABLE C.1.

12 HOUR FORECAST/REANALYSIS; SYSTEM A1; JANUARY CASE

	0	6 ST	13 ST	28 ST	48 ST	63 ST	TOT
ANALYSIS FROM ORIG. GUESS VS. ANALYSIS FROM REAN. GUESS							
SRMS	3.5	2.9	1.6	1.2	1.0	1.0	1.0
SCC	0.86	0.94	0.98	0.99	0.99	0.90	0.99
DCC	0.74	0.83	0.90	0.98	0.98	0.97	0.98
TRMS	23	19	8	6	5	5	4
TCC	0.87	0.94	0.98	1.00	1.00	1.00	1.00
ANALYSIS FROM ORIG. GUESS VS. NMC ANALYSIS							
SRMS	4.5	6.8	6.5	4.9	3.7	3.5	2.6
SCC	0.73	0.59	0.64	0.76	0.84	0.86	0.91
DCC	0.59	0.55	0.44	0.61	0.64	0.72	0.75
TRMS	31	47	47	29	20	17	11
TCC	0.75	0.69	0.72	0.91	0.93	0.94	0.98
ANALYSIS FROM REAN. GUESS VS. NMC ANALYSIS							
SRMS	4.7	6.5	6.3	5.1	3.7	3.5	2.9
SCC	0.74	0.61	0.67	0.75	0.85	0.87	0.90
DCC	0.61	0.60	0.41	0.63	0.72	0.81	0.76
TRMS	23	42	46	30	19	17	11
TCC	0.88	0.77	0.75	0.90	0.93	0.94	0.98
ANALYSIS FROM ORIG. GUESS VS. ORIG. GUESS							
SRMS		5.0	6.5	5.3	4.4	4.5	4.6
SCC		0.80	0.62	0.68	0.75	0.76	0.76
DCC		0.71	0.54	0.59	0.59	0.59	0.55
TRMS		37	49	41	31	30	32
TCC		0.89	0.75	0.67	0.75	0.77	0.73
ANALYSIS FROM REAN. GUESS VS. REAN. GUESS							
SRMS		5.4	6.6	5.1	4.3	4.4	4.7
SCC		0.74	0.61	0.78	0.81	0.80	0.78
DCC		0.76	0.49	0.66	0.56	0.56	0.61
TRMS		36	46	35	25	25	25
TCC		0.88	0.77	0.82	0.85	0.86	0.85

TABLE C.2.

12 HOUR FORECAST/REANALYSIS; SYSTEM A2; JANUARY CASE

	0	6 ST	13 ST	28 ST	48 ST	63 ST	TOT
ANALYSIS FROM ORIG. GUESS VS. ANALYSIS FROM REAN. GUESS							
SRMS	3.5	3.3	3.1	2.4	1.6	1.6	1.4
SCC	0.86	0.88	0.88	0.94	0.98	0.98	0.99
DCC	0.74	0.72	0.73	0.87	0.88	0.90	0.95
TRMS	23	21	19	15	8	8	7
TCC	0.87	0.89	0.90	0.95	0.98	0.98	0.99
ANALYSIS FROM ORIG. GUESS VS. NMC ANALYSIS							
SRMS	4.5	4.6	4.4	4.0	3.7	3.5	2.7
SCC	0.73	0.74	0.77	0.80	0.83	0.84	0.91
DCC	0.59	0.59	0.63	0.66	0.66	0.68	0.69
TRMS	31	31	29	23	21	19	11
TCC	0.75	0.76	0.76	0.89	0.90	0.91	0.98
ANALYSIS FROM REAN. GUESS VS. NMC ANALYSIS							
SRMS	4.7	4.6	4.4	4.1	3.9	3.6	3.0
SCC	0.74	0.76	0.79	0.80	0.83	0.85	0.90
DCC	0.61	0.65	0.66	0.65	0.71	0.73	0.79
TRMS	23	24	23	22	20	19	11
TCC	0.88	0.88	0.87	0.93	0.92	0.94	0.98
ANALYSIS FROM ORIG. GUESS VS. ORIG. GUESS							
SRMS		1.3	2.3	3.7	4.3	4.3	4.5
SCC		0.98	0.92	0.80	0.78	0.80	0.79
DCC		0.97	0.91	0.71	0.59	0.55	0.58
TRMS		7	11	26	28	27	30
TCC		1.00	0.98	0.84	0.80	0.82	0.78
ANALYSIS FROM REAN. GUESS VS. REAN. GUESS							
SRMS		1.26	2.0	3.7	4.2	4.2	4.5
SCC		0.98	0.95	0.84	0.82	0.83	0.82
DCC		0.94	0.87	0.72	0.62	0.60	0.60
TRMS		5	7	22	23	22	24
TCC		1.00	0.99	0.88	0.86	0.88	0.88

TABLE C.3.

36 HOUR FORECAST/REANALYSIS; SYSTEM A1; JANUARY CASE

	0	6 ST	13 ST	28 ST	48 ST	63 ST	TOT
ANALYSIS FROM ORIG. GUESS VS. ANALYSIS FROM REAN. GUESS							
SRMS	6.1	6.0	5.3	4.0	2.7	2.6	1.6
SCC	0.33	0.67	0.77	0.85	0.92	0.92	0.98
DCC	0.46	0.53	0.64	0.77	0.81	0.82	0.92
TRMS	49	44	40	21	17	15	7
TCC	0.62	0.80	0.80	0.93	0.96	0.97	0.99
ANALYSIS FROM ORIG. GUESS VS. NMC ANALYSIS							
SRMS	7.7	8.5	7.3	5.3	4.3	4.1	2.4
SCC	0.36	0.32	0.50	0.72	0.81	0.83	0.95
DCC	0.24	0.22	0.32	0.51	0.56	0.63	0.77
TRMS	66	74	62	35	27	25	12
TCC	0.48	0.52	0.62	0.88	0.92	0.93	0.98
ANALYSIS FROM REAN. GUESS VS. NMC ANALYSIS							
SRMS	7.0	8.4	6.8	4.9	3.7	3.6	2.5
SCC	0.51	0.38	0.61	0.76	0.85	0.86	0.93
DCC	0.45	0.35	0.42	0.61	0.63	0.65	0.78
TRMS	40	59	47	30	21	21	11
TCC	0.80	0.70	0.78	0.90	0.95	0.95	0.98
ANALYSIS FROM ORIG. GUESS VS. ORIG. GUESS							
SRMS		4.3	6.7	7.2	6.6	6.5	7.6
SCC		0.80	0.42	0.38	0.39	0.40	0.39
DCC		0.75	0.38	0.31	0.32	0.32	0.24
TRMS		28	52	57	53	53	64
TCC		0.94	0.70	0.54	0.58	0.58	0.50
ANALYSIS FROM REAN. GUESS VS. REAN. GUESS							
SRMS		6.5	7.8	6.7	6.1	6.1	7.0
SCC		0.55	0.48	0.57	0.57	0.57	0.53
DCC		0.70	0.40	0.34	0.46	0.45	0.43
TRMS		42	50	41	35	34	39
TCC		0.84	0.75	0.78	0.80	0.82	0.79

TABLE C.4.

36 HOUR FORECAST/REANALYSIS; SYSTEM A2; JANUARY CASE

	0	6 ST	13 ST	28 ST	48 ST	63 ST	TOT
ANALYSIS FROM ORIG. GUESS VS. ANALYSIS FROM REAN. GUESS							
SRMS	6.1	5.7	5.8	4.7	4.2	3.9	2.7
SCC	0.33	0.43	0.47	0.70	0.79	0.81	0.92
DCC	0.46	0.47	0.46	0.64	0.70	0.77	0.88
TRMS	49	48	48	35	27	23	12
TCC	0.62	0.65	0.65	0.79	0.88	0.91	0.97
ANALYSIS FROM ORIG. GUESS VS. NMC ANALYSIS							
SRMS	7.7	7.5	7.4	6.4	5.4	5.3	3.6
SCC	0.36	0.39	0.42	0.57	0.69	0.71	0.89
DCC	0.24	0.24	0.25	0.39	0.50	0.57	0.65
TRMS	66	66	64	45	35	32	18
TCC	0.48	0.50	0.53	0.74	0.84	0.86	0.96
ANALYSIS FROM REAN. GUESS VS. NMC ANALYSIS							
SRMS	7.0	6.8	6.5	5.6	4.4	4.4	3.1
SCC	0.51	0.55	0.59	0.68	0.80	0.81	0.91
DCC	0.45	0.43	0.44	0.52	0.63	0.65	0.73
TRMS	40	39	37	28	23	22	12
TCC	0.80	0.81	0.83	0.90	0.94	0.94	0.98
ANALYSIS FROM ORIG. GUESS VS. ORIG. GUESS							
SRMS		1.2	2.9	5.5	6.4	6.7	7.8
SCC		0.97	0.86	0.56	0.42	0.40	0.39
DCC		0.92	0.78	0.47	0.36	0.31	0.23
TRMS		6	13	37	47	49	60
TCC		0.99	0.97	0.79	0.68	0.67	0.56
ANALYSIS FROM REAN. GUESS VS. REAN. GUESS							
SRMS		1.5	3.0	4.7	5.7	5.8	6.8
SCC		0.96	0.87	0.71	0.60	0.61	0.57
DCC		0.94	0.75	0.52	0.49	0.49	0.44
TRMS		7	13	21	33	32	38
TCC		0.99	0.97	0.87	0.82	0.83	0.81

TABLE C.5.

12 HOUR FORECAST/BOGUS; SYSTEMS A1 AND A2; JANUARY CASE

	0	13 ST	19 ST	34 ST	54 ST	69 ST	TOT
A1 ANALYSIS WITHOUT BOGUS VS. A1 ANALYSIS WITH BOGUS							
SRMS		8.3	6.6	3.5	2.5	1.9	1.0
SCC		0.65	0.71	0.84	0.88	0.93	0.99
DCC		0.50	0.60	0.89	0.88	0.89	0.96
TRMS		60	53	22	14	11	6
TCC		0.72	0.75	0.91	0.92	0.96	1.00
A1 ANALYSIS WITH BOGUS VS. NMC ANALYSIS							
SRMS	4.5	9.3	7.2	5.2	4.1	3.7	2.7
SCC	0.73	0.54	0.64	0.73	0.80	0.82	0.90
DCC	0.59	0.44	0.53	0.63	0.68	0.70	0.78
TRMS	31	54	46	33	24	20	12
TCC	0.75	0.73	0.77	0.86	0.88	0.91	0.98
A1 ANALYSIS WITH BOGUS VS. ORIG. GUESS							
SRMS		8.6	7.0	5.4	4.6	4.5	4.5
SCC		0.62	0.62	0.68	0.73	0.74	0.77
DCC		0.53	0.55	0.56	0.52	0.53	0.54
TRMS		56	49	41	33	31	32
TCC		0.70	0.73	0.71	0.74	0.76	0.75
A2 ANALYSIS WITHOUT BOGUS VS. A2 ANALYSIS WITH BOGUS							
SRMS		3.9	3.9	3.1	2.8	2.0	1.0
SCC		0.80	0.82	0.86	0.90	0.93	0.99
DCC		0.76	0.75	0.82	0.76	0.81	0.96
TRMS		23	23	18	13	12	6
TCC		0.87	0.87	0.91	0.92	0.94	1.00
A2 ANALYSIS WITH BOGUS VS. NMC ANALYSIS							
SRMS	4.5	5.3	5.1	4.6	3.8	3.6	2.4
SCC	0.73	0.70	0.71	0.76	0.82	0.83	0.92
DCC	0.59	0.63	0.65	0.65	0.72	0.72	0.82
TRMS	31	30	30	25	21	19	11
TCC	0.75	0.82	0.82	0.88	0.91	0.92	0.98
A2 ANALYSIS WITH BOGUS VS. ORIG. GUESS							
SRMS		4.0	4.3	4.7	4.5	4.5	4.3
SCC		0.80	0.76	0.73	0.75	0.76	0.79
DCC		0.76	0.69	0.57	0.51	0.51	0.56
TRMS		24	27	33	30	30	29
TCC		0.87	0.85	0.75	0.76	0.77	0.78

TABLE C.6.

36 HOUR FORECAST/BOGUS; SYSTEMS A1 AND A2; JANUARY CASE

	0	12 ST	19 ST	34 ST	54 ST	69 ST	TOT
A1 ANALYSIS WITHOUT BOGUS VS. A1 ANALYSIS WITH BOGUS							
SRMS		8.0	6.3	3.8	2.7	2.0	1.2
SCC		0.53	0.74	0.87	0.91	0.95	0.99
DCC		0.43	0.62	0.80	0.80	0.89	0.91
TRMS		47	42	20	14	10	8
TCC		0.66	0.78	0.94	0.97	0.98	0.99
A1 ANALYSIS WITH BOGUS VS. NMC ANALYSIS							
SRMS	7.7	8.9	7.8	5.8	4.8	4.4	2.6
SCC	0.36	0.38	0.55	0.68	0.77	0.80	0.94
DCC	0.24	0.29	0.48	0.60	0.56	0.57	0.75
TRMS	66	55	48	34	28	27	13
TCC	0.48	0.72	0.79	0.88	0.91	0.93	0.98
A1 ANALYSIS WITH BOGUS VS. ORIG. GUESS							
SRMS		8.3	8.5	7.7	6.8	6.5	7.5
SCC		0.47	0.39	0.34	0.36	0.39	0.37
DCC		0.44	0.35	0.27	0.35	0.33	0.21
TRMS		53	51	53	50	50	59
TCC		0.62	0.65	0.59	0.59	0.62	0.57
A2 ANALYSIS WITHOUT BOGUS VS. A2 ANALYSIS WITH BOGUS							
SRMS		3.9	3.9	3.4	2.9	2.1	1.3
SCC		0.75	0.78	0.85	0.90	0.95	0.99
DCC		0.70	0.67	0.75	0.76	0.88	0.93
TRMS		23	23	19	16	11	6
TCC		0.90	0.90	0.93	0.96	0.98	1.00
A2 ANALYSIS WITH BOGUS VS. NMC ANALYSIS							
SRMS	7.7	7.1	7.0	6.0	5.4	5.2	3.2
SCC	0.36	0.45	0.48	0.64	0.70	0.72	0.91
DCC	0.24	0.32	0.33	0.51	0.53	0.60	0.70
TRMS	66	55	52	38	33	30	16
TCC	0.48	0.68	0.71	0.85	0.89	0.90	0.97
A2 ANALYSIS WITH BOGUS VS. ORIG. GUESS							
SRMS		4.3	4.9	6.4	6.8	6.7	7.5
SCC		0.70	0.63	0.43	0.37	0.39	0.39
DCC		0.68	0.55	0.35	0.34	0.31	0.24
TRMS		24	27	41	46	47	57
TCC		0.89	0.87	0.73	0.68	0.67	0.60

TABLE C.7.

12 HOUR FORECAST/REANALYSIS; SYSTEM A1; MAY CASE

	0	8 ST	14 ST	29 ST	56 ST	TOT
ANALYSIS FROM ORIG. GUESS VS. ANALYSIS FROM REAN. GUESS						
SRMS	3.9	1.0	1.5	1.3	0.8	0.8
SCC	0.85	0.94	0.98	0.98	0.99	1.00
DCC	0.72	0.81	0.91	0.92	0.96	0.98
TRMS	32	16	11	9	5	5
TCC	0.89	0.97	0.99	0.99	1.00	1.00
ANALYSIS FROM ORIG. GUESS VS. NMC ANALYSIS						
SRMS	5.6	6.5	6.0	4.3	3.5	2.4
SCC	0.75	0.54	0.65	0.75	0.85	0.92
DCC	0.55	0.63	0.58	0.70	0.76	0.78
TRMS	46	59	54	32	23	16
TCC	0.86	0.79	0.83	0.87	0.95	0.97
ANALYSIS FROM REAN. GUESS VS. NMC ANALYSIS						
SRMS	4.3	6.2	6.1	4.0	3.3	2.2
SCC	0.80	0.59	0.65	0.79	0.86	0.93
DCC	0.56	0.59	0.58	0.68	0.78	0.78
TRMS	31	52	53	30	31	14
TCC	0.90	0.84	0.85	0.90	0.96	0.98
ANALYSIS FROM ORIG. GUESS VS. ORIG. GUESS						
SRMS		6.7	6.6	5.4	5.1	5.0
SCC		0.64	0.60	0.71	0.77	0.78
DCC		0.56	0.52	0.51	0.56	0.60
TRMS		58	65	47	42	40
TCC		0.82	0.72	0.78	0.86	0.88
ANALYSIS FROM REAN. GUESS VS. REAN. GUESS						
SRMS		6.8	5.7	4.9	4.5	4.1
SCC		0.62	0.69	0.75	0.78	0.79
DCC		0.55	0.57	0.60	0.61	0.66
TRMS		58	58	43	35	29
TCC		0.77	0.77	0.78	0.88	0.90

TABLE C.8.

12 HOUR FORECAST/REANALYSIS; SYSTEM A2; MAY CASE

	0	8 ST	14 ST	29 ST	56 ST	TOT
ANALYSIS FROM ORIG. GUESS VS. ANALYSIS FROM REAN. GUESS						
SRMS	3.9	3.2	3.1	2.3	1.2	0.9
SCC	0.85	0.89	0.91	0.93	0.99	0.99
DCC	0.72	0.79	0.80	0.86	0.92	0.96
TRMS	32	27	24	17	9	6
TCC	0.89	0.93	0.95	0.97	1.00	1.00
ANALYSIS FROM ORIG. GUESS VS. NMC ANALYSIS						
SRMS	5.6	5.2	4.8	4.9	3.6	2.8
SCC	0.75	0.75	0.81	0.73	0.86	0.91
DCC	0.55	0.54	0.54	0.63	0.69	0.78
TRMS	46	42	37	34	23	19
TCC	0.86	0.87	0.91	0.88	0.95	0.96
ANALYSIS FROM REAN. GUESS VS. NMC ANALYSIS						
SRMS	4.3	4.1	4.1	4.0	3.2	2.5
SCC	0.80	0.82	0.82	0.81	0.88	0.93
DCC	0.56	0.57	0.57	0.65	0.73	0.80
TRMS	31	29	29	25	20	17
TCC	0.90	0.93	0.92	0.93	0.96	0.97
ANALYSIS FROM ORIG. GUESS VS. ORIG. GUESS						
SRMS		2.0	2.8	4.6	4.9	4.8
SCC		0.94	0.89	0.76	0.80	0.83
DCC		0.84	0.73	0.58	0.58	0.59
TRMS		14	21	36	37	36
TCC		0.98	0.93	0.86	0.88	0.89
ANALYSIS FROM REAN. GUESS VS. REAN. GUESS						
SRMS		1.6	2.0	4.2	4.1	4.0
SCC		0.96	0.95	0.80	0.82	0.82
DCC		0.92	0.86	0.67	0.58	0.64
TRMS		11	14	33	29	26
TCC		0.97	0.98	0.84	0.89	0.91

TABLE C.9.

12 HOUR FORECAST/BOGUS; SYSTEMS A1 AND A2; MAY CASE

	0	13 ST	19 ST	34 ST	61 ST	TOT
A1 ANALYSIS WITHOUT BOGUS VS. A1 ANALYSIS WITH BOGUS						
SRMS		7.1	5.1	4.2	3.1	2.3
SCC		0.51	0.71	0.79	0.89	0.94
DCC		0.67	0.71	0.79	0.85	0.90
TRMS		65	48	36	23	15
TCC		0.77	0.82	0.85	0.95	0.98
A1 ANALYSIS WITH BOGUS VS. NMC ANALYSIS						
SRMS	5.6	6.8	6.1	5.1	4.2	3.1
SCC	0.75	0.60	0.66	0.71	0.80	0.89
DCC	0.55	0.61	0.64	0.70	0.73	0.76
TRMS	46	67	46	37	28	21
TCC	0.86	0.82	0.84	0.84	0.93	0.96
A1 ANALYSIS WITH BOGUS VS. ORIG. GUESS						
SRMS		7.7	7.4	6.2	5.7	5.3
SCC		0.59	0.57	0.68	0.74	0.78
DCC		0.58	0.54	0.54	0.61	0.75
TRMS		59	57	47	44	39
TCC		0.75	0.76	0.78	0.85	0.88
A2 ANALYSIS WITHOUT BOGUS VS. A2 ANALYSIS WITH BOGUS						
SRMS		4.4	4.0	4.0	2.7	1.8
SCC		0.80	0.86	0.81	0.91	0.96
DCC		0.72	0.75	0.73	0.79	0.82
TRMS		29	28	28	19	12
TCC		0.89	0.91	0.88	0.96	0.98
A2 ANALYSIS WITH BOGUS VS. NMC ANALYSIS						
SRMS	5.6	5.2	5.0	4.8	3.8	3.0
SCC	0.75	0.70	0.75	0.73	0.83	0.90
DCC	0.55	0.58	0.61	0.60	0.69	0.75
TRMS	46	37	34	32	25	20
TCC	0.86	0.87	0.89	0.88	0.94	0.97
A2 ANALYSIS WITH BOGUS VS. ORIG. GUESS						
SRMS		4.9	5.3	5.6	5.4	5.0
SCC		0.78	0.77	0.73	0.78	0.82
DCC		0.66	0.65	0.57	0.61	0.63
TRMS		34	38	41	41	38
TCC		0.87	0.86	0.83	0.87	0.89

BIBLIOGRAPHY

Alaka, M.A. and F. Lewis, 1967: Numerical Experiments Leading to the Design of Optimum Global Meteorological Networks, ESSA technical memorandum WBTM TDL-7, Washing, D.C., 14pp.

Barr, S., M.B. Lawrence and F. Sanders. 1966: TIROS Vorticies and Large-Scale Vertical Motion. Monthly Weather Review, 94, No. 12, 675-696.

Bergthorssen, P. and B.R. Döös, 1955: Numerical Weather Map Analysis. Tellus, 7, No. 3,329-340.

Bjerknes, J., 1951: Extratropical Cyclones. Compendium of Meteorology, American Meteorological Society, 577-598.

Blinova, E.N., 1963: Determination of Initial Pressure on Wind Fields from Distributions of Temperature and Vertical Air Movements. Doklady Alcadami Nauk SSSR, 149, No. 4.

Bonner, W.D. and F. Winninghoff, 1967: Satellite Studies of Clouds and Cloud Bands Near the Low-Level Jet. Final Report, Contract No. Cwb-11210, Department of Meteorology, University of California, Los Angeles. 50pp.

Boucher, R.J. and R.J. Newcomb, 1962: Synoptic Interpretation of Some TIROS Vortex Patterns: A Preliminary Cyclone Model. Journal of Applied Meteorology, 1, No. 2, 127-136.

Bradley, J.H.S., C.M. Hayden and A.C. Wiin-Nielsen, 1966: An Attempt to Use Satellite Photography in Numerical Weather Prediction. Final Report, Contract No. Cwb-11145, Department of Meteorology, University of Michigan, 72pp.

_____, 1967: The Transient Part of the Atmospheric Planetary Waves. Technical report No. 5, Grant GP-2561, Department of Meteorology, University of Michigan.

Brodrick , H.J., 1964: TIROS Cloud Pattern Morphology of Some Mid-latitude Weather Systems. Meteorological Satellite Laboratory Report, No. 24, U.S. Weather Bureau, Washington, D.C., 31pp.

Cressman, G.P., 1959: An Operational Objective Analysis System. Monthly Weather Review, 87, No. 10, 367-374.

Deardorff, J.W., 1963: Satellite Cloud Photographs and Large Scale Vertical Motions. Journal of Applied Meteorology, 2, No. 1, 173-175.

Doos, B.R., 1962: Theoretical Analysis of Lee Wave Clouds observed by TIROS I. Tellus, 14, No. 3, 301-309.

Eddy, A., 1967: The Statistical Objective Analysis of Scalar Data Fields. Journal of Applied Meteorology, 6, No. 4, 597-609.

Elliott, R.D. and J.R. Thompson, 1965: Relationships Between TIROS Cloud Patterns and Air Mass (Wind and Thermal Structure) Final Report, Contract No. N189(188)-58870A, Aerometric Research, Inc., 54pp.

Erickson, C.O. and F.S. Erickson, 1965: Early History of Tropical Storm Katherine, 1963. Monthly Weather Review, 93, No. 3, 145-153.

Felt, R.W., 1966: Life Cycle of Tropical Cyclone Judy as Revealed by ESSA II and Nimbus II. Monthly Weather Review, 94, No. 10, 605-610.

Frank, N.L., 1963: Synoptic Case Study of Tropical Cyclogenesis utilizing TIROS Data. Monthly Weather Review, 91, No. 8, 355-366.

Fritz, S., 1962: Satellite Pictures and the Origin of Hurricane Anna. Monthly Weather Review, 90, No. 12, 507-513.

_____, 1963: Research with Satellite Cloud Pictures. Astronautics and Aerospace Engineering, 1, No. 3, 70-74.

_____, 1965: Significance of Mountain Lee Waves as seen from Satellite Pictures. Journal of Applied Meteorology, 4, No. 1, 31-37.

_____, L.F. Hubert and A Timchalk, 1966: Some Inferences from Satellite Pictures of Tropical Disturbances. Monthly Weather Review, 94, No. 4, 231-236.

Gandin, L.S., 1963: Objective Analysis of Meteorological Fields, Leningrad 1963. Israel Program for Scientific Translations, 1965, 242pp.

Gustafson, A.F. and J.E. McDonell, 1965: The Derivation of First-Guess Fields for Objective Analysis. National Meteorolgical Center Technical Memorandum No. 31, Washington, D.C., 7pp.

Holmström, I., 1963: On a Method for Parametric Representation of the State of the Atmosphere. Tellus, 15, No. 1, 26-32.

_____, 1964: On the Vertical Structure of the Atmosphere. Tellus, 16, No. 3, 288-308.

Hubert. L.F., 1961: A Subtropical Convergence Line of the South Pacific. A Case Study Using Meteorological Satellite Data. Journal of Geophysical Research, 66, No. 3, 797-812.

Krishnamurti, T.N., M.L. Altinger and O.M. Ciliberti, 1964: Inversion of the Ω-Equation. Final Report, Grant WBG-11, Department of Meteorology, University of California at Los Angles, 31pp.

Leese, J.A., 1962: The Role of Advection in Vortex Cloud Patterns. GRD Research Notes NO. 78, Air Force Cambridge Research Laboratories, Bedford, Mass., 27pp.

McClain, E.P., M.A. Ruzecki and H.J. Brodrick, 1965: Experimental Use of Satellite Pictures In Numerical Prediction. Monthly Weather Review, 93, No. 7, 445-452.

_____, 1966: On the Relation of Satellite Viewed Cloud Conditions to Vertically Integrated Moisture Fields. Monthly Weather Review, 94, No. 8, 509-514.

Merritt, E.S., 1964: Easterly Waves and Perturbations, A Reappraisal. Journal of Applied Meteorology, 3, No. 4, 367-382.

Musayelyan, Sh.A., 1964: Certain Problems Dealing With the Numerical Interpretation of Cloud Information Received from Artificial Earth Satellites. Trudy Glavnaya Geofizicheskaya Observatoria, No. 166, 203-213.

Nagle, R.E. and S.M. Serebreny, 1962: Radar Precipitation Echo and Satellite Cloud Observations of a Maritime Cyclone. Journal of Applied Meteorology, 1, No. 3, 279-295.

_____, J.R. Clark and M.M. Holl, 1966: Tests of the Diagnostic-Cycle Routine in the Interpretation of Layer-Cloud Evolutions. Monthly Weather Review, 94, No. 1, 55-66.

Nemchinov, S.V., 1963: Determination of the Stream Function from Vertical Motion. Tellus, 15, No. 2, 120-126.

Obukhov, A.M., 1960: The Statistically Orthogonal Expansion of Empirical Functions. Izvestiya Akademii Nauk SSSR, Seriya Geofizicheskaya, No. 3, 432-439.

Oliver, V.J., 1962: TIROS fills a void for World Weather Watch. Weatherwise, 15, No. 4, 160-163.

Richardson, N.N., Numerical Tests of a Method for Dynamic Analysis in Regions of Poor Data Coverage. Tellus, 13, No. 3, 353-362.

Riehl, H., 1954: Tropical Meteorology. McGraw-Hill Book Co., Inc. 392pp.

Rogers, C.W.C. and P.E. Sherr, 1966: Toward the Dynamical Interpretation of Satellite Observed Extratropical Vortical Cloud Patterns. Final Report, Contract No. Cwb-11123, ARACON Geophysics Division, Allied Research Associates, Inc., 125pp.

_____, 1967: A Study of Dynamical Relationships Between Cloud Patterns and Extratropical Cyclogenesis. Final Report, Contract No. E-47-67(N), ARACON Geophysics Division, Allied Research Associates, Inc., 74pp.

Sadler, J.C., 1963: Utilization of Meteorological Satellite Cloud Data in Tropical Meteorology. Rocket and Satellite Meteorology, North-Holland Publishing Co., Amsterdam, 333-356.

Shuman, F.G., 1957: Numerical Methods in Weather Prediction II: Smoothing and Filtering. Monthly Weather Review, 35, No. 11, 357-361.

Smith, F.B., 1962: Objective Analysis of the Vorticity Field within a Region of No Data. Tellus, 14, No. 3, 281-289.

Thomasell, A., 1962: The Areal-Mean-Error Method of Analysis Verification. Technical Report 7083-12, Travelers Research Center, Inc., 18pp.

Thompson, P.D., 1961: A Dynamical Method of Analyzing Meteorological Data. Tellus, 13, No. 3, 1961, 345-352.

Timchalk, A. and L.F. Hubert, 1961: Satellite Pictures and Meteorological Analyses of a Developing Low in the Central United States. Monthly Weather Review, 89, No. 11, 429-445.

Whitney, L.F. Jr., 1961: Another View from TIROS I of a Severe Weather Situation, May 16, 1060. Monthly Weather Review, 89, No. 11, 447-460.

_____, 1963: Severe Storm Clouds as seen from TIROS. Journal of Applied Meteorology, 2, No. 4, 501-507.

_____, A. Timchalk and T.I. Gray, 1966: On Locating Jet Stream from TIROS photographs. Monthly Weather Review, 94, No. 3, 127-138.

Widger, W.K., P.E. Sherr and C.W.C. Rogers, 1964: Practical Interpretation of Meteorological Satellite Data. Final Report, Contract No. AF 19(628)-2471, Aracon Geophysics Co., 380pp.

Wiin-Nielsen, A.C., 1959: On a Graphical Method for an Approximate Determination of the Vertical Velocity in the Mid-Troposphere. Tellus, 11, No. 4, 432-440.